

**EVALUATION OF THE PHARMACEUTICAL
POTENTIAL OF COMPONENTS OF ANISEED AND
FLAXSEED AGAINST SHIGELLOSIS (*SHIGELLA
SONNEI*) THROUGH IN SILICO AND IN VITRO
ANALYSIS**

**A Thesis Submitted to
the Graduate School of Engineering and Science of
Izmir Institute of Technology
in Partial Fulfillment of the Requirement for the degree of**

MASTER OF SCIENCE

in Molecular Biology and Genetics

**by
Tosin Felicia FAJEMBOLA**

December 2023

Izmir

We approve of the thesis of **Tosin Felicia FAJEMBOLA**

Examining Committee Members:

Prof. Dr. Anne FRARY

Molecular Biology and Genetics, İYTE

Dr. Muse OKE

Molecular Biology and Genetics, İYTE

Prof. Dr. Fatma Aykut TONK

Field Crops, Ege University

12 December 2023

Prof. Dr. Anne FRARY

Supervisor, Molecular Biology
and Genetics, İYTE

Prof. Dr. Özden Yalcin ÖZUYSAL

Head of Department, Molecular Biology
and Genetics

Prof. Dr. Mehtap EANES

Dean of the Graduate School

ACKNOWLEDGEMENTS

I want to express my deep appreciation to my supervisor, Prof. Dr. Anne Frary, who provided valuable feedback and advice during this study, especially the experiment and writing process which has significantly led to my academic and intellectual growth. I am also thankful to Prof. Dr. Sami Doğanlar for his support, guidance, and generosity.

Additionally, I want to express my gratitude to Ezgi Keskin who by sharing her knowledge and expertise contributed greatly to the success of this study. I am deeply appreciative of all members of Doğanlar and Frary and my friends from other labs for their kindness, support, and assistance.

I am grateful to TUSEB for providing me with the financial support that allowed me to carry out my research and complete my thesis.

Furthermore, I am grateful to my family, especially my parents, Mr. and Mrs. Fajembola for their prayers, encouragement, moral and financial support.

ABSTRACT

EVALUATION OF THE PHARMACEUTICAL POTENTIAL OF COMPONENTS OF ANISEED AND FLAXSEED AGAINST SHIGELLOSIS (*SHIGELLA SONNEI*) THROUGH IN SILICO AND IN VITRO ANALYSIS

Shigella sonnei is a human pathogen that causes shigellosis (dysentery) disease. Due to its resistance to currently available antibiotics in the market, shigellosis has been identified as a global crisis by the World Health Organization. Hence, there is a need to discover new drug candidates for this disease. Plant-based drug candidates have received attention for their wide variety of bioactive components and because plants are often easily accessible and inexpensive to grow. Anise seed and flaxseed essential oils have been shown to have therapeutic effects on several human diseases. In this research, the pharmaceutical potential of these essential oils was evaluated through in silico and in vitro analysis. The results of molecular docking, molecular dynamics simulation and ADMET analysis showed that isoeugenol and p-anisaldehyde from aniseed and secoisolariciresinol from flaxseed are the most promising candidates as they exhibited good binding affinities to the enzymes of the shikimate pathway and T3SS ATPase and showed promising ADMET profiles. The qualitative inhibitory assay showed that isoeugenol exerted the most inhibitory activity followed by p-anisaldehyde. The bacterium was also susceptible to SDG. The quantitative inhibition assay also indicated isoeugenol as the most potent compound with a minimum inhibitory concentration (MIC) of 0.04 mg/ml and minimum bactericidal concentration (MBC) of 0.08 mg/ml followed by p-anisaldehyde and SDG. In conclusion the in silico and in vitro assays showed that specific components of aniseed and flaxseed essential oils have potential bioactivity as drugs against *S. sonnei*.

ÖZET

ANASON VE KETEN TOHUMU BİLEŞENLERİNİN SIGELLOZ'A (*SHIGELLA SONNEI*) KARŞI FARMASÖTİK POTANSİYELİNİN IN SILICO VE IN VITRO ANALİZ YOLUYLA DEĞERLENDİRİLMESİ

Shigella sonnei, şigeloz (dizanteri) hastalığına neden olan bir insan patojenidir. Şu anda piyasada bulunan antibiyotiklere karşı direnci nedeniyle şigeloz, Dünya Sağlık Örgütü tarafından küresel bir kriz olarak tanımlanmıştır. Bu nedenle bu hastalığa yönelik yeni ilaç adaylarının keşfedilmesine ihtiyaç vardır. Bitki bazlı ilaç adayları, geniş çeşitlilikteki biyoaktif bileşenleri ve bitkilere genellikle kolayca erişilebilmesi ve yetiştirilmesinin ucuz olması nedeniyle dikkat çekmektedir. Anason ve keten tohumu esansiyel yağlarının çeşitli insan hastalıkları üzerinde tedavi edici etkileri olduğu gösterilmiştir. Bu araştırmada bu esansiyel yağların farmasötik potansiyeli in silico ve in vitro analizlerle değerlendirildi. Moleküler yerleştirme, moleküler dinamik simülasyonu ve ADMET analizinin sonuçları, anasondan elde edilen izoöjenol ve p-anisaldehitin ve keten tohumundan elde edilen sekoizolarisiresinolün, şikimat yolu ve T3SS ATPaz enzimlerine iyi bağlanma afiniteleri sergiledikleri ve umut verici ADMET gösterdikleri için en umut verici adaylar olduğunu gösterdi. profiller. Kalitatif inhibitör tahlili, izoöjenolün en fazla inhibitör aktiviteyi sergilediğini ve bunu p-anisaldehitin izlediğini gösterdi. Bakteri aynı zamanda SDG'ye de duyarlıydı. Kantitatif inhibisyon tahlili aynı zamanda izoöjenolün minimum inhibitör konsantrasyonu (MIC) 0,04 mg/ml ve minimum bakterisit konsantrasyonu (MBC) 0,08 mg/ml ile en güçlü bileşik olduğunu ve ardından p-anisaldehit ve SDG'yi gösterdi. Sonuç olarak, in silico ve in vitro analizler, anason ve keten tohumu esansiyel yağlarının spesifik bileşenlerinin, *S. sonnei*'ye karşı ilaç olarak potansiyel biyoaktiviteye sahip olduğunu gösterdi.

TABLE OF CONTENTS

LIST OF FIGURES.....	ix
LIST OF TABLES.....	x
CHAPTER 1. INTRODUCTION.....	1
1.1. Shigellosis.....	1
1.2. Computer-aided drug discovery (CADD).....	3
1.3. Targeting shigellosis.....	4
1.4. Plant-based drugs.....	8
1.4.1 Aniseed.....	8
1.4.2 Flaxseed.....	9
1.5. Aim of the study.....	11
CHAPTER 2 METHODS AND MATERIALS.....	12
2.1. Collection and identification of plant samples.....	12
2.2. Extraction of essential oil from seeds of plant samples.....	12
2.3. Gas chromatography-mass spectrometry (GC-MS) analysis of the essential oil of aniseed.....	12
2.4. Extraction of secoisolariciresinol diglucoside (SDG) from flaxseed.....	13
2.5. Molecular docking analysis and molecular dynamics (MD) simulations.....	13
2.5.1. Preparation of ligands for molecular docking.....	13
2.5.2. Preparation of molecular targets for molecular docking.....	13
2.5.3. Molecular docking with protein targets.....	15
2.5.4. Virtual screening.....	15
2.5.5. Molecular dynamic (MD) simulations.....	16
2.5.5.1. Preparation of ligand–protein complexes for MD.....	16
2.5.5.2. MD simulation of ligand-protein target.....	16
2.6. ADME and toxicity analysis.....	17
2.7. Antimicrobial test.....	17
CHAPTER 3. Results and Discussion.....	19
3.1. Percentage yield of essential oil (EO) from aniseed and flaxseed.....	19
3.2. Metabolic profiling of aniseed EO.....	19
3.3. Secoisolariciresinol diglucoside (SDG) extraction from flaxseed.....	26
3.4. Molecular docking.....	26

3.4.1. Selection of protein targets	27
3.4.2. Binding energies, sites, and interactions.....	34
3.5. Molecular dynamics (MD) simulation.....	73
3.6. Absorption, Distribution, Metabolism, Excretion and Toxicity (ADMET) profiles of the most promising compounds.....	79
3.7. Qualitative and quantitative analysis of the inhibitory ability of the aniseed and flaxseed EO and their bioactive components.....	84
3.7.1. Qualitative analysis of aniseed and flaxseed EO for inhibition of <i>S. sonnei</i> growth.....	84
3.7.2. Quantitative analysis of <i>S. sonnei</i> growth inhibition by aniseed and flaxseed EO.....	85
3.7.3. Qualitative and quantitative analysis of the most promising compounds from aniseed and flaxseed.....	93
3.7.4 Mode of action	101
3.8. The bioactive compounds.....	102
CHAPTER 4.0 Conclusion.....	104
REFERENCES.....	105

LIST OF FIGURES

<u>Figure</u>	<u>Page</u>
Figure 1. The shikimate pathway and genes encoding each enzyme.....	6
Figure 2. Pictorial representation of the T3SS.....	7
Figure 3a and b. Anise plant and anise seeds.....	10
Figure 4a and b. Flax plant and flax seeds.....	11
Figure 5. GC-MS spectrum of aniseed EO showing time on the x-axis and relative abundance on the y-axis.	20
Figure 6. Protein sequence and structures employed for in silico analysis.....	27
Figure 7. 3D and 2D interactions of ligands with their respective controls in the active sites of the proteins.....	56
Figure 8. RMSD and RMSF of ligand-protein complex.....	74
Figure 9. Agar disc diffusion assay of aniseed and flaxseed EO.	84
Figure 10. MIC assay of aniseed EO dissolved in DMSO.....	86
Figure 11. MIC assay of aniseed EO dissolved in Tween 20.....	88
Figure 12. Histogram showing the growth rate of <i>S. sonnei</i> at decreasing concentrations of aniseed EO + 1% Tween 20.....	91
Figure 13. Histogram showing the growth rate of <i>S. sonnei</i> at decreasing concentrations of flaxseed EO + 1% tween 20.....	93
Figure 14. A and B show the zones of growth inhibition by antibiotic control, ceftriaxone, and cefuroxime respectively.....	94
Figure 15. Chemical structures of most promising antimicrobial agent from aniseed and flaxseed	102

LIST OF TABLES

<u>Table</u>	<u>Page</u>
Table 1. Protein targets and their sources.....	14
Table 2. Constituents of aniseed EO. The phytochemicals are arranged in descending order of the percent area of peaks from the GC-MS spectrum.....	21
Table 3. Binding affinities and interactions of ligands with protein targets.....	32
Table 4. ADMET profiles of most promising compounds from aniseed and flaxseed...81	
Table 5. Qualitative result of EO from aniseed and flaxseed.....	85
Table 6. Minimum inhibitory assay of aniseed EO.....	90
Table 7. Minimum inhibitory assay of flaxseed EO.....	92
Table 8. Minimum inhibitory assay of ampicillin.....	96
Table 9. Minimum inhibitory assay of p-anisaldehyde.....	97
Table 10. Minimum inhibitory assay isoeugenol.....	98
Table 11. Minimum inhibitory assay of anethole.....	99
Table 12. Minimum inhibitory assay of SDG.....	100
Table 13. Minimum inhibitory concentrations of most promising compounds against <i>S. sonnei</i>	100
Table 14. Minimum bactericidal concentrations of EO and phytochemicals.....	101

CHAPTER 1

INTRODUCTION

1.1. Shigellosis

Diarrheal diseases are one of the major public health problems caused by pathogenic bacteria, viruses, and parasites (Schroeder and Hilbi. 2008). Of the causes of diarrhea, 5-15% of cases are attributed to *Shigella* spp. *Shigella* spp are Gram-negative, non-spore-forming, and rod-shaped bacteria, which belong to the Enterobacteriaceae family (Shahin et al. 2019). These bacteria cause a disease known as shigellosis (dysentery) which is characterized by fever, diarrhea (watery or bloody), abdominal pain and abundant leukocytes, blood and mucus in the stool (Koffloff et al., 2018). There are four different types of *Shigella* spp: *S. dysenteriae*, *S. flexneri*, *S. boydii*, and *S. sonnei*. *S. flexneri* and *S. sonnei* serotypes are responsible for 90% of the occurrences of this disease. While shigellosis originates from *S. flexneri* in small and middle-income countries (Kahsay et al. 2016; Kottloff et al. 2018; Livivo et al. 2014), it originates from *S. sonnei* in high-income countries (Bovee et al. 2012; Cohen et al. 2014; Kottloff et al. 2018). Shigellosis is highly contagious and there are many reasons for its incidence worldwide. According to the World Health Organization (WHO), every year there are 700,000 deaths from 80 million cases of shigellosis with ~56 million cases and ~420,000 deaths occur among children less than five years of age (WHO, 2022). *Shigella* can be transmitted through contaminated food, water, and flies. Malnutrition is one of the causes of the emergence of *Shigella* infection and, as a result, this infection is commonly seen in low and middle-income countries (Khalil et al. 2018; Platts et al. 2017; Rogawski et al. 2018). However, people in high income countries are not safe from contracting this infection and this can be because of people who travel to regions where the infection is endemic which causes it to spread to other areas (Cohen et al. 2001; Porter et al. 2017). Owing to its low infective dose (10-100 bacteria), the disease can spread rapidly, making prevention of bacteria spread an imperative task in containing the infection (WHO, 2022).

The WHO in 2014 announced shigellosis as a global crisis (WHO, 2014) not only for its threats to the public health, but also because of the economic burden. This is

because it has become more difficult to get a successful result from treatment and this lengthens the duration of hospitalization (Shahin et al. 2020). *Shigella* has inevitably evolved to develop resistance of the current antibiotics in use, thereby restricting the options of treating shigellosis and reducing the success rate of treatment (Baker et al. 2018; Gu et al. 2012; Kottloff et al. 2018).

Over the years, *Shigella* has significantly increased its resistance to antibiotics and emerged to be a multi-drug resistant bacterium. As of March 2022, nine European countries, Italy, Spain, Austria, Belgium, Denmark, France, Ireland, Norway, and Germany have reported new cases of drug resistant *S. sonnei* (WHO, 2022). The acquisition of resistance has occurred through mechanisms including mutations, gene transfer, efflux of the drug by efflux pumps (the bacteria's mechanism of discarding antimicrobial drugs from its cells), poor penetration of the drug, hydrolysis of the drug (Blair et al. 2015) or broad and abusive use of antibiotics. (Hajipour et al. 2012). Although over 100 types of antibiotics are available today, their effectiveness has gradually reduced towards multi-drug resistance infectious diseases (Nordmann et al. 2007). For the treatment of *Shigella* infection, a list of antibiotics has been administered with sulphonamides being the first antibiotics used in intravenous treatment (Hardy, 1946). Afterwards, tetracycline, chloramphenicol, ampicillin, and co-trimoxazole were used (Haltalin and Nelson, 1965). As a matter of fact, ampicillin was the first line of oral therapeutic treatment of shigellosis (Haltalin et al. 1967). However, due to observed resistance to these antibiotics, nalidixic acid and fluoroquinolones were then administered in succession, but *Shigella* has also developed resistance against these compounds (Haltalin et al. 1973). Today WHO recommends the use of ciprofloxacin, as the first line treatment, and ceftriaxone, pivmecillinam, or azithromycin as alternative therapy for shigellosis (Taneja and Meware 2016; Williams and Berkley 2018). Ceftriaxone is administered in severe cases of shigellosis (Ud-Dine et al. 2013; Afronze et al. 2017). Sadly, drug resistance against ceftriaxone and azithromycin has been reported in some regions (Rahman et al. 2007). The current WHO guidelines for treatment of shigellosis are based on region specific antibacterial resistance patterns (Williams and Berkley, 2018). Thus, ciprofloxacin or azithromycin is administered in regions with a prevalence of the ampicillin resistant strain. Likewise, in regions with azithromycin resistant strains, ceftriaxone or ampicillin are administered. In Bangladesh, for example, 70% of *Shigella* isolates are resistant to ciprofloxacin so azithromycin is administered in treatment of shigellosis (Ud-Dine et al. 2013; Afronze et al. 2017).

Resistance to antimicrobial drugs is one of the most critical concerns of public health. As a result, much research has been done to discover and develop novel antibacterial alternatives (Hyde et al. 2019). However, the conventional method of drug discovery and development is time-consuming, risky, and laborious. This method generally involves the generation of large libraries of compounds and high-throughput virtual screen of bioactivity. On average, development of a new drug is estimated to take more than 15 years and US\$2.8 billion in recent years (Fleming, 2018). Even then, the attrition rate of drugs is as high as 96% (Paul et al. 2010). The reason for this low success rate is because of poor drug efficacy and failure to fulfill the required absorption, distribution, metabolism, excretion, and toxicity (ADMET) criteria (Giri and Bader. 2015). Therefore, a better approach to lessen the time, labor and cost issues faced by the conventional approach is required in developing drugs against shigellosis.

1.2. Computer-aided drug discovery (CADD)

Computer-aided drug discovery (CADD) provides a functional alternative method through modelling and docking (Billones et al. 2017). This approach includes computational identification of potential drug targets, virtual screening of large chemical libraries for effective drug candidates, further optimization of candidate compounds, and *in silico* assessment of their potential toxicity (Bilal et al. 2021). After these analyses, the potential drug candidate can be subjected to *in vitro*/*in vivo* experiments for confirmation. A good number of drugs have been brought to the market to tackle diverse diseases through this approach, including human immunodeficiency virus (HIV)-1-inhibiting drugs [atazanavir (Robinson et al. 2000), saquinavir (Krohn et l. 1991), indinavir (Chen et al. 1994, and ritonavir (Kempf et al. 1995)], anti-cancer drugs (raltitrexed, Anderson. 2003), and antibiotics [norfloxacin, (Rutenber and Stroud et al., 1996)].

Two different approaches are used in CADD: structure-based drug discovery (SBDD) (Jhoti and Leach. 2007) and ligand-based drug discovery (LBDD) (Vidal et al. 2011). SBDD involves identification of a target protein which is usually obtained experimentally by nuclear magnetic resonance analysis or X-ray crystallography (Jhoti and Leach. 2007) and investigating the binding abilities and stability of compounds with the protein. There are two major computational modelling approaches employed here. These are molecular docking and molecular dynamic simulation. Molecular docking is

employed to screen ligands based on their binding affinities to the receptor (protein target). Usually during the docking process, the receptor is made rigid while the ligand's conformation is slightly remodeled and strategically analyzed for its binding affinities to different grooves or regions in the protein. In contrast, during molecular dynamic simulation, the receptor is made flexible. The fundamental idea behind molecular dynamic simulation is that the macromolecule (target protein) is provided with an identical environment as that found in nature (in water or lipid bilayer). Then, the ligand is added to react with the protein. Here, unlike in molecular docking where the protein is made rigid, the protein is flexible and the forces controlling its binding and dissociation kinetics to the ligand are determined (Buch et al. 2011), that is, the forces exerted on each atom of the protein by the inhibitor are determined. In addition, using Newton's law of motion, position and movement pattern of the atoms in respect to time can be captured. LBDD, on the other hand, involves the screening of compounds based on prior knowledge of active drugs to predict the biological activity of the novel compounds (Martain et al. 2002). Given the availability of the complete genome of *Shigella spp* and the primary and tertiary structures of unique proteins that are required for the survival of this organism, SBDD can help to circumvent the limitations of conventional drug discovery in identifying lead molecules that are pharmacologically active against shigellosis.

1.3. Targeting shigellosis

Targeting shigellosis strategically involves interfering with its essential metabolic pathway(s). The shikimate pathway is a good candidate because it is important for the survival of microbes, algae, and plants as it leads to the production of aromatic amino acids. The attractiveness of the shikimate pathway as an antimicrobial target goes beyond its usefulness to the bacteria as a source of aromatic amino acids. This pathway is absent in higher eukaryotic animals including humans which implies that the successful discovery of antimicrobial targets against the shikimate pathway would have no adverse effect on humans. The shikimate pathway as shown in Figure 1, is a seven catalytic step pathway for the synthesis of aromatic compounds in microorganisms, fungi, and plants. This metabolic pathway converts the metabolic substrates D-erythrose 4-phosphate and phosphoenolpyruvate to chorismate and ultimately leads to the synthesis of phenylalanine, tyrosine, and tryptophan (Herrmann 1995; Knagg., 2003). A few studies

have been carried out on the shikimate pathway as targets for drug design. Ahmad et al. (2018) worked on in silico identification of potential inhibitors against shikimate kinase from *S. sonnei*. Similarly, Arora et al. (2010) worked on identification of potential inhibitors against shikimate kinase from *Shigella flexneri* via in silico analysis. Apart from shigellosis, treatment of other diseases has been investigated by targeting the shikimate pathway. Kumar et al. (2010) and Reichau et al. (2011) reported studies on in silico identification of anti-tuberculosis drugs. Similarly, Tapas et al. (2011) worked on the structural analysis of chorismate synthase in the discovery of antimalaria drugs.

Interfering with the shikimate pathway would inevitably impede the bacteria's ability to synthesize aromatic amino acids. This would invariably affect the bacteria's ability to survive let alone carry out pathogenesis.

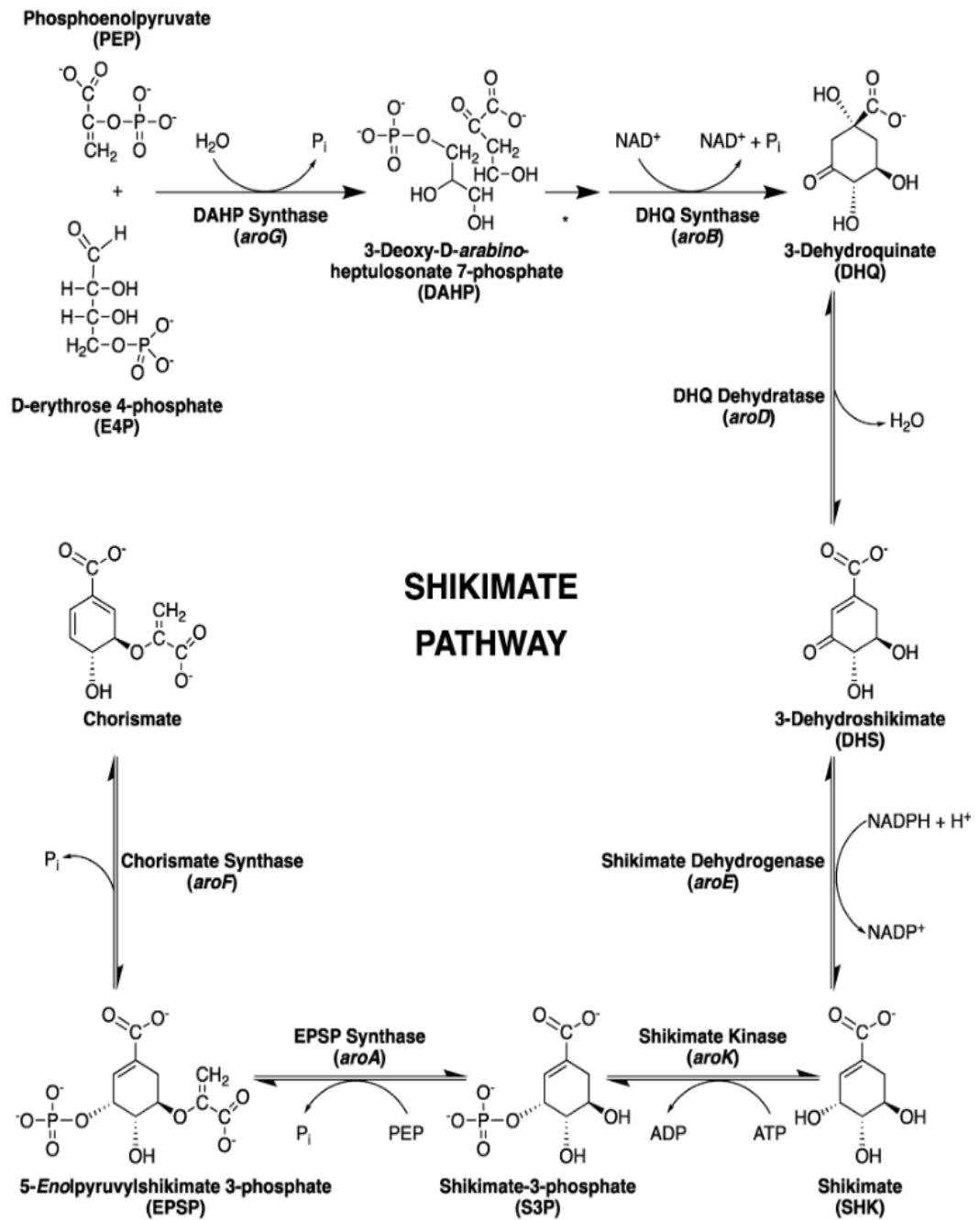


Figure 1. The shikimate pathway and genes encoding each enzyme (Nunes et al. 2020).

As a result of *Shigella* species' resistance to multiple antibiotics, another enticing solution is to target its virulence proteins. These proteins are responsible for the bacteria's ability to disrupt its host defense and cause disease. Anti-virulence drugs would stop or slow infection while exerting minimal selective pressure (Keyser et al. 2008). The Type III secretion system (T3SS) is a notable anti-virulence target. *Shigella spp* and many other important Gram-negative bacterial pathogens use T3SS to initiate contact with eukaryotic

cells to manipulate those cells for the benefit of the pathogen (Galan et al. 2018). *Shigella* invasion and pathogenesis is dependent on a complex T3SS which includes effector proteins that are secreted into the host cell and the needle-like structural system which induces the effector transfer (Carayol and Nhieu. 2013). The T3SS can be broken down into five major regions as shown in Figure 2. The translocon is a protein hexamer pore that is formed in the host cell membrane and allows secreted proteins to pass into the host (Nissim-Eliraz et al. 2017; Browne et al. 2008; Berube et al. 2017; Marteyn et al 2010). The part responsible for puncturing the cells (Zhang et al. 2016) is called the needle. The basal body anchors the needle to the cell surface (Bergeron et al. 2019). Lastly, the export apparatus and cytoplasmic complex work together in sorting, guiding and powering secretion (Bernal et al., 2019). The export apparatus and cytoplasmic complex receive effectors from chaperone proteins and unfold the effectors for secretion as folded proteins and function as a recognition domain for the effectors (Steven et al., 2014; Duncan et al. 2012; Minamino et al. 2019). Primarily, secretion of the effector through the T3SS is powered by the ATPase of the cytoplasmic complex (Bernal et al. 2013; Majewski et al., 2019; Case and Dickenson, 2018). Strategic interference of the *Shigella spp* T3SS ATPase can reduce the secretion of effector proteins to the host cells, thereby promoting host cell defense against *Shigella*.

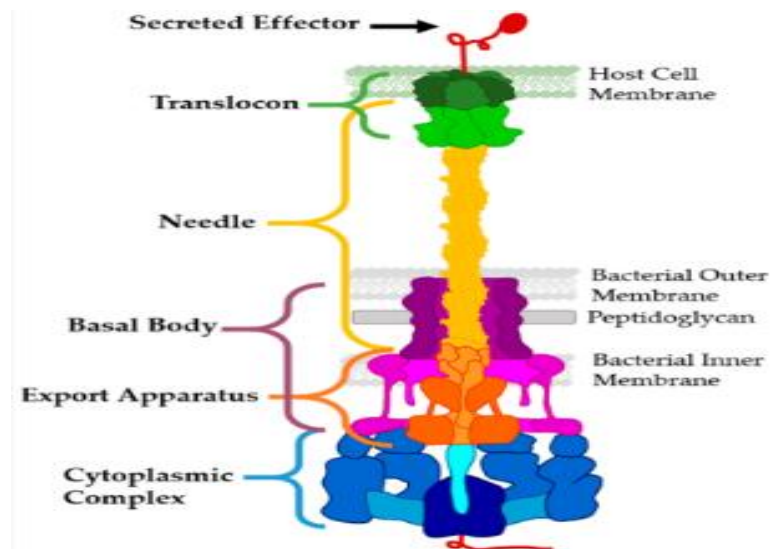


Figure 2. Pictorial representation of the T3SS (Wagner and Diepold. 2020).

1.4. Plant-based drugs

Having identified the enzymes of the shikimate pathway and T3SS ATPase as the antimicrobial targets for this study, it is crucial to identify compounds capable of inhibiting their biological activity. Medicinal plants have received significant attention due to their abilities in treating many diseases which can be attributed to diversity in their chemical composition (Gullece et al. 2006; Maregesi et al. 2008). Plant essential oils and their components are powerful potential antimicrobial agents (Cowan et al. 1999; Gyawali and Ibrahim 2014; Jeon et al. 2017; Tepe et al. 2005). Research suggests that plants contain potent antimicrobial compounds which, unlike synthetic antimicrobial compounds, are easily accessible, minimize drug resistance developed by bacteria, are low cost and have fewer side effects (Cowan et al. 1999; Gyawali and Ibrahim 2014; Jeon et al. 2017; Tepe et al. 2005). A few studies have been done on the investigation of plant-based antimicrobials in the treatment of shigellosis. Jeong et al. (2018) reported antimicrobial activity of 4-methoxysalicylaldehyde isolated from *Periploca sepium* oil. Similarly, Medina-Galván et al. (2018) reported the antimicrobial effect of flower scape extracts of *Agave salmiana*. In the same vein, Oyedeji-Amusa and Ashafa (2019) reported the antimicrobial activity of whole fruit extracts of *Nauclea latifolia* against shigellosis. Pacheco-Cano et al. (2017) described the antimicrobial activity of broccoli (*Brassica oleracea*) cultivar Avenger against pathogenic bacteria. Pereira et al. (2018) also indicated the antimicrobial activities of *Aristolochia triangularis* against shigellosis.

1.4.1. Aniseed

Aniseed (*Pimpinella anisum*) (Figure 3a and 3b) belongs to the Apiaceae family and has diverse bioactivities including antioxidant (Odeh and Allaf et al. 2017; Rebey et al. 2019), antifungal (Özcan 2005, Yutani et al. 2011; Vieira et al. 2019), antibacterial (see below), antiviral (e.g. Shukla 1989), anticancer [e.g. triple-negative breast cancer (Sumathi et al. 2018); fibrosarcoma (Choo et al. 2011)], antidiabetic (e.g. Shobha et al. 2013), analgesic (e.g. Tas 2009), and insecticidal (e.g. Erler et al. 2006; Lee 2004; Park et al. 2006; Prajapati et al. 2005) activities. It is also used as a growth promoter for broiler chickens (Ciftci et al. 2005). In terms of aniseed's antibacterial effects, Ahmed et al. (2019) reported its effect against *Salmonella typhimurium*, *Escherichia coli*, *Bacillus*

cereus and *Staphylococcus aureus*. Gulcin et al. (2003) reported its antimicrobial effect on *Pseudomonas aeruginosa*, *Escherichia coli*, *Proteus mirabilis*, *Citrobacter koseri*, *Enterobacter aerogenes*, *Staphylococcus aureus*, *Streptococcus pneumoniae*, *Micrococcus luteus*, *Staphylococcus epidermidis*, and *Candida albicans*. Ibrahim et al. (2017) reported aniseed's effect on *Staphylococcus spp.*, *Streptococcus spp.*, *Escherichia coli*, *Klebsiella spp.*, *Acinetobacter spp.* and *Pseudomonas spp.* Sağdıç and Özcan (2003) also reported the effects of aniseed on *Bacillus amyloliquefaciens*, *B. brevis*, *B. cereus*, *B. subtilis* var. *niger*, *Enterobacter aerogenes*, *Escherichia coli*, *Klebsiella pneumoniae*, *Proteus vulgaris*, *Salmonella enteritidis*, *S. gallinarum*, *S. typhimurium*, *Staphylococcus aureus*, *S. aureus*, and *Yersinia enterocolitica*.

1.4.2. Flaxseed

Flaxseed (*Linum usitatissimum*) (Figure 4a and b), which belongs to the Linaceae family, has been reported to show antioxidant, Hepatitis C antibody (Barbary et al., 2010), antifungal (Basma et al. 2018), anticancer (Franklyn and Jane, 2019) and antimicrobial activities. More specifically, flaxseed has activity against *Porphyromonas gingivalis*, *Aggregatibacter actinomycetemcomitans* and *Tannerella forsythia* (Badiger et al. 2019), *Staphylococcus aureus*, *Streptococcus agalactiae*, *Enterococcus faecalis*, *Micrococcus luteus*, *Bacillus subtilis*, *Bacillus pumilus*, *Staphylococcus epidermidis*, *Escherichia coli*, *Lactobacillus sporogenes*, *Bacillus brevis*, *Bacillus cereus*, *Pseudomonas aeruginosa* and *Candida* (Kaithwas et al. 2011). Similarly, Alahmad et al. (2018) investigated the antimicrobial effect of flaxseed on *Streptococcus mutans*, *Streptococcus pyogenes* and *Pseudomonas aeruginosa*. Hussein and Aziz (2021) also reported the antimicrobial effect of flaxseed against *Shigella flexneri*, *Salmonella typhimurium* and *Escherichia coli*. Additionally, Barbary et al. (2010) reported the antimicrobial activity of flax lignans against *Shigella flexneri*, *Salmonella typhimurium* and *Escherichia coli*. The major phytochemical in flaxseed is a lignin, secoisolariciresinol (SECO), which is present in the form of the diglucoside (i.e., secoisolariciresinol diglucoside SDG) (Dobbins and Wiley. 2004) and has been reported to have therapeutic effects including antioxidant activities, decreased tumor growth, reduction of serum cholesterol levels and decreased formation of breast, prostate, and colon cancers (Hosseini et al. 2006; Prasad.

1997; Prasad. 2002; Zhang et al. 2008; Penumathsa et al. 2008; Bloedon et al. 2008). However, there is no report about the main bioactive components in aniseed and flaxseed and their possible antimicrobial effects against *Shigella sonnei*.

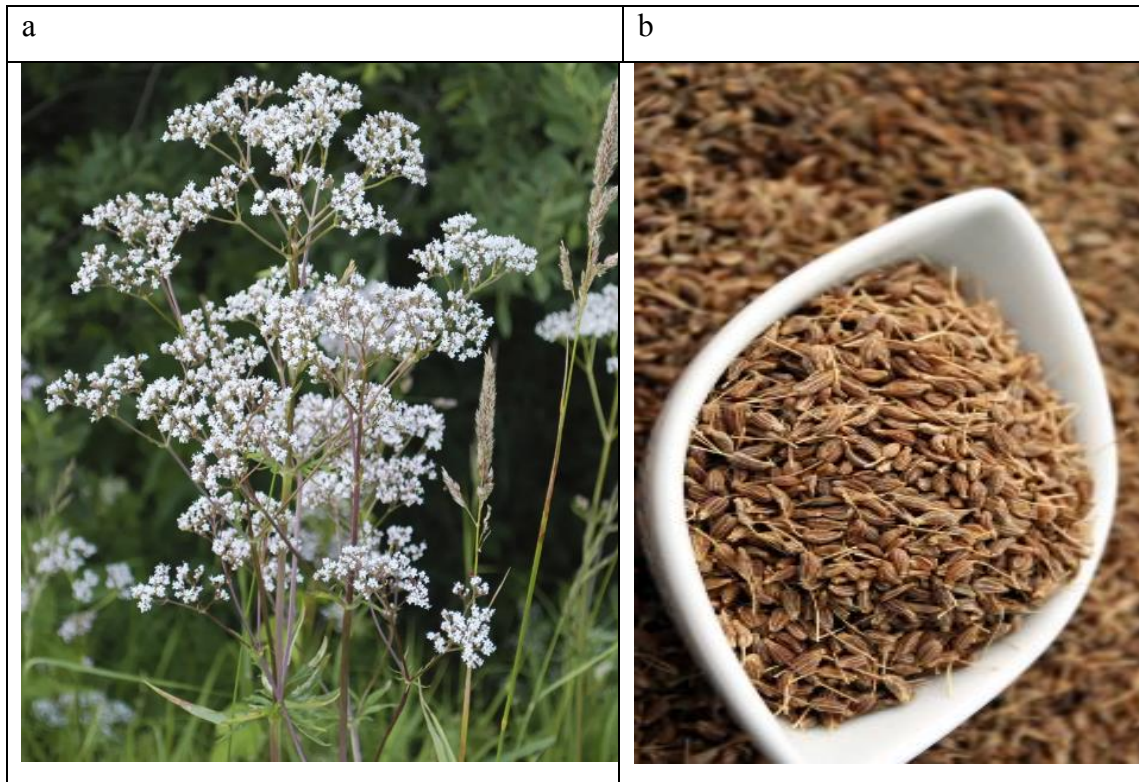


Figure 3a and b. Anise plant and seeds, respectively (The Encyclopedia Britannica, 2023).

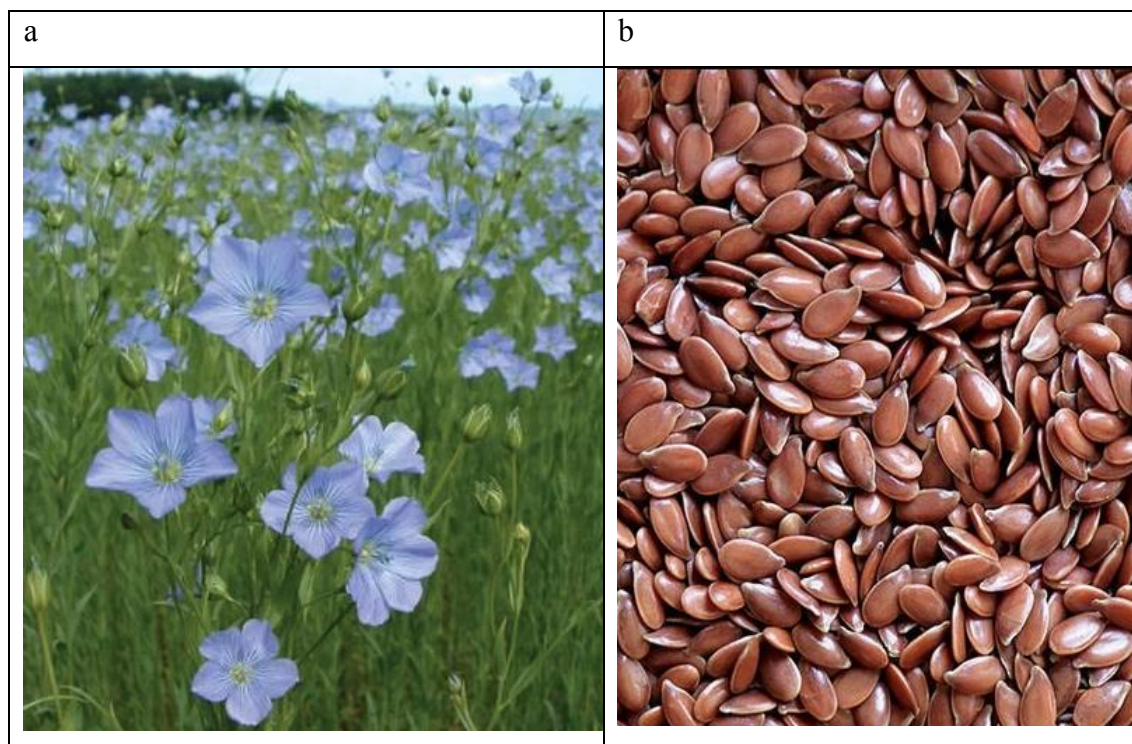


Figure 4a and b. Flax plant and flax seeds (Downloaded from seedman's.com).

1.5. Aim of the study

The aim of this study was to identify the chemical constituents of aniseed oil and flaxseed oil and investigate their pharmacodynamic potentials by inspecting their binding affinities with specific molecular targets-- the enzymes of the shikimate pathway and T3SSATPase. The potential drug candidate compounds which were expected to bind with high affinity to *Shigella* target proteins that play crucial roles in the bacterium's survival and pathogenesis were further screened for their ability to form a stable complex with the target proteins through molecular dynamic simulation studies. The ADMET features of the stable compounds with their targets were inspected to detect cases of poor drug bioavailability and toxicity. Furthermore, the most promising compounds were tested against *Shigella sonnei* in vitro to determine their minimum inhibitory and minimum bactericidal concentrations. Ultimately, it is hoped that this research can lead to a new plant-based drug candidate active against shigellosis, which causes thousands of deaths every year.

CHAPTER 2

METHODS AND MATERIALS

2.1. Collection and identification of plant samples

The commercially purchased aniseed (unknown cultivar) and Sari Dane cultivar flaxseed were collected from Aegean Agricultural Research Institute.

2.2. Extraction of essential oil from seeds of plant samples

Initially, the plant seeds were milled to a fine powder in an Emir ‘ogutucu makinesi’ grinder, then the essential oil was extracted. The extraction of essential oil from ground plant samples was performed by an automatic Soxhlet device. The Soxhlet apparatus conditions were adjusted as follow: extraction temperature 45°C, reduction interval 3 min, reduction pulse 2 sec, hot extraction 45 min, evaporation A 1x interval, rinsing time 1 h 20 min, evaporation B 3x interval and evaporation C 2 min. The extraction solvent was recovered, and the essential oil was then placed in a vacuum concentrator for complete evaporation of the solvent. The extraction yield of essential oil was determined.

2.3. Gas chromatography-mass spectrometry (GC-MS) analysis of the essential oil of aniseed

GC-MS analysis of essential oil of aniseed was performed on an HP-5 MS capillary column (5% phenylmethyl polysiloxane, 30 m, 0.25 mm i.d., 0.1 µm film thickness). The temperature program was adjusted as follows: 5 min at 60°C, 4°C/min up to 220°C, 11°C/min up to 280°C, held for 15 min, for a total run of 65 min. Helium was used as the carrier gas (1 mL/min). The mass range was 29–400 m/z and mass spectra were recorded at 70 eV. Peaks were analyzed with TurboMass software (PerkinElmer

Inc.) and searched within the National Institute of Standards and Technology (NIST) library to identify the compounds.

2.4. Extraction of secoisolariciresinol diglucoside (SDG) from flaxseed

GC-MS analysis of flaxseed was not carried out due to the great number of reports on its prominent phytochemical: secoisolariciresinol diglucoside (Imran et al. 2015). Secoisolariciresinol diglucoside (SDG) is the main dietary lignan present in flaxseed (Frank et al. 2004) and it was extracted using the protocol reported by Johnson et al. (2000). Briefly, 10 g of flaxseed was milled into fine powder and then defatted with hexane for 1 h under magnetic stirring for 1 h. Then, 5 g of the defatted material was extracted with 70 mL of ethanol/water (80:20, v/v) for 4 h at 55 °C in a shaking water bath and then concentrated to 10 mL. The concentrated ethanolic extract was subjected to acid hydrolysis with 1M HCl for 1 h at 95°C.

2.5. Molecular docking analysis and molecular dynamics (MD) simulations

2.5.1. Preparation of ligands for molecular docking

The structural data formats (SDF) of each component of aniseed obtained from the GC-MS analysis were retrieved from Pubchem (Kim et al. 2019). Their energies were minimized and then they were converted to a dockable format (PDBQT) using Open Babel (O'Boyle et al. 2011).

2.5.2. Preparation of molecular targets for molecular docking

A total of eight proteins were utilized as molecular targets, seven of which are the enzymes of the shikimate pathway and one of the crucial enzymes of the Type III secretion system as described in Table 1. Due to the absence of experimentally generated structures of the enzymes from *Shigella sonnei*, a sequence alignment was carried out

using NCBI-Blast and protein structures of *Escherichia coli* k12 strain were selected from the protein data bank (PDB) due to sequence identify > 90%. However, for enzymes 3-dehydroquinate synthase, 3- dehydroquinate dehydratase and chorismate synthase, Alphafold, an artificial intelligence program, was used to predict their structures from their sequences due to lack of sequence similarity and coverage with the available experimentally generated structures of the enzymes. The 3D crystal structure of each protein was retrieved, bound ligands were removed, the structures were cleaned and ready for molecular docking.

Table 1. Protein targets and their sources.

Protein	source	Reference
3-Deoxy-d-arabino-heptulosonate 7-phosphate (DAHP) synthase	PDB ID: 5CKS	Balanchandran et al., 2016
3-Dehydroquinate synthase	Alphafold	Jumper et al. 2021
3-Dehydroquinate dehydratase	Alphafold	Jumper et al. 2021
Shikimate dehydrogenase	PDB ID: 1NYT	Michel et al. 2003
Shikimate kinase	PDB ID: IKAG	Romanowski and Burley 2002
5-Enolpyruvylshikimate 3-phosphate (EPSP) synthase	PDB ID: 1G6S	Schonbrunn et al. 2001
Chorismate synthase	Alphafold	Jumper et al. 2021
T3SS ATPase	PDB ID: 5YBH	Gao et al. 2018

2.5.3 Molecular docking with protein targets

Docking studies of the phytochemicals that were present at > 0.10% abundance (as revealed from the GC-MS of aniseed oil) were performed by Autodock vina (Trott and Olson, 2010) with the protein targets. Similarly, docking studies were performed with the same program for SDG, secoisolariciresinol (SECO), enterolactone and enterodiol from flaxseed. Enterolactone and enterodiol are the product of bacteria metabolism of SECO in mammals' gut (Borriello et al. 1985). Although the prominent lignan in flaxseed is SDG, its monomeric form and mammal phytoestrogens were investigated in silico for their antimicrobial activity to determine the bioactive form of secoisolariciresinol against shigellosis. For each protein target studied, the respective substrate or coenzyme was used as control to compare its binding affinity to that of each selected ligand. Polar hydrogen bonds were added to the proteins while the Gasteiger charges were computed (Gasteiger and Marsili. 1980). Water and all other non-amino acids residues were removed and a cubic docking box in which the entire protein structure fits was employed. Autodock vina uses a hybrid scoring function that applies empirical and knowledge-based function bases (Trott and Olson. 2010). This scoring function is a simulated annealing, genetic algorithm, and particle swarm optimization which makes up the stochastic global optimization approaches (Trott and Olson. 2010) and was used to perform automated docking of each of the proteins with each of the ligands. The target proteins were kept rigid while the torsion bonds and side chains of the ligands were allowed to rotate freely.

2.5.4. Virtual screening

The compound's binding site to the proteins and types of interactions between the protein's amino acid residues and ligands were investigated by Discovery Studio Visualizer (BIOVIA 2015). Each enzyme's substrate or co-enzyme binding site to the protein was used as control and the strength of the interactions between the amino acid residues and ligands was used as the screening criterion.

2.5.5. Molecular dynamic (MD) simulations

2.5.5.1. Preparation of ligand–protein complexes for MD

Crystal structure of proteins as drug targets were prepared using USCF Chimera (Eric et al. 2004). Initially, all the non-amino acid compounds, water molecules, and ions were removed from the downloaded structures and then the Gasteiger charges were added (Gasteiger and Marsili. 1980). For each complex, Charmm27 Forcefield (Vanommeslaeghe et al. 2010) was used for both protein and ligand. Prior to the complex formation, the PDB structure of the ligands with the best binding conformations and energies were selected and polar hydrogens were added. This was then converted to MOL2 structure using Avogadro software (Hanwell et al .2012). Swissparam was used in the generation of ligand topology (Zoete et al. 2011). The generated ligand coordinate was then added to the protein coordinate to form the protein-ligand complex.

2.5.5.2 MD simulation of ligand-protein target

To analyze the structural stability of the receptor-ligand complexes which were selected based on molecular docking studies, GROMACS 2022.6 software was used for MD simulations (Berendsen et al. 1995; Abraham et al. 2015) with the CHARMM27 force field (Bjerkmar et al. 2010; Vanommeslaeghe et al. 2010). Protein-ligand complexes were solved using TIP3P water; a MD simulation water model selected based on the force field employed (Jorgensen et al. 1983) in a dodecahedral box. After the neutralization of the system by addition of appropriate amount of sodium ions, MD simulation of each ligand–protein complex was performed in four consecutive stages: (1) energy minimization, (2) canonical ensemble (NVT) heating, (3) isothermal–isobaric (NPT) equilibration, and (4) production simulation. Energy minimization was performed using a steepest-descent gradient method for a maximum of 50,000 steps. Isothermal-isochloric (NVT) ensemble and isothermal-isobaric ensemble (NPT) were utilized in restraining each complex for 100 ps. Temperature was maintained at 310 K with a modified Berendsen thermostat (Berendsen et al. 1984), and pressure at 1.0 bar with the Parrinello-Rahman barostat (Parrinello and Rahman, 1980). LINCS algorithm was used to constrain

the bond lengths (Hess et al. 1997), and particle-mesh Ewald scheme (PME) (Darden et al. 1993) was used for long-range electrostatic forces calculation.

Visual Molecular Dynamic Simulation 1.9.3 (Humphrey et al. 1996) and USCF Chimera (Pettersen et al. 2004) were used to visualize the molecular dynamics trajectories. The root mean square deviation (RMSD) and root mean square fluctuation (RMSF) were determined for the protein backbone residues and the ligand within the binding site of the simulated system to decipher the protein-ligand stability.

2.6. ADME and toxicity analysis

The compounds which formed stable complexes with the protein targets as revealed by the MD simulation studies were further screened based on their ADMET (absorption, distribution, metabolism, excretion and toxicophore) properties using the Admetlab program (Xiong et al. 2021).

2.7. Antimicrobial test

Antibacterial activities of the essential oils from aniseed and flaxseed were tested using simple agar diffusion according to Alkowni et al. (2018) and Baron et al. (1990), against a *S. sonnei* strain [ATCC 9290]. A Mueller-Hinton agar medium plate which contains beef extract, acid casein hydrolysate, starch, and agar, was gently swabbed with bacterial suspension of 1.5×10^8 CFU/ml from a 24-hour old bacterium colony grown on Mueller-Hinton agar. Different concentrations of aniseed, flaxseed oil or the identified promising antimicrobial agent was added to a 6 mm sterile filter paper placed in the plate. The plates were then incubated for 16–18 h at 37°C and the antibacterial activity was evaluated by measuring the diameter of clear zones surrounding the sample.

The minimal inhibitory concentrations (MIC) of the aniseed oil, flaxseed oil and promising antimicrobial agents from the plant samples against the bacteria were determined using the micro-broth dilution method. Mueller-Hinton broth (MHB) was used for this test in a polystyrene plate containing 96 wells including sterility control (just the Mueller-Hinton broth) and growth control (Mueller-Hinton broth + bacteria without

the antimicrobial agent). Different starting concentrations of aniseed, flaxseed oil or the identified promising antimicrobial agent were added to the first wells which already contain 100 μ l MHB and then serially diluted with MHB in the remaining wells. The bacteria at concentration 5×10^5 CFU/ml were then added. The plate was covered and incubated at 35°C for 16–20 h before analysis of the results using a micro plate reader at an absorbance of 600 nm. Each of the experiments was carried out in three biological replicates and each value reported represented the average of the three different replicates \pm standard deviation (SD).

CHAPTER 3

RESULTS AND DISCUSSION

3.1. Percentage yield of essential oil (EO) from aniseed and flaxseed

A yield of 11% (v/w) essential oil was obtained from the commercially purchased aniseed (unknown cultivar) using the Soxhlet extraction technique. The EO yield obtained from flaxseed (Sari Dane cultivar) was 28% (v/w).

3.2. Metabolic profiling of aniseed EO

GC-MS technique was used to analyze the chemical constituents of aniseed EO. The mass spectra were 70 ev and each of the peaks was analyzed with Turbomass software. Table 2 summarizes the phytochemicals identified by comparing the constituents' spectra with the National Institute of Standards and Technology (NIST) mass spectral library. The GC-MS spectra showed 111 phytochemicals as shown in Figure 5. Out of these phytochemicals, anethole (39.11%), linoleic acid (16.49%), elaidic acid (10.05%), 3,4-dimethoxystyrene (4.98%), thellungianin g (2.47%) and cis-(-)-2,4a,5,6,9a-hexahydro-3,5,5,9-tetramethyl(1h) benzocycloheptene (2.20%) were the major phytochemicals (Table 2). In contrast to this study, Iannarelli et al. (2018) reported anethole (97.9%), methyl chavicol (1.7%) and γ -himachalene (0.3%) as the major phytoconstituents of aniseed. Similarly, Samajlik et al. (2012) reported anethole (88.49%), γ -himachalene (3.43%), cis-isoeugenol (1.99%) and linalool (1.79%) as major phytoconstituents of aniseed. In contrast to the 39.11% anethole reported in this work, many studies (Orav et al. 2008; Rodrigues et al. 2003; Ondarza and Sanchez. 1990; Santos et al. 1998; Chouksey et al., 2010; Dzamic et al., 2009; Tuan and Ilangantileket, 1997; Ozcan and Chalchat, 2006) reported higher concentrations of anethole (more than 80%) in aniseed. Anethole is a phenylpropanoid and phenylpropanoids are synthesized via the shikimate pathway as protectants against harm, UV light and herbivores (Schmid and Amrhein, 1995). The shikimate pathway can be compromised using herbicides, for

example, glyphosate inhibits the sixth enzyme of the shikimate pathway (Nuria de Maria et al. 2006). Although application of herbicide protects maximal crop production, the production of secondary metabolites e.g., phenylpropanoid could be impeded. This may be the reason for the low quantity of anethole observed in the aniseed used in this study as it was purchased commercially, and it is unknown if chemical control was used during its growth. Of the detected phytochemicals, 36 were present at less than 0.10% and were not considered for further study (Table 2).

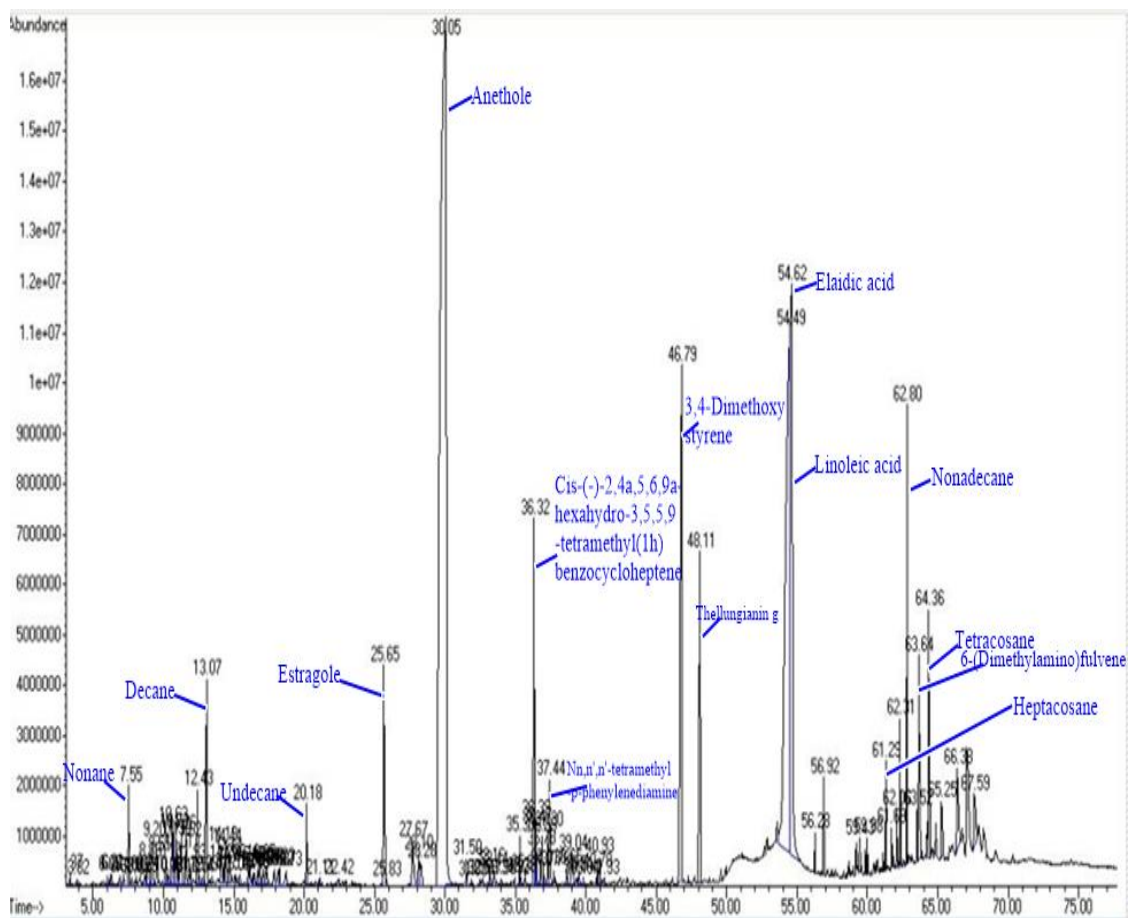


Figure 5. GC-MS spectrum of aniseed EO showing time on the x-axis and relative abundance on the y-axis. Retention time (RT) of major aniseed phytochemicals indicated.

Table 2. Constituents of aniseed EO. The phytochemicals are arranged in descending order of the percent area of peaks from the GC-MS spectrum.

Compound name	Pubchem CID	Rt (min)	Area %	Molecular formula	Molecular weight g/mol
Anethole	637563	30.05	39.11	C ₁₀ H ₁₂ O	148.20
Linoleic acid	5280450	54.49	16.49	C ₁₈ H ₃₂ O ₂	280.4
Elaidic acid	637517	54.63	10.05	C ₁₈ H ₃₄ O ₂	282.5
3,4-Dimethoxystyrene	61400	46.79	4.98	C ₁₀ H ₁₂ O ₂	164.20
Thellungianin g	545130	48.11	2.47	C ₁₅ H ₂₀ O ₄	264.32
Cis-(-)-2,4a,5,6,9a-hexahydro-3,5,5,9-tetramethyl(1h) benzocycloheptene	564747	36.32	2.20	C ₁₅ H ₂₄	204.35
Nonadecane	12401	62.80	1.56	C ₁₉ H ₄₀	268.5
Decane	15600	13.07	1.51	C ₁₀ H ₂₂	142.28
6-(Dimethylamino)fulvene	136523	63.64	1.41	C ₈ H ₁₁ N	121.18
Estragole	8815	25.65	1.40	C ₁₀ H ₁₂ O	148.20
Tetracosane	12592	64.36	0.94	C ₂₄ H ₅₀	338.7
Adrenaline tetraacetate	536776	66.38	0.93	C ₁₇ H ₂₁ NO ₇	351.4
Nn,n',n'-tetramethyl-p-phenylenediamine	7490	37.44	0.70	C ₁₀ H ₁₆ N ₂	164.25
2(1h) Naphthalenone, 3,5,6,7,8,8a-hexahydro-4,8a-dimethyl-6-(1-methylethenyl)-	612605	67.59	0.68	C ₁₅ H ₂₂ O	218.33
1,2,3-Trimethylbenzene	10686	12.43	0.64	C ₉ H ₁₂	120.19
Undecane	14257	20.17	0.61	C ₁₁ H ₂₄	156.31
Nonane	8141	7.55	0.53	C ₉ H ₂₀	128.25

D-carvone	16724	27.67	0.52	C ₁₀ H ₁₄ O	150.22
3-Methylnonane	22202	11.27	0.49	C ₁₀ H ₂₂	142.28
1-Ethyl-2-methylbenzene	11903	10.63	0.44	C ₉ H ₁₂	120.19
2,6,10,14,18-Pentamethyl-2,6,10,14,18-eicosapentaene	5366013	62.32	0.43	C ₂₅ H ₄₂	342.6
4-Methylnonane	28455	10.73	0.41	C ₁₀ H ₂₂	142.28
Bicyclo[4.2.0]octa-1,3,5-triene-7-carboxylic acid	302324	56.92	0.41	C ₉ H ₈ O ₂	148.16
3-(3,4-dimethoxyphenyl)propanenitrile	319932	65.25	0.41	C ₁₁ H ₁₃ NO ₂	191.23
4-Hydroxy-3-methoxyphenylacetone	17262	39.04	0.33	C ₁₀ H ₁₂ O ₃	180.20
Germacrene D	5317570	36.39	0.31	C ₁₅ H ₂₄	204.35
Alpha-curcumene	92139	36.47	0.30	C ₁₅ H ₂₂	202.33
Anethole	637563	28.10	0.30	C ₁₀ H ₁₂ O	148.20
1-Ethyl-2-methylbenzene	11903	11.62	0.29	C ₉ H ₁₂	120.19
2-Methylnonane	13379	10.90	0.29	C ₁₀ H ₂₂	142.28
Heptacosane	11636	61.29	0.29	C ₂₇ H ₅₆	380.7
4-Methyldecane	17835	14.44	0.28	C ₁₁ H ₂₄	156.31
Beta-bisabolene	10104370	37.30	0.27	C ₁₅ H ₂₄	204.35
Hemimellitene	10686	14.13	0.27	C ₉ H ₁₂	120.19
Octane, 2,6-dimethyl-	16319	9.20	0.27	C ₁₀ H ₂₂	142.28
P-anisaldehyde	31244	28.28	0.25	C ₈ H ₈ O ₂	136.15
Zingiberene	92776	36.89	0.23	C ₁₅ H ₂₄	204.35
Alpha,2,4,5-tetramethylstyrene	94566	11.01	0.23	C ₁₂ H ₁₆	160.25
Alpha-himachalene	11830551	35.30	0.23	C ₁₅ H ₂₄	204.35

3-Ethyl-2-methylheptane	139803	9.55	0.23	C ₁₀ H ₂₂	142.28
Propylcyclohexane	15505	8.88	0.20	C ₉ H ₁₈	126.24
1-Methyl-2-propylbenzene	14091	16.15	0.19	C ₁₀ H ₁₄	134.22
Ent-spathulenol	13854255	40.93	0.19	C ₁₅ H ₂₄ O	220.35
5-Methyldecane	93071	16.85	0.18	C ₁₁ H ₂₄	156.31
P-cymene	7463	18.73	0.18	C ₁₀ H ₁₄	134.22
Octacosane	12408	62.06	0.18	C ₂₈ H ₅₈	394.8
Benzene, propyl	7668	10.16	0.17	C ₉ H ₁₂	120.19
M-menthane, (1s,3r)-(+)-	101946252	11.93	0.17	C ₁₀ H ₁₈ CIN O ₂	219.71
Methyl isoeugenol	637776	36.78	0.17	C ₁₁ H ₁₄ O ₂	178.23
D-limonene	440917	14.62	0.16	C ₁₀ H ₁₆	136.23
Benzoicyclobutyl-1-carboxylic acid	302324	56.28	0.16	C ₉ H ₈ O ₂	148.16
Octadecane	11635	63.52	0.16	C ₁₈ H ₃₈	254.5
2-Ethyl-m-xylene	17877	18.23	0.15	C ₁₀ H ₁₄	134.22
Decane, 3-methyl	101671334	17.88	0.14	C ₁₁ H ₂₄	156.31
1-Methyl-4-propylbenzene	14095	17.24	0.14	C ₁₀ H ₁₄	134.22
Eugenol	3314	14.76	0.14	C ₁₀ H ₁₂ O ₂	164.20
M-cymene	10812	14.25	0.14	C ₁₀ H ₁₄	134.22
8-Ethyl-6-oxa-3,12-diazapentacyclo [9.7.0.02,8.05,7.01 3,18] octadecal(11),2,13, 15,17-pentaene	22295473	59.43	0.14	C ₁₇ H ₁₈ N ₂ O	266.34
Isoeugenol	853433	17.38	0.13	C ₁₀ H ₁₂ O ₂	164.20
4-Ethyl-1,2-dimethylbenzene	13629	18.12	0.13	C ₁₀ H ₁₄	134.22
Delta-elemene	89316	31.50	0.13	C ₁₅ H ₂₄	204.35

4-Ethyl-1,2-dimethylbenzene	13629	16.70	0.12	C ₁₀ H ₁₄	134.22
2,4,6-Trimethylheptane	137658	8.36	0.12	C ₁₀ H ₂₂	142.28
4-Ethyl-1,2-dimethylbenzene	13629	16.70	0.12	C ₁₀ H ₁₄	134.22
1,3-Diethylbenzene	8864	16.03	0.11	C ₁₀ H ₁₄	134.22
Linalool	6549	16.46	0.11	C ₁₀ H ₁₈ O	154.25
4-Methyldecane	17835	17.08	0.11	C ₁₁ H ₂₄	156.31
4-Ethylphenyl 4-methoxybenzoate	346059	38.65	0.11	C ₁₆ H ₁₆ O ₃	256.30
Diisooctyl phthalate	33934	61.69	0.11	C ₂₄ H ₃₈ O ₄	390.6
Tetradecane	12389	15.44	0.10	C ₁₄ H ₃₀	198.39
Anisketone	31231	33.16	0.10	C ₁₀ H ₁₂ O ₂	164.20
Bis(2-ethylhexyl) phthalate	8343	59.98	0.10	C ₂₄ H ₃₈ O ₄	390.6
2,5-Dimethyloctane	139988	8.74	0.09	C ₁₀ H ₂₂	142.28
3-Ethyl-2-methylhept-2-ene	140589	12.79	0.08	C ₁₀ H ₂₀	140.27
Himachalene	11586487	37.01	0.08	C ₁₅ H ₂₄	204.35
Cyclohexylmesitylene	608751	39.51	0.08	C ₁₅ H ₂₂	202.33
M-xylene	7929	7.17	0.07	C ₈ H ₁₀	106.16
2,5,6-Trimethyldecane	112466	10.29	0.07	C ₁₃ H ₂₈	184.36
4-Ethyloctane	85925	10.38	0.07	C ₁₀ H ₂₂	142.28
2-Phenylbutane	8680	16.39	0.07	C ₁₀ H ₁₄	134.22
Durene	7269	21.11	0.07	C ₁₀ H ₁₄	134.22
2,5-Dimethylheptane	16662	6.31	0.06	C ₉ H ₂₀	128.25
P-xylene	7809	6.22	0.06	C ₈ H ₁₀	106.16
2-Methyloctane	18591	6.04	0.06	C ₉ H ₂₀	128.25

3-Ethyl-3-methylpentane	14018	8.08	0.06	C ₈ H ₁₈	114.23
1-Methyl-3-propylcyclohexane	138178	11.79	0.06	C ₁₀ H ₂₀	140.27
Pentylcyclopentane	19540	15.08	0.06	C ₁₀ H ₂₀	140.27
Beta-sesquiphellandrene	12315492	37.76	0.06	C ₁₅ H ₂₄	204.35
Apiol	10659	40.78	0.06	C ₁₂ H ₁₄ O ₄	222.24
1-Ethyl-4-methylcyclohexane	19503	6.92	0.05	C ₈ H ₁₀	126.24
1-Ethyl-4-methylcyclohexane	19503	7.75	0.05	C ₉ H ₁₈	126.24
Cumene	7406	8.65	0.05	C ₉ H ₁₂	120.19
1-Methyl-2-propylcyclohexane	107252	12.55	0.05	C ₁₀ H ₂₀	140.27
2-Phenylbutane	8680	13.47	0.05	C ₁₀ H ₁₄	134.22
3-Methyl-hexatriene	141124	22.42	0.05	C ₇ H ₁₀	94.15
Elemene	10583	33.44	0.05	C ₁₅ H ₂₄	204.35
Toluene	1140	3.37	0.04	C ₇ H ₈	92.14
Trans-beta-farnesene	5281517	35.67	0.04	C ₁₅ H ₂₄	204.35
Methyl-3,5-dimethoxybenzoate	75074	39.40	0.04	C ₁₀ H ₁₂ O ₄	196.20
1-Methylcyclopentanol	73830	3.82	0.03	C ₆ H ₁₂ O	100.16
Dodecane	8182	25.83	0.03	C ₁₂ H ₂₆	170.33
Longipinene	12311396	31.88	0.03	C ₁₅ H ₂₄	204.35
Hexamethylbenzene	6908	32.51	0.03	C ₁₂ H ₁₈	162.27
Ylangene	20055075	32.68	0.03	C ₁₅ H ₂₄	204.35
Alpha-bergamotene	86608	34.92	0.03	C ₁₅ H ₂₄	204.35
4'-Methoxypropionone	67144	35.38	0.03	C ₁₀ H ₁₂ O ₂	164.20

1,7,7-Trimethyl-2-vinyl bicyclo[2.2.1]hept-2-ene	576719	39.85	0.03	C ₁₂ H ₁₈	162.27
Alpha-cedrene	6431015	41.33	0.03	C ₁₅ H ₂₄	204.35

3.3. Secoisolariciresinol diglucoside (SDG) extraction from flaxseed

GC-MS analysis of flaxseed was not carried out due to the great number of reports on its prominent phytochemical: secoisolariciresinol diglucoside (Imran et al. 2015). Secoisolariciresinol diglucoside (SDG) is the main dietary lignan present in flaxseed (Frank et al. 2004). The potential therapeutic impacts of SDG as an anti-cancer (Jenab and Thompson, 1996), anti-diabetic (Prasad, 2011; Prasad, 2009; Prasad, 2007; Peterson et al. 2010) and cardiovascular protector (Zhang et al. 2008) agent have been studied. Moreover, SDG's effects on liver necrosis (Fukumitsu et al. 2010), kidney diseases (Ogboron et al. 2016), mental stress and immunity (Spence et al. 2003; Ma et al. 2013; Rhee et al. 2007) have also been examined. SDG was extracted from flaxseed and its antimicrobial potency was investigated *in silico* and *in vitro*. The percentage yield of SDG was 6% (w/w).

3.4. Molecular docking

Molecular docking was performed to get detailed information about ligand-receptor binding affinities. Aniseed phytochemicals that were present in EO at a concentration of at least 0.10% based on GC-MS analysis were analyzed. Although SDG is the form of secoisolariciresinol lignan present in flaxseed, its monomer, secoisolariciresinol (SECO), and its mammalian phytoestrogens, enterodiol and enterolactone, were also investigated. These four compounds from flaxseed were analyzed for their antimicrobial activity to understand the bioactive form of flaxseed lignan against *S. sonnei*. The protein targets were seven enzymes of the shikimate pathway and Type III secretion system ATPase (T3SS ATPase). Compounds with binding affinity of ≤ -5 kcal/mol were visualized by Discovery Studio Visualizer (Biovia 2015).

3.4.1. Selection of protein targets

Due to the absence of experimental crystallized structures of the *S. sonnei* protein targets in the Protein Data Bank (PDB), selection of protein target structures was based on the extent of protein sequence coverage in *S. sonnei*. Protein structures from *Escherichia coli* (*E. coli*) k12 strain and *Shigella flexneri* were selected because they have the highest protein sequence identity (>90%) with *S. sonnei* which suggests highly similar structures. For T3SS ATPase (PDB ID:5YBH), 3-deoxy-d-arabinoheptulosonate 7-phosphate (DAHP) synthase (PDB ID: 5CKS), shikimate dehydrogenase (SDHase) (PDB ID: 1NYT), shikimate kinase (SK) (PDB ID: 1KAG) and 5-enolpyruvylshikimate-3-phosphate (EPSP) synthase (PDB ID: 1G6S) were selected. Alpha fold prediction was used for 3-dehydroquinase synthase (DHQS), 3-dehydroquinase dehydratase (DHQH) and chorismate synthase (CS), due to the absence of similar protein structures.

SHISO	MSYTKLLTQLSFPNRISGPILETSLSDVSIQAGIESNEIVARAQVVGHFHDEKTI	60
SHIFL	MSYTKLLTQLSFPNRISGPILETSLSDVSIQAGIESNEIVARAQVVGHFHDEKTI	60

SHISO	LSLIGNSRGLSRQTLIKPTAQFLHTQVGRLLGAVVNPLGEVTDKFAVTDNSEILYRPVD	120
SHIFL	LSLIGNSRGLSRQTLIKPTAQFLHTQVGRLLGAVVNPLGEVTDKFAVTDNSEILYRPVD	120

SHISO	NAPPLYSERAAIEKPFLTGIKVIDSLLTCGEGQRMGIFASAGCGKTFMNMNLIHSGADI	180
SHIFL	NAPPLYSERAAIEKPFLTGIKVIDSLLTCGEGQRMGIFASAGCGKTFMNMNLIHSGADI	180

SHISO	YVIGLIGERGREVTETVDYLNSEKKSRCVLYVYATSDYSSVDRCNAAIATAIAEFFRTE	240
SHIFL	YVIGLIGERGREVTETVDYLNSEKKSRCVLYVYATSDYSSVDRCNAAIATAIAEFFRTE	240

SHISO	GHKVALFIDSLTRYARALRDVALAAGESPARRGYPVSVFDSLPRLLERPGKLGAGGSITA	300
SHIFL	GHKVALFIDSLTRYARALRDVALAAGESPARRGYPVSVFDSLPRLLERPGKLGAGGSITA	300

SHISO	FYTVLLEDDDFADPLAEVRSILDGHIYLSRNLAQKGFPAIDSLKSISRVTQVVDEKH	360
SHIFL	FYTVLLEDDDFADPLAEVRSILDGHIYLSRNLAQKGFPAIDSLKSISRVTQVVDEKH	360

SHISO	RIMAAAFRELLSEIEELRTHIDFGEYKPGENASQDKIYNKISVVESFLKQDYRLGFTYEQ	420
SHIFL	RIMAAAFRELLSEIEELRTHIDFGEYKPGENASQDKIYNKISVVESFLKQDYRLGFTYEQ	420

SHISO	TMELIGETIR	430
SHIFL	TMELIGETIR	430

A. T3SS ATPase- Sequence alignment of *S. sonnei* and *Shigella flexneri*.

SHISO	MNYQNDDLRIKEIKELLPVALLEKFPATENAANTVAHARKAIHKILKGNDRLLVVIGP	60
ECOLI	MNYQNDDLRIKEIKELLPVALLEKFPATENAANTVAHARKAIHKILKGNDRLLVVIGP	60

SHISO	CSIHDPVAAKEYATRLALREELKDELEIVMRVYFEKPRTTVGWKGLINDPHMDSFQIN	120
ECOLI	CSIHDPVAAKEYATRLALREELKDELEIVMRVYFEKPRTTVGWKGLINDPHMDSFQIN	120

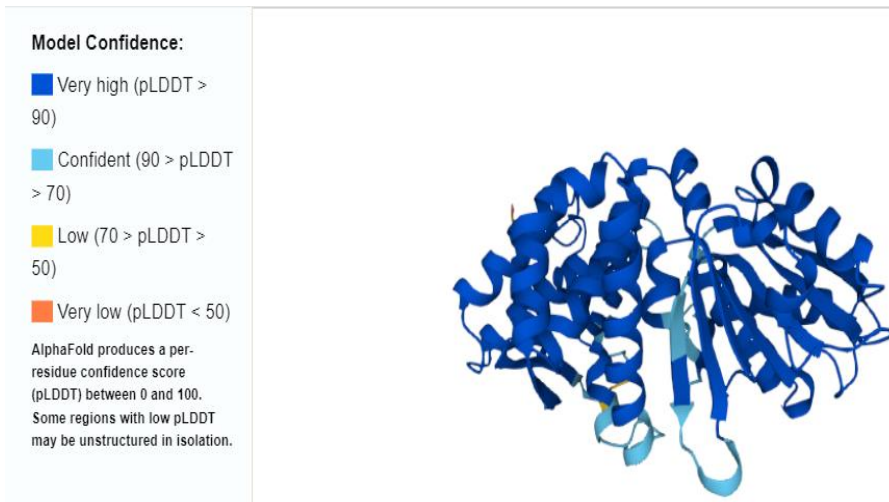
SHISO	DGLRIARKLLLNDINDSGLPAAGEFLDMITPQYLADLMSWGAIGARTTESQVHRELASGLS	180
ECOLI	DGLRIARKLLLNDINDSGLPAAGEFLDMITPQYLADLMSWGAIGARTTESQVHRELASGLS	180

SHISO	CPVGFKNGTDGTIKVAIDAINAAGAPHCFLSVTKWGHSAIVNTSGNGDCHIILRGGKEPN	240
ECOLI	CPVGFKNGTDGTIKVAIDAINAAGAPHCFLSVTKWGHSAIVNTSGNGDCHIILRGGKEPN	240

SHISO	YSAKHVAEVKEGLNKAGLPAQVMIDFSHANSSKQFKKQMDVCADVCQIAGGEKAIIGVM	300
ECOLI	YSAKHVAEVKEGLNKAGLPAQVMIDFSHANSSKQFKKQMDVCADVCQIAGGEKAIIGVM	300

SHISO	VESHLVEGNQSLDSGEPLAYGKSITDACIGWEDTDALLRQLVNAVKARRG	350
ECOLI	VESHLVEGNQSLDSGEPLAYGKSITDACIGWEDTDALLRQLANAVKARRG	350

B. 3-Deoxy-D-arabinoheptulosonate 7-phosphate (DAHP) synthase- Sequence alignment of *S.sonnei* and *E. coli* K-12.



C. Alpha fold prediction of DHQS

Model Confidence:

- Very high (pLDDT > 90)
- Confident (90 > pLDDT > 70)
- Low (70 > pLDDT > 50)
- Very low (pLDDT < 50)

AlphaFold produces a per-residue confidence score (pLDDT) between 0 and 100. Some regions with low pLDDT may be unstructured in isolation.



D. Alpha fold prediction of DHQH.

SHISO	MDVTAKYELIGLMAYPIRHSLSPMQNKALEKAGLPFTYMAFEVDNDSFPGAIEGLKALK	60
ECOLI	MDVTAKYELIGLMAYPIRHSLSPMQNKALEKAGLPFTYMAFEVDNDSFPGAIEGLKALK	60

SHISO	MRGTGVSMPNKQLACEYVDELTPAAKLVGAINIVNDDGYLRGYNTDGTGHIRAIKESGF	120
ECOLI	MRGTGVSMPNKQLACEYVDELTPAAKLVGAINIVNDDGYLRGYNTDGTGHIRAIKESGF	120

SHISO	DIKGMTVLLGAGGASTAIGAQGAIEGLKEIKLFNRRDEFFDKALAFQVRNENTDCVVT	180
ECOLI	DIKGMTVLLGAGGASTAIGAQGAIEGLKEIKLFNRRDEFFDKALAFQVRNENTDCVVT	180

SHISO	DTDLDLADQQAFAEALASADILTNGTKVGMKPLENESLVNDISLLHPGLLVTECVYNPHMTK	240
ECOLI	VTDLDLADQQAFAEALASADILTNGTKVGMKPLENESLVNDISLLHPGLLVTECVYNPHMTK	240

SHISO	LLQQAQQAGCKTIDGYGMLLWQAEQFTLWTGKDFPLEYVKQVMGFGA	288
ECOLI	LLQQAQQAGCKTIDGYGMLLWQAEQFTLWTGKDFPLEYVKQVMGFGA	288

E. Shikimate dehydrogenase- Sequence alignment of *S. sonnei* and *E. coli* K-12.

SHISS	MAEKRNI FLV GPMGAGKSTIGRQLA QQLNMEFYDSDQEIEKRTGADV G W V F D L E G E E G F R	60
ECOLI	MAEKRNI FLV GPMGAGKSTIGRQLA QQLNMEFYDSDQEIEKRTGADV G W V F D L E G E E G F R	60

SHISS	DREKVINELTEKQGIVLATGGGSVKSRETRNRLSARGVVVYLETIEKQLARTQRDKKR	120
ECOLI	DREKVINELTEKQGIVLATGGGSVKSRETRNRLSARGVVVYLETIEKQLARTQRDKKR	120

SHISS	PLLHVETPPREVLEALANERNPLYEEIADVTIRTDDQSAKVVANQIIHMLESN	173
ECOLI	PLLHVETPPREVLEALANERNPLYEEIADVTIRTDDQSAKVVANQIIHMLESN	173

F. Shikimate kinase- Sequence alignment of *S. sonnei* and *E. coli* K-12.

SHISO	MESLTLQPIARVDGTINLPGSKSVSNRALLLAALAHGKTVLTNLLDSDDVRRHMLNALTAL	60
ECOLI	MESLTLQPIARVDGTINLPGSKSVSNRALLLAALAHGKTVLTNLLDSDDVRRHMLNALTAL	60

SHISO	GLSYTLSADRTRCEIIGNGGPLHAEGALELFLGNAGTAMRPLAAALCLDSNDIVLTGEPR	120
ECOLI	GVSYTLSADRTRCEIIGNGGPLHAEGALELFLGNAGTAMRPLAAALCLGSNDIVLTGEPR	120
*.*****		
SHISO	MKERPIGHLVDALRLGGAKITYLEQENYPPLRLQGGFTGGNVDVDGVSQFLTALLMTA	180
ECOLI	MKERPIGHLVDALRLGGAKITYLEQENYPPLRLQGGFTGGNVDVDGVSQFLTALLMTA	180

SHISO	PLAPEDTVIRIKGDLVSKPYIDITLNLMTKTFGVEIENQHYQQFVVKGGQSYQSPGYLVE	240
ECOLI	PLAPEDTVIRIKGDLVSKPYIDITLNLMTKTFGVEIENQHYQQFVVKGGQSYQSPGYLVE	240

SHISO	GDASSASYFLAAAAIKGGTVKVTGIGRNSMQGDIRFADVLEKMGATICWGDDYISCTRGE	300
ECOLI	GDASSASYFLAAAAIKGGTVKVTGIGRNSMQGDIRFADVLEKMGATICWGDDYISCTRGE	300

SHISO	LNAIDMDMNHIPDAAMTIATAALFAKGTTLRNIYNWRVKETDRLFAMATELRKVGAEVE	360
ECOLI	LNAIDMDMNHIPDAAMTIATAALFAKGTTLRNIYNWRVKETDRLFAMATELRKVGAEVE	360

SHISO	EGHDYIRITPPEKLNFAEIATYNDHRMAMCFSLVALSDTPVTILDPKCTAKTFPDYFEQL	420
ECOLI	EGHDYIRITPPEKLNFAEIATYNDHRMAMCFSLVALSDTPVTILDPKCTAKTFPDYFEQL	420

SHISO	ARISQAA	427
ECOLI	ARISQAA	427

G. Shikimate kinase- Sequence alignment of *S.sonnei* and *E.coli* K-12.



H. Alpha fold prediction of CS.

Figure 6. Protein sequence and structures employed for in silico analysis. A: protein sequence alignment between *S.sonnei* T3SS ATPase and *Shigella flexneri* T3SS ATPase. B: protein sequence alignment between *S.sonnei* DAHP synthase and *E. coli* K-12 DAHP synthase. E: protein sequence alignment between *S.sonnei* shikimate

dehydrogenase and *Escherichia coli* K-12 shikimate dehydrogenase. F: protein sequence alignment between *S.sonnei* shikimate kinase and *Escherichia coli* K-12 shikimate kinase. G: protein sequence alignment between *S.sonnei* EPSP synthase and *Escherichia coli* K-12 EPSP synthase. C, D and H show Alpha fold prediction of DHQS, DHQH and CS. The confidence score of each residue is shown in different colors. Royal blue: very high confident score, sky blue: confident score, yellow: low and orange: very low.

3.4.2. Binding energies, sites, and interactions

To identify promising antimicrobial compounds from aniseed and flaxseed, their phytochemicals were individually made to interact with each of the protein targets through molecular docking. From aniseed, 94 phytochemicals were analyzed and four compounds were analyzed from flaxseed. To decipher the binding region of the compounds, the enzyme's substrate or co-enzyme was used as control. The binding affinities, hydrogen bonds, interacting amino acids and non-covalent interactions of the phytochemicals from aniseed and flaxseed with binding affinities of ≤ -5 kcal/mol were selected and are shown in Table 3. The number of compounds which met the screening criteria of binding affinity of ≤ -5 kcal/mol with the protein targets differed. For DAHP, 16 compounds from aniseed and 4 from flaxseed were identified. DHQS was the target for which the most compounds met the screening criteria: 21 compounds from aniseed and four from flaxseed. For DHQH, nine compounds from aniseed and three compounds from flaxseed were identified. For SDHase, 14 compounds from aniseed and four compounds from flaxseed were identified. For SK, 15 compounds from aniseed and four compounds from flaxseed were selected. For EPSP synthase, 16 compounds from aniseed and four from flaxseed were identified. For T3SS ATPase, only SDG from flaxseed was selected.

Table 3. Binding affinities and interactions of ligands with protein targets.

DAHP	Pubchem ID	Binding affinity(kcal/mol)	Hydrogen Bond Interactions (Å)	Non-Covalent Interactions (Å)
	3-phosphoenolpyruvate (PEP): control	-4.5	Asn120 (2.11, 2.26), Ile119 (2.48), Gln 118 (2.50), Phe 117 (1.96)	Lys 14 (5.56)
	637563	-5.8	Asn 109 (2.78)	Leu145 (4.9), Tyr 94 (4.88), Ile 108(3.67), Glu 96 (3.44)
	545130	-5.5	Gln 151 (2.88)	Ala 154 (5.28, 3.77)
	8815	-5.6	Asn 109 (2.68)	Tyr94 (4.96), Leu 145(4.70), Glu 96 (3.55), Ile 108 (3.58, 4.54)
	17262	-5.2	Ser180 (3.43), Gln 151(2.96)	Ala 154(3.69, 4.85), Leu 179 (5.09, 3.90)
	5317570	-5.7	-	-
	92139	-5.4	-	Leu16(5.15), Lys 14(4.99, 3.80), Ile 119 (4.12, 5.10)

10104370	-5.8	-	Ile148(4.99), Tyr152(4.42), Leu 123(4.44), Ile 119 (4.57, 4.35, 3.97), Leu 16(3.99, 4.96)
11830551	-5.6	-	Val221(4.83), Leu179(5.19), Pro150(5.46), Ala154(4.05)
13854255	-6.3	-	Ala154(5.38)
7463	-5.7	-	Leu145(5.02), Glu96(3.75), Ile108(3.92)
637776	-5.2	Glu 96(3.49)	Ile108(5.01), Asp146(3.64), Leu145(4.49), Glu96(3.34), Phe95(5.17)
3314	-5.6	-	Ile108(3.70), Glu96(3.38), Leu145(4.36)
853433	-5.4	Asn120(2.93,2.41,2.07), Phe117(3.73)	Lys14(5.03), Ile119(4.16), Phe117(4.03)
89316	-5.2	-	Leu16(5.09), Ile119(4.46)

346059	-6.7	Asn109(2.15)	Glu96(3.56), Ile148(4.08), Asp 146(3.78), Leu 145 (4.40), Ile 108(3.65)
31231	-6.1	Phe95(1.89), Asn 109(2.84)	Leu145(5.46), Glu96(3.29),Ile108(3.87,4. 95)
SDG	-7.3	Ala327(2.25), Gly236(2.66, 2.25), Lys186(2.29), Ala164(2.93), Glu143(2.29)	Asp326(3.77), Lys273(4.05), Arg234(1.63), Lys97(4.02), Arg99(5.28), Thr100(1.63)
Enterolactone	-7.1	Gly178(2.17,2.20), Ser180(2.90,2.16), Pro150(2.85), Gln151(2.26), Ala154(2.08), Asp 155(2.08)	Val221(5.19), Ser180(2.98), Ala154(4.77)
Enterodiol	-6.6	Ser180(2.63)	Ala154(4.24), Leu179(5.46), Ser180(1.56)
SECO	-6.3	Met147(2.26), Gln151(3.55), Ala154(2.69), Ser180(2.17)	Phe209(4.77), Val221(4.00), Asp155(4.92)

DHQS	Pubchem ID	Binding affinity(kcal/mol)	Hydrogen Bond Interactions (Å)	Non-Covalent Interactions (Å)
	NAD+	-10.1	Gly104(3.61), Asn42(3.03), Glu73(3.64, 3.30), His264(3.40), Lys76(2.74), Ser137(3.37), Asn152(2.04,2.34), Lys323(2.58), Thr 2.27(2.96)	Gly77(4.12, 4.66), Asp71(3.77), Asn 42(1.78), Glu73(4.21), His264(4.41), Lys76(4.77), Asp109(5.04), Lys142(2.61)
	637563	-5.1	-	His264(4.06), Leu132(5.03, 5.06)
	545130	-6.5	-	-
	8815	-5.1	Lys226(2.44, 2.79), Leu243(3.57)	Ala144(3.55), Lys142(3.84,3.92, 4.36), Leu243(4.65), His247(4.71)
	16724	-5.2	-	Lys142(5.11), Leu243(4.16)

17262	-5.6	Lys76(2.35, 2.92), His264(1.87), Glu177(1.94)	Leu263(4.58), His264(3.97), Leu132(4.66)
5317570	-5.7	-	Tyr158(5.48), Arg11(5.21)
92139	-6.3	-	Leu132(4.28, 5.40), Leu263(3.83), Val106(4.81), Asp71(4.69), Leu45(5.36, 5.02), Leu173(5.03), Pro174(4.76), Leu263(3.83), Leu132(4.28,5.40)
10104370	-6.2	-	Leu263(4.63,4.99), Leu45(4.11)
10686	-5	-	Phe85(3.65)
31244	-5	Trp262(3.68), Glu254(3.70), Leu263(3.40), Gly105(2.08)	Leu263(5.26), Glu177(4.95), Leu132(5.19), Thr130(2.96)
11830551	-6.5	-	Leu263(4.81), Leu132(5.32), Val106(5.05)
13854255	-7	Gly105(2.51)	Leu263(4.89)

7463	-5.2	-	Leu263(5.22), Glu177(4.80), Leu132(3.65,5.37)
637776	-5.2	Gly104(3.38), Thr130(3.37)	Glu73(4.78), Val106(3.60), Leu132(4.21)
440917	-5.3	-	-
10812	-5.2	-	Lys142 (4.39,3.99, 4.31)
853433	-6.0	Gly105 (2.62,2.03)	Val106(4.03), Glu177(4.05), Leu132(5.14)
89316	-5.7	-	Val106(3.92, 4.52), Val107(5.10)
346059	-7.3	Gly104(3.40, 3.54), Gly105(2.23), His264(2.01), Trp262(3.49)	Asp71(4.53), Leu45(4.93), Glu177(4.78), Leu173(4.86), Pro174(4.76), Thr130(2.97), Leu263(4.83,5.47)
31231	-5.4	Asn42(1.94)	Val106(5.36), Leu45(4.16), Val106(5.36), Gly105(3.89)

SDG	-6.5	Arg95(2.07,1.95), Gly121(2.08), Tyr158(2.99), Arg11(2.58), Ser12(2.04), Pro160(3.00)	Arg123(4.07,4.87)
Enterolactone	-7.1	Arg308(2.40), Gly306(2.53), Trp262(1.87)	Pro303(5.15,3.81,4.17), Arg308(5.18), Glu309(3.61)
Enterodiol	-6.2	Met153(3.25), Ala156(1.78)	Lys323(4.85,4.32), Lys142(4.91), Phe157(4.51)
SECO	-6.2	Trp262(3.52), Asn261(2.79), Glu266(2.73)	Arg308(5.20), Glu309(3.77), Pro303(5.22), Trp262(4.23,3.87)

DHQH	Pubchem ID	Binding affinity(kcal/mol)	Hydrogen Bond Interactions (Å)	Non-Covalent Interactions (Å)
	3-dehydroquinate	-5.2	Gly14(2.30), Gln192(1.94), Gly220(2.58,2.65), Gly216(2.72), Gly217(2.52), Pro16(3.04)	-
	545130	-5.0	Tyr37(3.47), Ala24(3.48), His51(2.45)	His51(4.83), Lys230(3.97,4.64,4.20), Lys229(3.89), Met23(5.72), Arg29(4.22)
	5317570	-5.2	-	Phe118(4.69), Lys85(4.08)
	92139	-5	-	Phe118(3.53,5.11), Ly85(5.39,5.22)
	10686	-5.5	-	Arg82(5.50,4.51), Ala233(4.62,4.45), Met203(4.78), Ala233(4.45,4.62), Phe225(3.64,5.34)
	11830551	-5.2	-	-
	13854255	-5.3	Gly216(2.00)	-
	10812	-5.0	-	Val58(4.91), Ala99(4.47), Ala96(4.36,3.63), Ile92(4.73)

853433	-5.1	Gly14(2.04, 2.72), Ser 221(3.36)	Met 1(4.53), Ala 196(4.02), Ile 200(3.90), Pro16(3.72), Ala 222 (5.43)
346059	-5.4	Arg159(2.19)	Arg159(5.30,4.80,4.16), Lys160(5.04,3.63)
SDG	-6.6	Glu39(2.27), Arg38(2.45), Thr71(2.60), Met72(3.30), Glu74(3.41),Asp43(2.09),Phe42 (2.74,2.59),Asp41(1.93),Arg243 (2.63)	Pro73(4.24), Glu74(2.78), Asp8(1.97),Lys75(5.39)
Enterolactone	-5.8	Phe145(2.25), His143(2.09,2.72), Asp144(3.70),Asn142(2.08)	Lys85(3.71,4.92)
SECO	-5.1	Ala84(3.54), Lys85(3.58,3.03), Phe145(2.25),Asp144(3.30,3.65) ,Arg157(2.60)	Lys85(4.73,4.87)

SDHase	Pubchem ID	Binding affinity(kcal/mol)	Hydrogen Bond Interactions (Å)	Non-Covalent Interactions (Å)
	NADP+	-10	Thr61(2.05)	Asp102(4.69), Phe214(5.04), Ile192(4.56),Val62(5.14), Ala130(4.31),Asp10(4.63), Lys65(5.47)
	3-Dehydroshikimate	-6.6	Lys65(2.37), Asn86(2.94), Gln244(3.04)	-
	637563	-5.1	-	Ala130(4.08), Met213(5.24), Lys65(3.78), Val62(3.79,4.40,3.93)
	545130	-7	Gln244(3.50), Asn86(3.75), Val60(3.47), Thr61(3.40)	Leu241(5.00)
	16724	-5.6	Asn86(2.11)	Leu241(4.89)
	17262	-5.9	Gln244(2.76, 3.57), Ser14 (2.69), Ser16(2.11)	Leu241(4.74)
	5317570	-6.8	-	Phe214(4.98), Val 62(5.20)

92139	-6.3	-	Met240(4.41), Leu241(4.32), Tyr215(5.23), Met213(5.09), Phe214(4.84,5.34), Ile192(5.20)
10104370	-5.9	-	Val62(4.82,4.86), Phe214(5.23), Met213(4.77), Ile192(3.74), Ala130(4.67)
10686	-5.3	-	Leu136(4.17), Pro137(4.75,4.11,4.38), Ala82(4.13),Arg78(4.86,3. 30,4.43)
637776	-5.5	Val60(3.79)	Ile11(4.99), Tyr215(5.18), Leu241(4.37,5.25)
10812	-5.2	-	Leu241(5.48)
346059	-6.7	Thr188(3.51)	Phe214(5.43,4.78), Met213(4.94)
31231	-5.1	Gly129(2.75,1.93)	Ala130(4.81), Val62(5.10), Ser189(4.07), Phe214(5.26)

853433	-6.0	Gly105(2.62,2.03)	Leu132(5.14), Val106(4.03), Glu177(4.05)
3314	-5.8	-	Met240(4.41), Leu241(4.94)
SDG	-7.9	Thr151(2.48), Arg150(1.97,2.63,2.48,1.81), Ser189(3.66), Ala187(3.13), Gly129(2.54),Ala130(3.66), Asp212(2.76),Met213(2.79)	Pro63(5.48), Lys65(5.14)
Enterolactone	-6.6	Val60(2.38), Asn86(2.46), Gly237(2.33), Tyr215(2.70)	-
Enterodiol	-7.9	Gly55(2.97), Thr46(2.31), Arg35(2.72)	Ala49(5.31), Phe50(4.63), Val36(5.12)
SECO	-7.0	Thr188(2.81), Asp102(3.72)	Pro10(4.37), Ala130(3.73), Met240(4.97), Met213(4.75)

SK	Pubchem ID	Binding affinity(kcal/mol)	Hydrogen Bond Interactions (Å)	Non-Covalent Interactions (Å)
	ATP	-8.0	Ala112(2.72), Gly14(2.39,2.26), Ala15(2.33),Gly16(2.28),Lys17(2.24),Ser18(1.79),Thr19(2.35)	Thr19(2.86), Lys109(5.31)
	Shikimate	-6.1	Pro12(2.82), Gly16(2.18),Lys17(2.16,3.45),Ser18(2.89),Asp34(2.63),Asp36(2.17)	Pro121(2.84)
	637563	-5.0	Ser18(1.81), Lys17(2.93)	Leu123(4.39),Lys17(3.86, 5.08)
	545130	-6.1	Asp34(3.23), Asp36(3.58), Ala79(3.54), Thr80(3.38),Lys17(2.80),Ser18(2.20),Gly14(2.17)	Ala76(4.13),Lys17(5.19,3.82),Met13(5.00),Leu122(4.06)
	16724	-5.1	Ala15(2.31),Gly16(1.94),Lys17(2.20,2.41)	Ala79(4.32),Pro121(5.42)
	3314	-5	Lys17(2.84,3.67),Ser18(1.94,2.51,2.69)	Lys17(4.25,5.47),Met13(3.87),Leu122(4.74)
	5317570	-5.5	-	-

31244	-5.0	Lys17(2.19),Gly16(2.20),Ala15(2.19),Gly14(2.44),Met13(2.41,3.01)	Leu122(4.93), Met13(5.04,3.85)
11830551	-5.6	-	Met13(4.31,5.07),Leu122(4.81)
13854255	-6.1	-	-
7463	-5.2	-	Ile167(4.38),Leu28(4.99), Glu3(3.31),Leu170(3.94)
637776	-5.4	Ser18(1.98,2.86)	Ser18(2.91),Lys17(3.99,5.35,4.23),Ala79(3.24),Leu123(4.14)
10812	-5.3	-	Glu3(2.41),Val99(4.43),Leu170(3.75,4.67,3.61),Ile167(4.43),Leu28(4.66)
89316	-5.0	-	Lys109(5.33)
346059	-6.1	Gly14(2.52),Asp34(3.44),Ala79(3.69),Thr80(3.55)	Ala79(3.86),Ly17(4.55,5.43),Met13(4.26,3.48),Leu122(4.93)
31231	-5.3	Gly14(2.38),Ala15(2.41),Gly16(2.13),Lys17(2.21,2.25),Leu123(1.93)	Leu122(4.97),Met13(3.78,5.14)

853433	-5.2	Lys17(2.87),Ser18(1.87,2.56,2.62)	Lys17(5.41,4.19),Met13(4.21),Leu122(4.20)
SDG	-7.4	Gln110(2.10),Lys109(2.40),Ala112(3.01),Gly14(3.56),Met13(2.37),Lys17(2.08,3.68),Ser18(2.64), Pro121(2.16,3.30,2.25)	Leu122(3.64),Met13(4.20,3.51)
Enterolactone	-6.2	Thr114(3.69),Pro121(1.94),Ser18(3.61)	Met13(3.63), Leu122(5.28,5.11)
Enterodiol	-5.7	Lys73(2.37),Thr71(2.31),Arg5(2.20), Asn6(2.63)	Arg97(4.38),Arg5(4.69),Lys4(5.03)
SECO	-6.5	Val125(2.20) His124(2.61),Ly17(2.56),Gly14(2.59),Thr114(3.52)	Met13(4.96,3.43)

EPSP synthase	Pubchem ID	Binding affinity(kcal/mol)	Hydrogen Bond Interactions (Å)	Non-Covalent Interactions (Å)
	PEP	-4.4	Ser269(2.07,2.48), Glu240(3.63), Asp292(2.08)	Asp292(5.02), Ser269(2.57, Glu240)
	3-Phosphoshikimate	-5.0	Asn17(2.28,2.68), Asp415(2.29)	Asp46(5.43), Asp415(4.28,5.47)
	545130	-5.1	Asp46(3.78), Asp415(3.44)	Asp (4.47)
	16724	-5.1	-	Pro19(4.24)
	17262	-5.5	Asn43(3.34,2.84)	Asn43(2.53), Thr71(3.81),Pro19(4.81)
	5317570	-5.7	-	Pro19(5.12)
	92139	-5.2	-	Lys209(4.51), Met208(4.56),Ile215(4.33) ,Leu205(5.38,4.43,3.96),A sn206(2.34)

10104370	-5.0	-	Phe324(5.16), Leu374(4.57), Pro370(5.44)
10686	-5.1	Gln171(3.43)	Tyr200(3.74)
11830551	-6.0	-	Leu205(4.87,4.79,3.95), Ile215(4.41), Lys209(4.89)
13854255	-6.6	Leu18(2.48)	Pro19(4.80)
7463	-5.3	-	Pro19(4.68)
10812	-5.4	-	Pro19(4.36), Asp415(3.90),Pro414(5.21)
89316	-5.9	-	Met208(4.77), Leu205(3.98,3.86),Ile215(4.43)
346059	-5.6	-	Pro19(4.56), Asp46(3.67),Asp415(3.70) ,Pro414(5.13,4.60)
853433	-5.2	Asp46(2.77)	Asp46(2.38), Asp415(4.05), Pro19(4.26,5.17)

3314	-5.3	Val213(2.43)	Lys209(4.21), Leu205(3.57), Tyr220(5.34)
31244	-5.0	Pro19(2.68), Asp46(2.74)	Pro19(4.36), Pro414(5.40, 3.81), Asp415(3.42)
SDG	-6.6	Asp292(2.07), Thr71(3.25,3.26), Thr263(3.22), Leu18(2.78), Asn1 7(3.65)	Thr263(2.70), Leu18(2.62)
Enterolactone	-6.5	-	Gly20(2.58)
Enterodiol	-5.5	Pro371(2.07)	Leu374(2.35,5.18)
SECO	-5.4	Arg298(2.14), Ile255(3.46,3.66), Glu372(1.85,2 .42)	Leu374(4.20), Lys373(5.19)

CS	Pubchem ID	Binding affinity(kcal/mol)	Hydrogen Bond Interactions (Å)	Non-Covalent Interactions (Å)
	FMN	-7.6	Arg125(2.76,2.92,2.64), Asn238(2.46), Glu130(2.28),Arg134(2.68),His 232(2.50,3.01)	Glu130(4.01,4.16), Arg134(3.65,3.87),Thr14(2.21)
	EPSP	-6.3	His320(3.69), Ser296(2.82), Arg327(2.22), Lys293(2.58), Tyr95(2.09)	Arg59(5.49), Arg103(3.61), Ser296(2.99)
	545130	-6.4	Ile298(3.65), Gly200(3.59)	Ile298(5.43), Pro322(4.30),Arg319(3.87) ,Lys197(4.83)
	8815	-5.0	-	Ala128(4.12,5.08), Arg(4.25),Pro50(.36),Arg5 9(4.23),Arg327(3.50)
	16724	-5.4	-	Arg125(4.50), Tyr111(5.18)
	17262	-6.0	Arg47(2.79),Gly155(2.55,2.25)	Glu174(4.17),Val173(4.85) ,Arg154(3.75)
	5317570	-6.2	-	Arg125(5.45),Tyr115(3.69)
	92139	-6.2	Asn238(3.29)	Ala107(107),Ala239(4.08, 4.84),Ala128(3.91),Val324

			(4.89,3.66),Arg327(4.35),Ile331(5.35)
10104370	-5.6	-	Val354(4.44),Arg348(4.09),Phe149(5.09,5.41),Pro215(4.82)
10686	-5.0	-	Arg125(5.31),Tyr115(4.10,3.81)
31244	-5.0	Arg48(2.10,1.88),Arg129(3.58),Arg327(2.18),Asp321(3.56),His320(3.68)	His320(5.23),Asp321(4.77),Arg327(3.61),Arg59(4.02)
11830551	-6.5	-	Arg125(4.14),Tyr115(3.90,4.36),Leu117(5.02)
13854255	-6.9	Ser126(1.95)	Ala239(4.86),His106(4.90)
7463	-5.2	-	Arg125(5.03),Tyr115(4.26,384),Met1(4.79)
637776	-5.2	Asp119(1.99,2.73),Gly123(3.50)	Leu117(4.10),Tyr115(4.71,4.36),Arg125(4.98,5.30),Tyr111(4.56)
3314	-5.8	Arg47(2.85),Glu333(1.76)	Arg154(3.76),Val173(4.82),Glu174(4.19)

10812	-5.4		
853433	-5.9	Gly155(2.22,2.23),Ile153(3.67)	Arg154(4.71,3.76),Val173(4.72)
89316	-5.5	-	Lys143(4.53),Ala146(3.86),Lys142(4.26)
346059	-6.0	Lys142(2.67),Ser171(3.48)	Arg154(4.90),Lys142(4.35,5.09,4.08),Glu174(3.47)
31231	-5.2	Thr56(3.64),Thr299(2.41,2.62)	Pro322(4.90),Lys197(4.57)
6549	-5.1	Leu196(2.57)	Arg319(4.61,4.12),Pro322(5.16,4.26),Ile298(5.49),Lys197(4.53)
SDG	-6.6	Asn271(1.97),Gln285(2.08),Gly246(2.27),His289(2.35),Lys206(2.15),Leu165(3.31)	Ile287(5.38),Val210(4.97),Ile167(4.84,4.51),Trp170(4.58),Asn271(5.20),His272(3.81),Lys206(2.39)
Enterolactone	-6.1	Asp40(2.89), Arg47(2.68), Glu174(3.35)	Lys142(4.50,4.06), Glu174(4.16), Arg154(3.71), Val173(4.98)

Enterdiol	-7.3	His320(2.10),Arg103(2.40)	Ser127(3.91), Ala239(4.33),Val324(4.63), Ser296(1.39),His106(4.77)
SECO	-7.8	Arg59(2.73,2.52), Tyr95(2.23),Gly122(3.49),Ser126(2.64), Arg48(2.48),Ala128(2.57)	Ala128(4.99,4.53), His106(4.74),Ala128(4.99,4.53), Pro50(5.25,4.07),Arg59(4.55)

T3SS ATPase	Pubchem ID	Binding affinity(kcal/mol)	Hydrogen Bond Interactions (Å)	Non-Covalent Interactions (Å)
	ATP	-7.0	Arg129(3.08), Pro124(2.14), Lys291(2.61), Gly152(1.94)	Glu287(4.51,4.44), Asp324(5.47), Ala131(5.12)
	SDG	-7.1	Ile322(3.54), Asp324(2.50), Gly152(1.9), Arg154(2.64,2.95), Arg129(2.75,3.09), Ala130(2.23)	Gln354(1.46), Ala131(3.77,5.02), Ile132(5.38), Arg350(2.04)

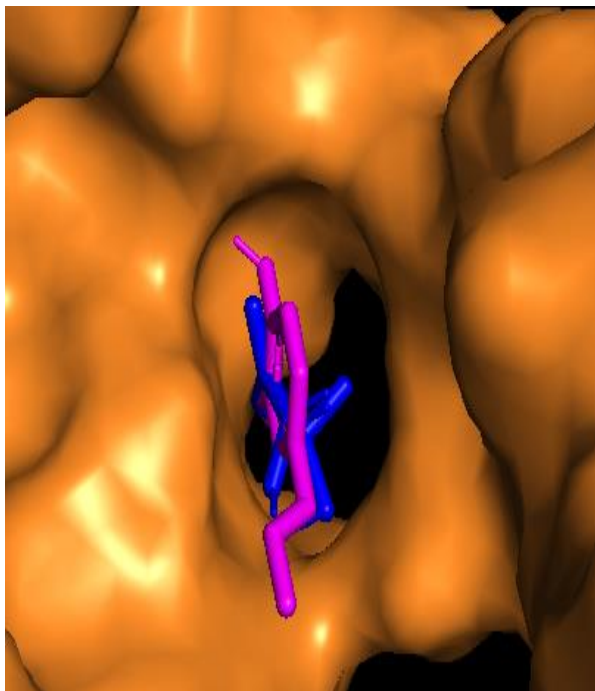
Three and two-dimensional binding conformations of the ligands at the active site of the enzyme with respect to the enzyme's substrate or coenzyme are shown in Figure 7. The number of compounds that interacted at the active site of each enzyme varied with shikimate kinase having the highest number of ligands which interacted at its active site. Among the compounds which had binding affinity of ≤ -5 kcal/mol with DAHP synthase, only isoeugenol was found to bind to the 3-phosphoenolpyruvate binding region with binding affinity of -5.4 kcal/mol. This was stronger than the binding affinity of -4.5 kcal/mol observed between 3-phosphoenolpyruvate and DAHP synthase (Figure 7A). At the substrate binding region of DHQS, four compounds: 4-hydroxy-3-methoxyphenylacetone (-5.6 kcal/mol), 4-ethylphenyl 4-methoxybenzoate (-7.3 kcal/mol), isoeugenol (-6.0 kcal/mol) and p-anisaldehyde (-5 kcal/mol) interacted with 3-dehydroquininate synthase at the NAD⁺ (-10.1 kcal/mol) binding site (Figure 7B). Here the binding affinity of NAD⁺ to DHQS was found to be the strongest followed by 4-ethylphenyl 4-methoxybenzoate and isoeugenol. Like DAHP, only isoeugenol interacted at the substrate binding region of DHQH. Isoeugenol had a binding affinity of -5.1 kcal/mol which is almost same as the binding affinity of the enzyme's substrate, 3-dehydroquininate (-5.2 kcal/mol).

Thellungianin g (-7 kcal/mol), isoeugenol (-6.0 kcal/mol), and 4-hydroxy-3-methoxyphenylacetone (-6.7 kcal/mol) interacted with SDHase at the NADP⁺ (-10 kcal/mol) and 3-dehydroshikimate (-6.6 kcal/mol) binding regions. This makes five compounds at the substrate binding region of the enzyme. Overall, NADP⁺ showed the strongest binding affinity to SDHase followed by thellungianin g and 4-hydroxy-3-methoxyphenylacetone whose binding affinities surpass that of the enzyme's substrate, 3-dehydroshikimate (Figure 7D). For SK, 11 compounds were found to interact with the amino acids at the substrate binding region of the enzyme. Isoeugenol (-5.2 kcal/mol), eugenol (-5.0 kcal/mol), enterolactone (-6.2 kcal/mol), methyl isoeugenol (-5.4 kcal/mol), p-anisaldehyde (-5.0 kcal/mol), thellungianin g (-6.1 kcal/mol), 4-ethylphenyl 4-methoxybenzoate (-6.1 kcal/mol), SECO (-6.5 kcal/mol), SDG (-7.4 kcal/mol), d-carvone (-5.1 kcal/mol), anethole (-5.0 kcal/mol), anisketone (-5.3 kcal/mol) bind to the ATP (-8.0 kcal/mol) and shikimate (-6.1 kcal/mol) binding site. ATP showed the strongest binding energy followed by SDG and enterolactone (Figure 7E).

At the EPSP synthase substrate binding region, six compounds: enterolactone (-6.5 kcal/mol), isoeugenol (-5.2 kcal/mol), p-anisaldehyde (-5.0 kcal/mol), enterodiol (-5.5

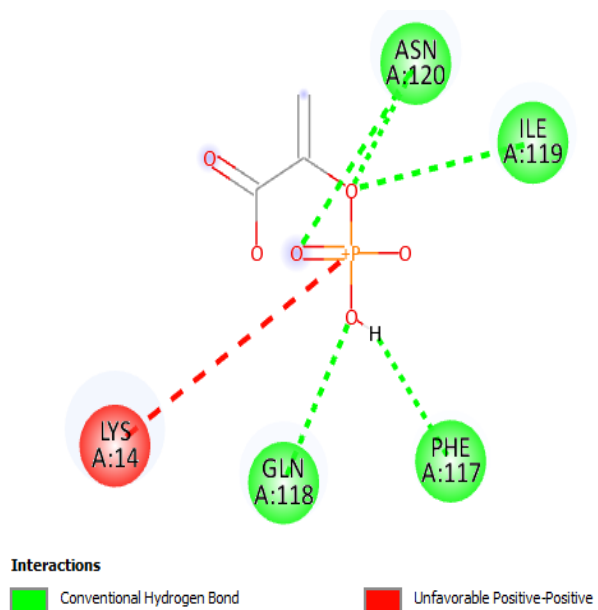
kcal/mol), 4-ethylphenyl 4-methoxybenzoate (-5.6 kcal/mol), thellungianin g (-5.1 kcal/mol) and SDG (-6.6 kcal/mol) were found to interact with EPSP synthase at its substrate, 3-phosphoshikimate (-5.0 kcal/mol) binding site. All the compounds had binding affinities stronger than that of 3-phosphoshikimate except for p-anisaldehyde with equal binding affinity with 3-phosphoshikimate (Figure 7F). For chorismate synthase, p-anisaldehyde (-5.2 kcal/mol) and SECO (-7.0 kcal/mol) interacted at its substrate, 5-enolpyruvylshikimate 3-phosphate (-6.8 kcal/mol) binding region where SECO showed the strongest binding affinity (Figure 7G). Finally, only SDG (-7.1 kcal/mol) formed a complex with T3SS ATPase at its ATP (-7.0 kcal/mol) binding site where both compounds showed similar binding affinities to the enzyme (Figure 7H).

A. DAHP synthase

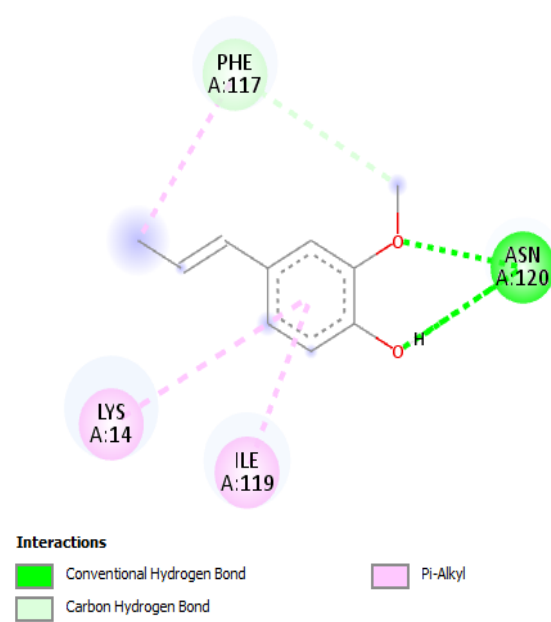


Blue: 3-phosphoenolpyruvate (PEP), purple: isoeugenol

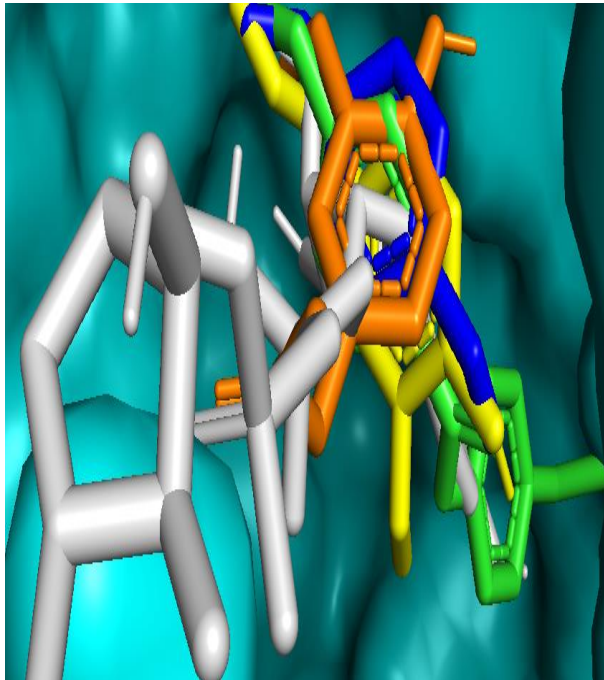
A1. PEP-DAHP



A2. Isoeugenol- DAHP

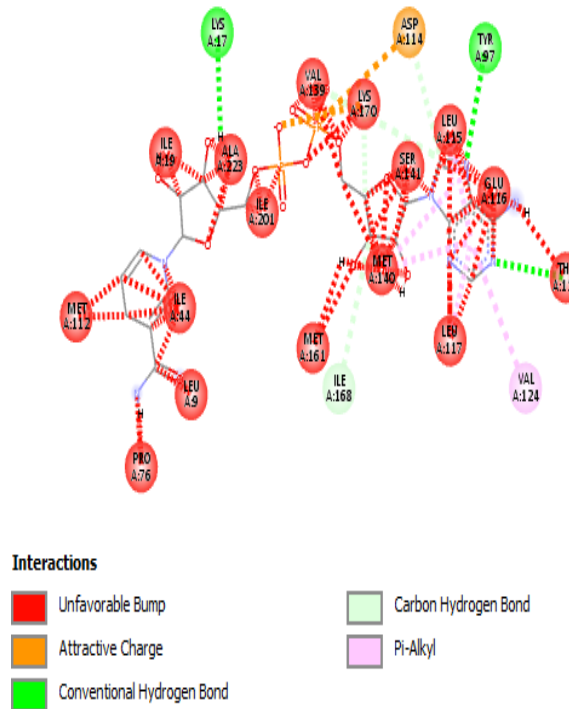


B. DHQS

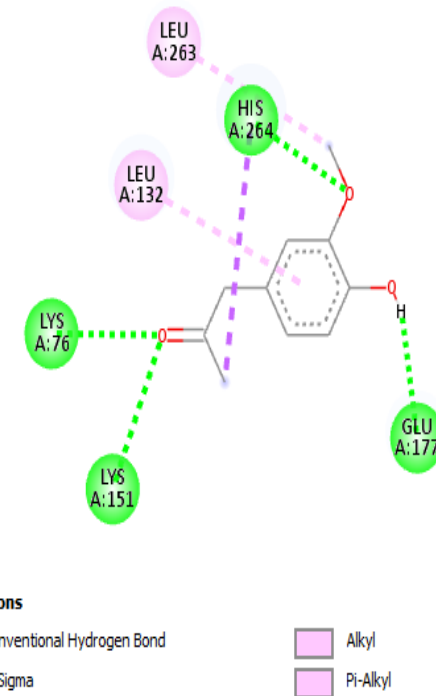


Gray: NAD+, orange: 4-hydroxy-3-methoxyphenylacetone, green: 4-ethylphenyl 4-methoxybenzoate, blue: p-anisaldehyde, yellow: isoeugenol.

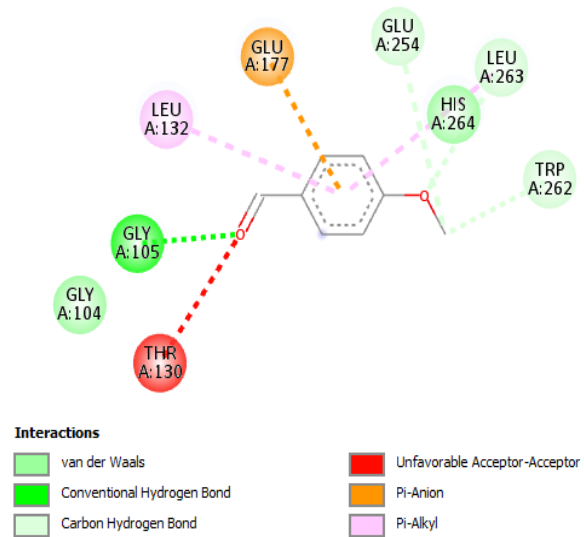
B1. NAD+-DHQS



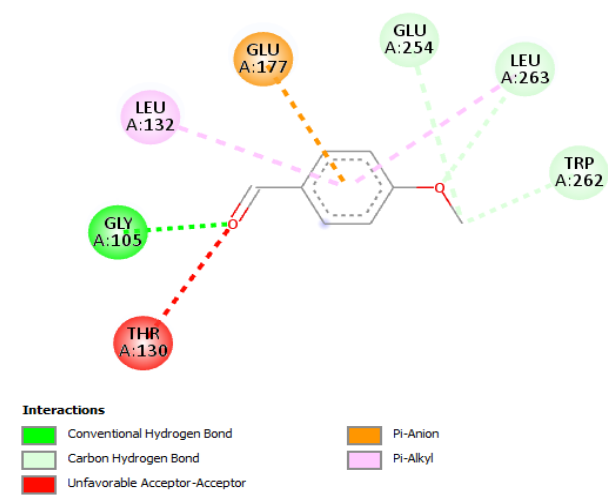
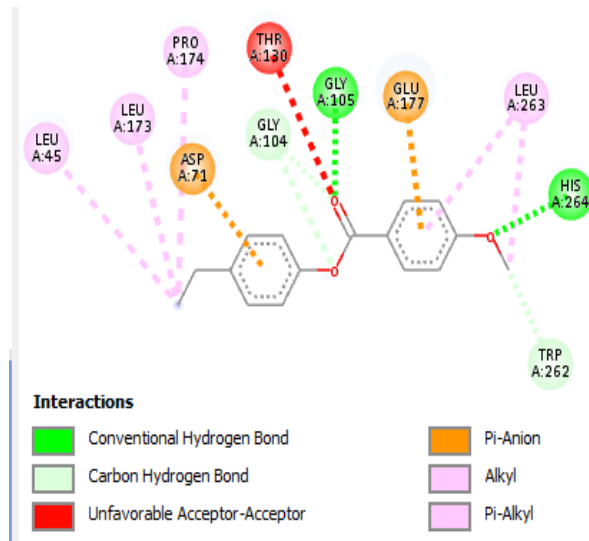
B2. Isoeugenol-DHQS



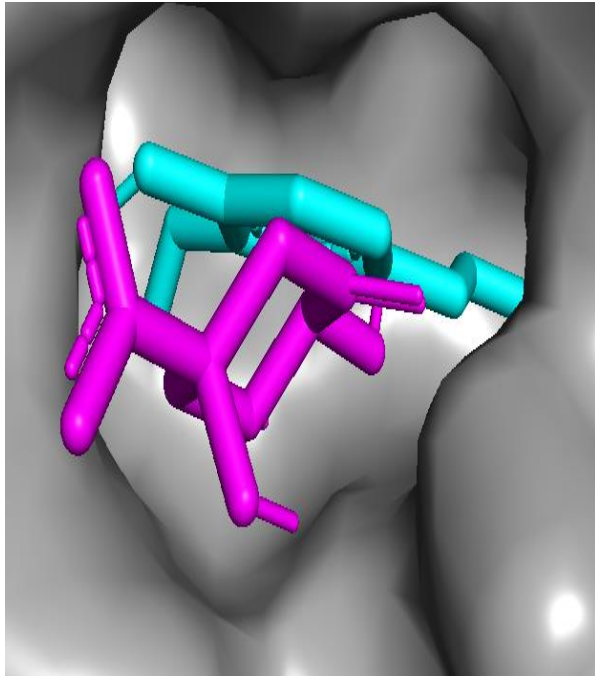
B3. 4-hydroxy-3-methoxyphenylacetone-DHQS



B4. 4-ethylphenyl 4-methoxybenzoate-DHQS B5. P-anisaldehyde-DHQS

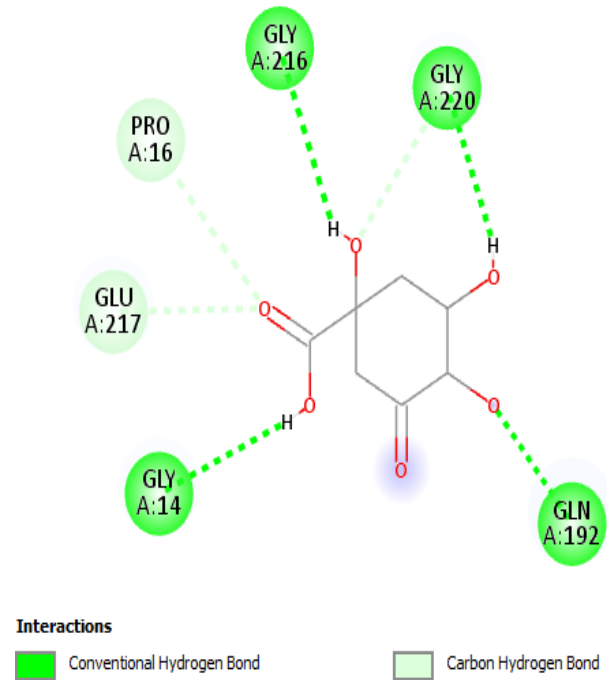


C. DQHH

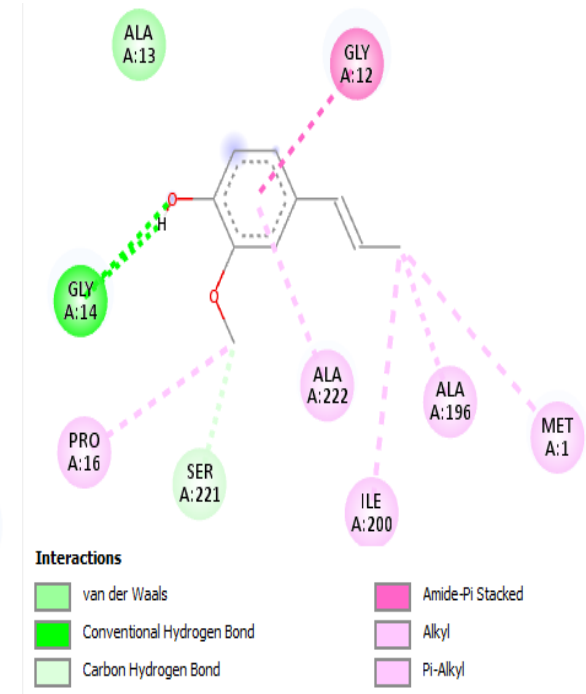


Magenta: 3-dehydroquininate, cyan: isoeugenol

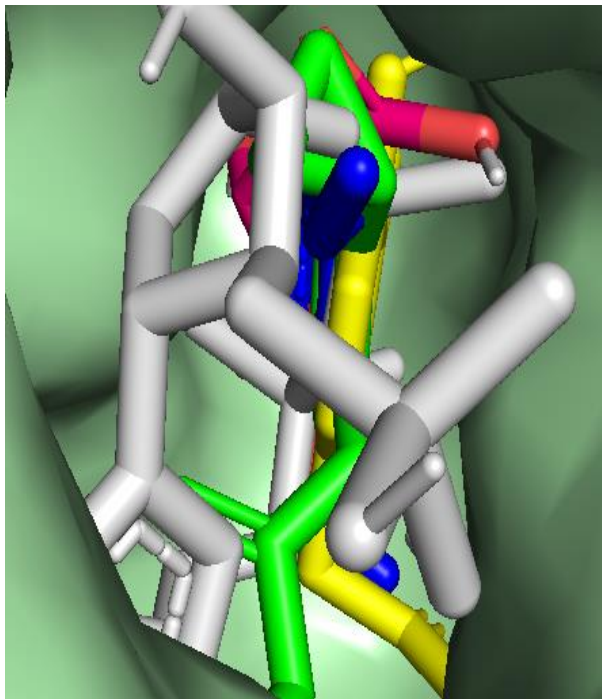
C1. 3-dehydroquininate-DHQH



C2. Isoeugenol-DHQH

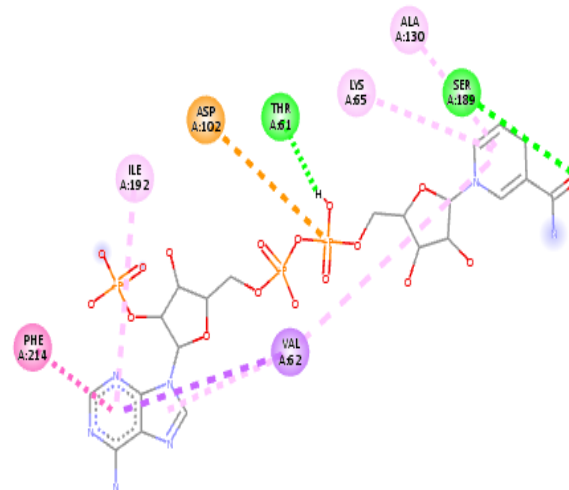


D. SDHase









White: NADP+, pink: 3-dehydroshikimate,
green: thellungianin g, blue: isoeugenol,
yellow: 4-hydroxy-3-methoxyphenylacetone

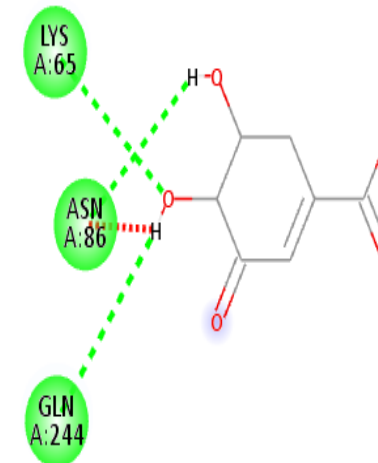
D1. NADP+-SDHase



Interactions

 Attractive Charge	 Pi-Pi T-shaped
 Conventional Hydrogen Bond	 Alkyl
 Pi-Sigma	 Pi-Alkyl

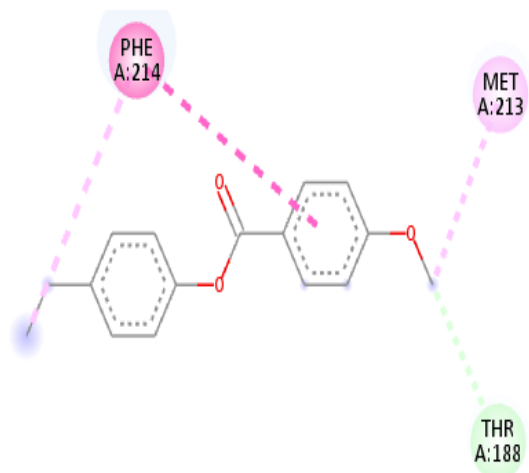
D2. 3-dehydroshikimate-SDHase



Interactions

 Conventional Hydrogen Bond	 Unfavorable Donor-Donor
--	---

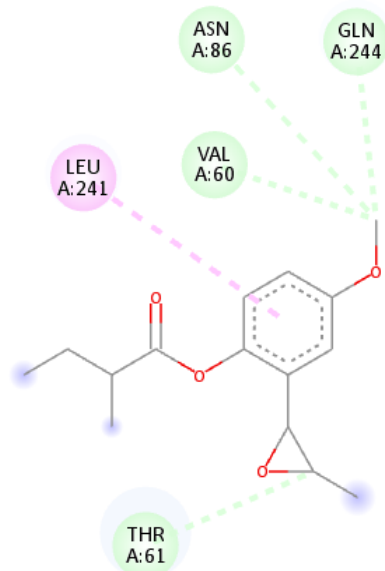
D3. 4-hydroxy-3-methoxyphenylacetone-SDHase



Interactions

- Carbon Hydrogen Bond
- Alkyl
- Pi-Pi T-shaped
- Pi-Alkyl

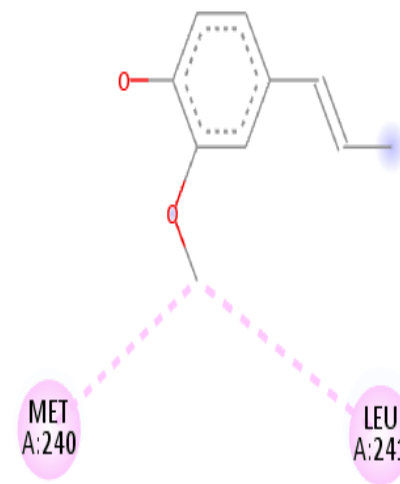
D4. Thellungianin g-SDHase



Interactions

- Carbon Hydrogen Bond
- Pi-Alkyl

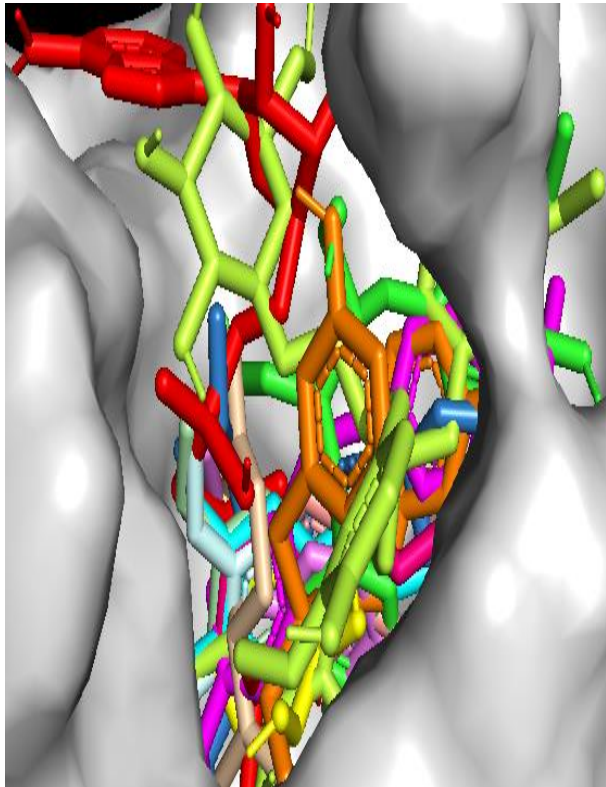
D5. Isoeugenol-SDHase



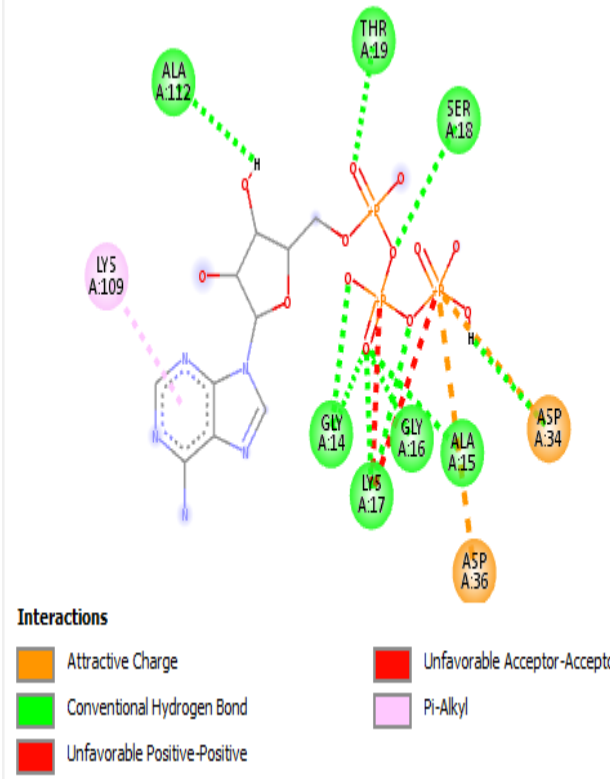
Interactions

- Alkyl

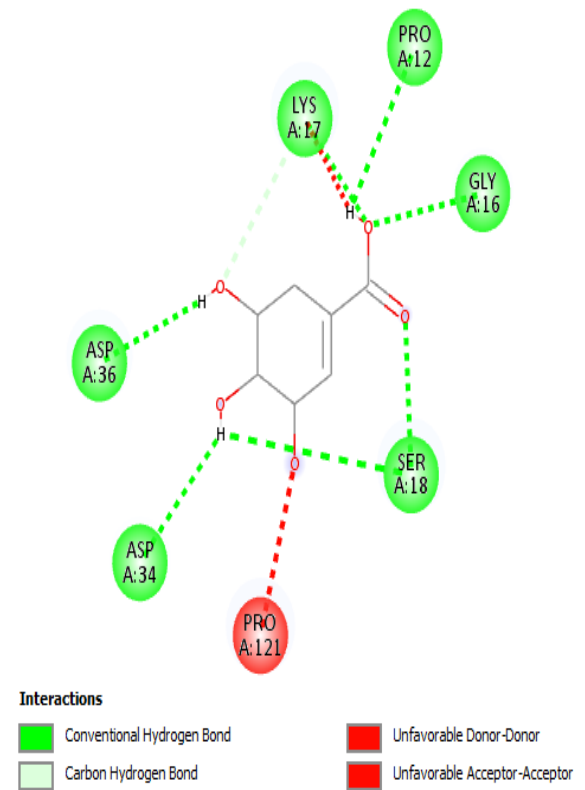
E. SK



E1. ATP-SK



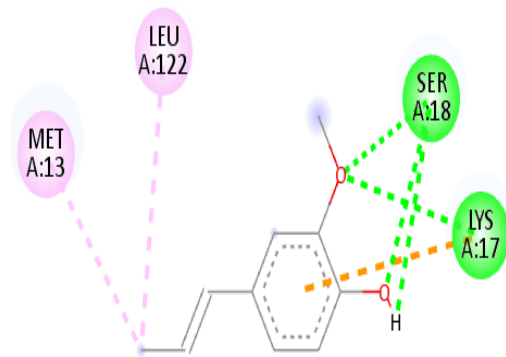
E2. Shikimate-SK



Yellow: shikimate, red: ATP green: SECO,
 pink: isoeugenol, orange: enterolactone, pale
 green: anethole, light cyan: methyl
 isoeugenol, violet: anisiketone, wheat: d-

carvone, salmon: p-anisaldehyde, magenta:
 4-ethylphenyl 4-methoxybenzoat, skyblue:
 thellungianin g, limon: SDG

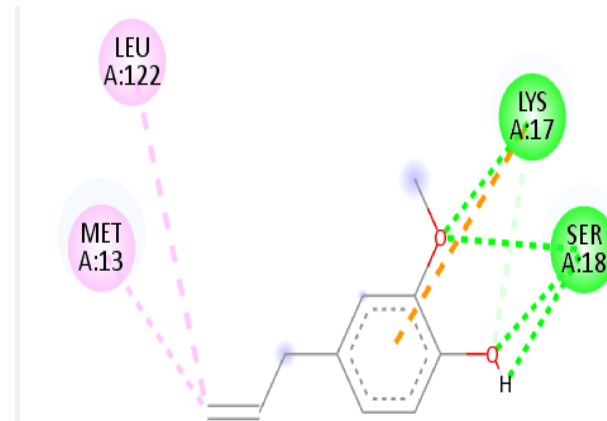
E3. Isoeugenol-SK



Interactions

- Conventional Hydrogen Bond
- Pi-Cation
- Alkyl
- Pi-Alkyl

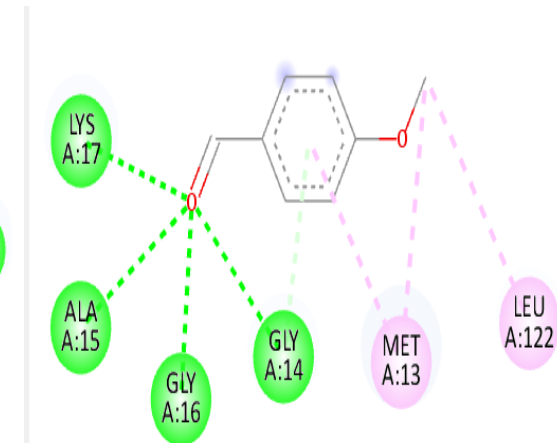
E4. Eugenol-SK



Interactions

- Conventional Hydrogen Bond
- Carbon Hydrogen Bond
- Pi-Cation
- Alkyl
- Pi-Alkyl

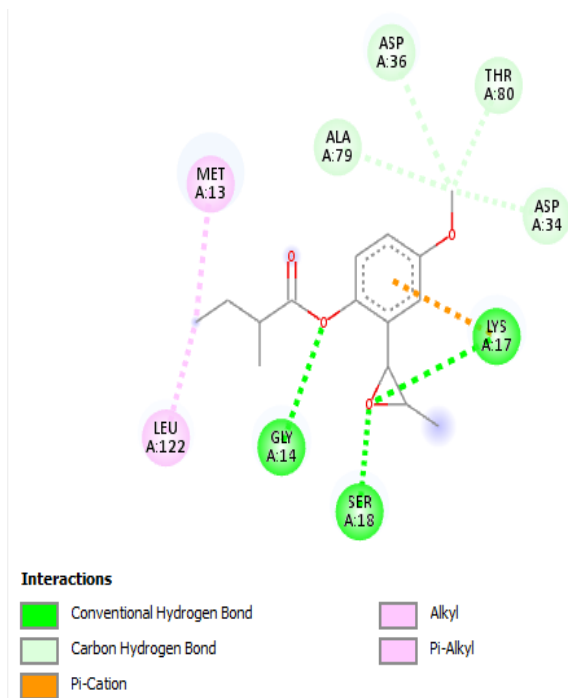
E5. P-anisaldehyde-SK



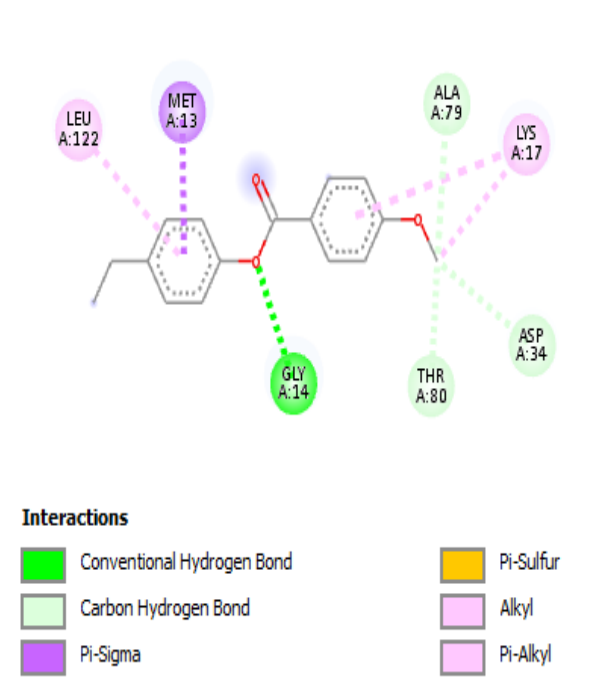
Interactions

- Conventional Hydrogen Bond
- Pi-Donor Hydrogen Bond
- Alkyl
- Pi-Alkyl

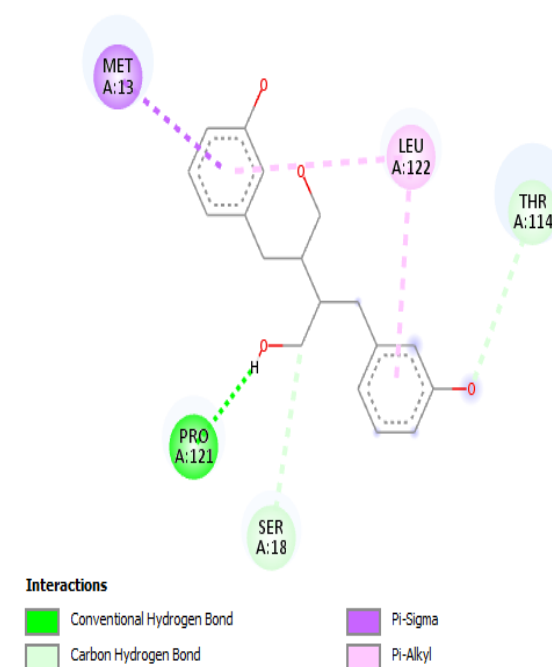
E6. Thellungianin SK



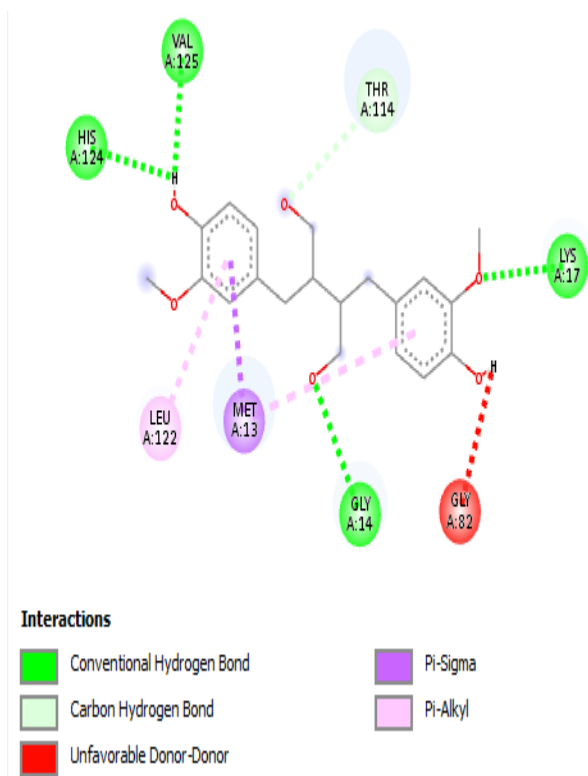
E7. 4-ethylphenyl 4-methoxybenzoate-SK



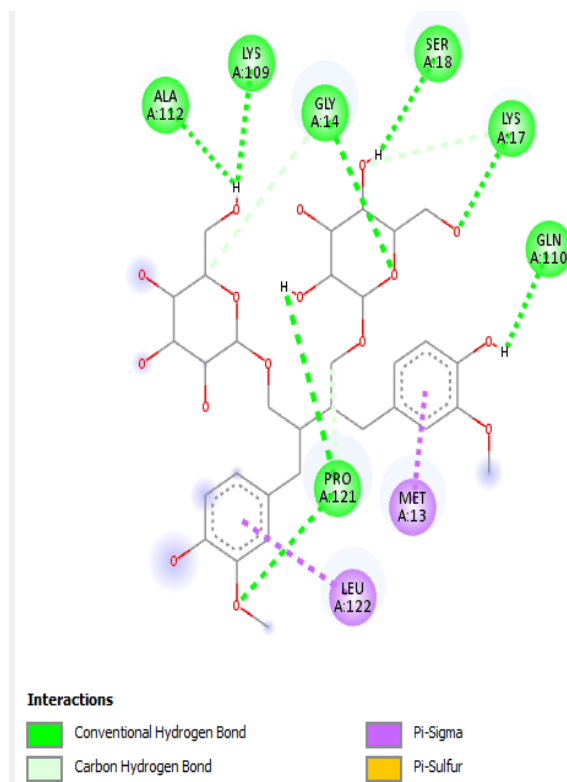
E8. Enterolactone-SK



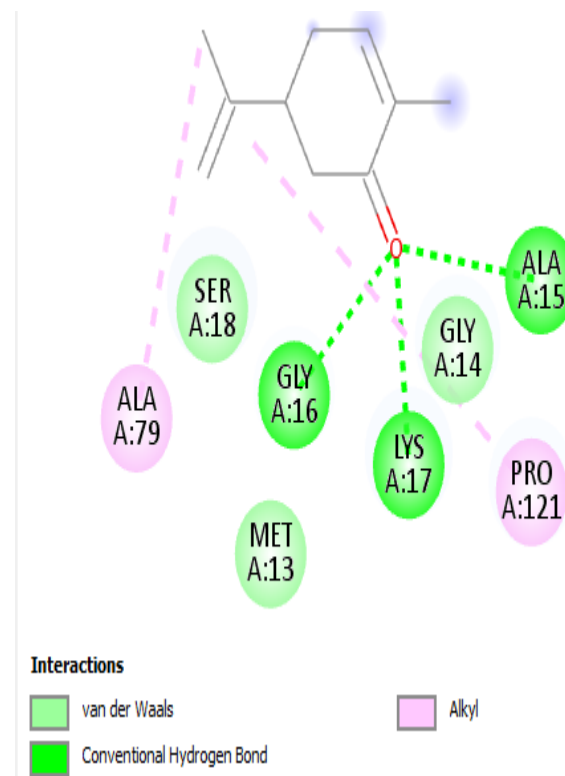
E9. SECO-SK



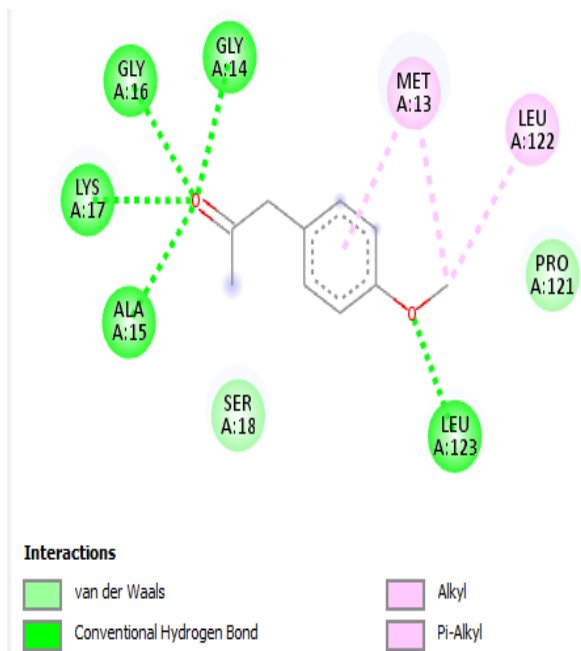
E10. SDG-SK



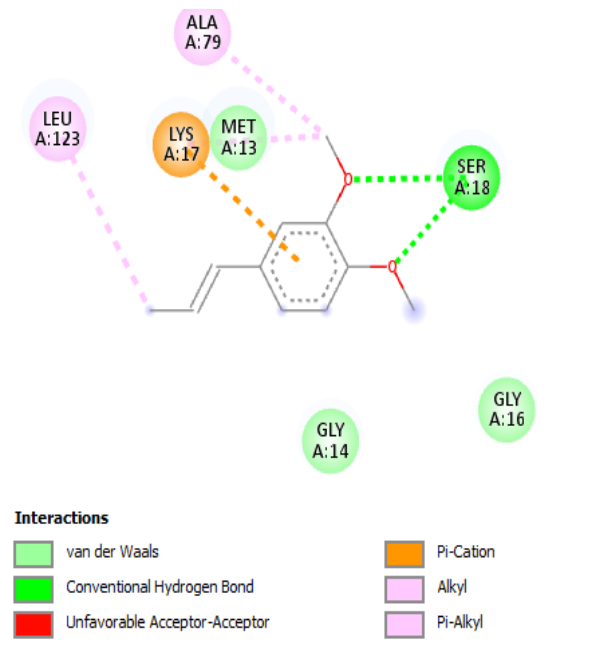
E11. d-Carvone-SK



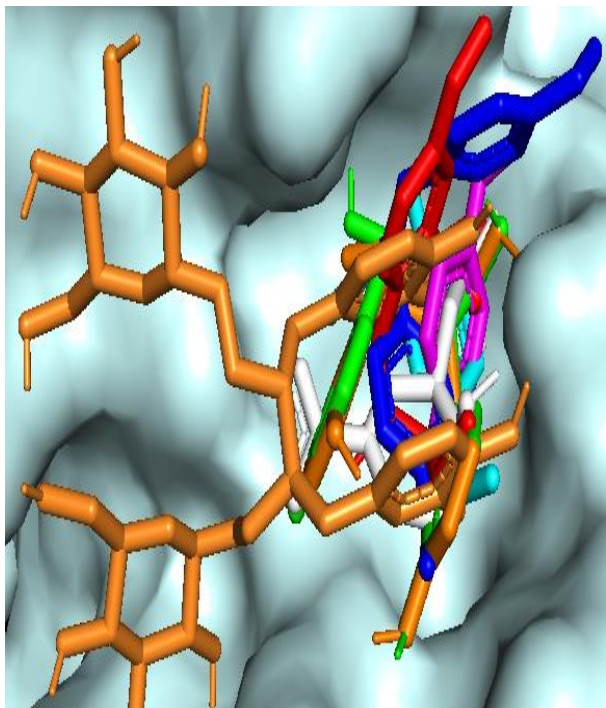
E12. Aniketone-SK



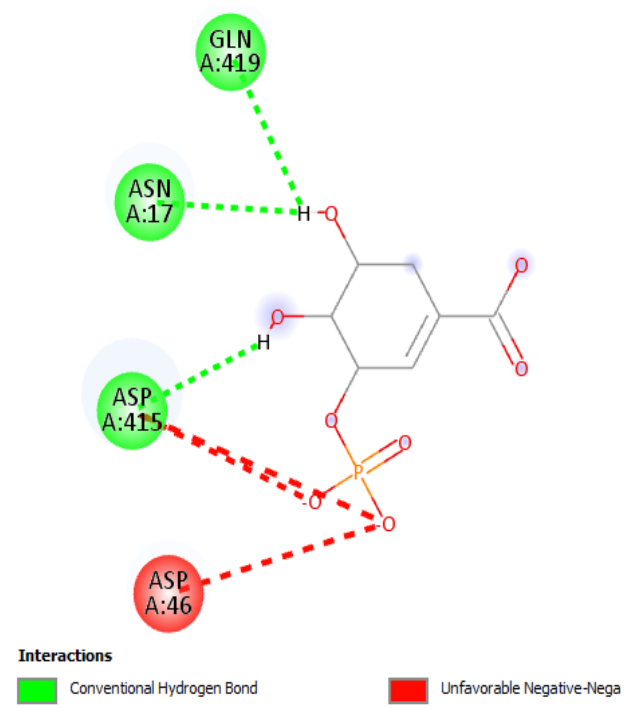
E13. Methylisoeugenol-SK



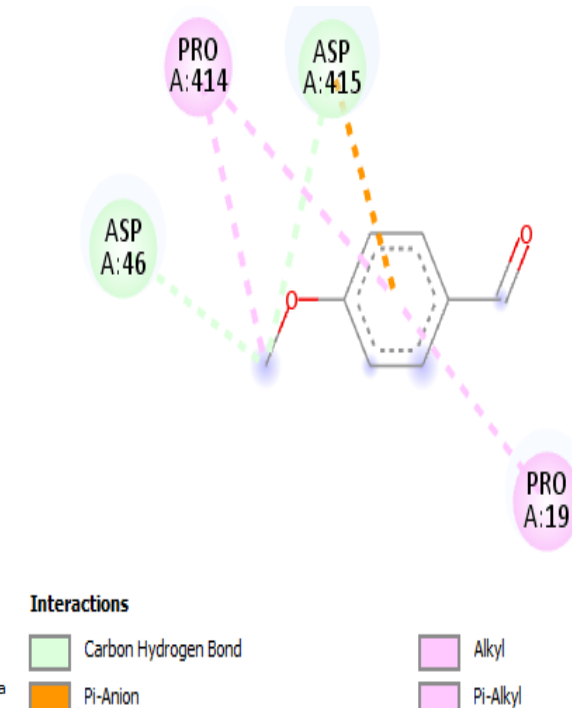
F. EPSP synthase



F1. 3-phosphoshikimate-EPSP synthase

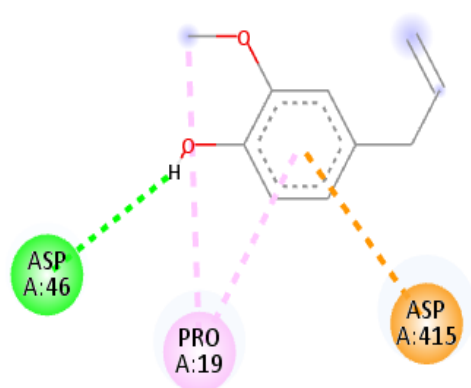


F2. P-anisaldehyde-EPSP synthase



White: 3-phosphoshikimate, orange: enterolactone, cyan: isoeugenol, green: enterodiol, blue: 4-ethylphenyl 4-methoxybenzoate, red: thellungianin g, magenta: p-anisaldehyde, red: SDG

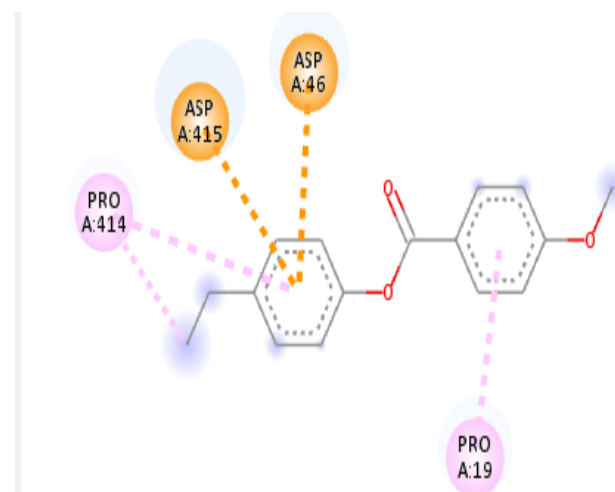
F3. Isoeugenol-EPSP synthase



Interactions

- Conventional Hydrogen Bond
- Unfavorable Donor-Donor
- Pi-Anion
- Alkyl
- Pi-Alkyl

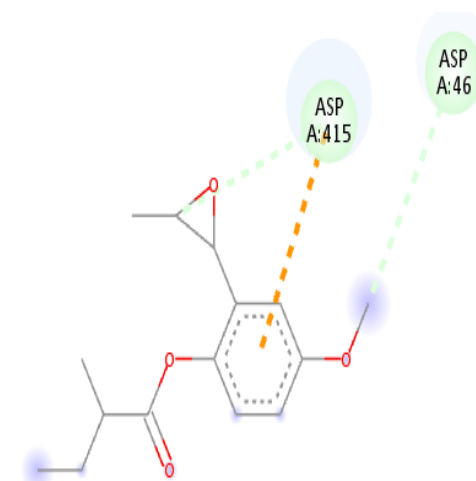
F4. 4-ethylphenyl 4-methoxybenzoate-EPSP synthase



Interactions

- Pi-Anion
- Alkyl
- Pi-Alkyl

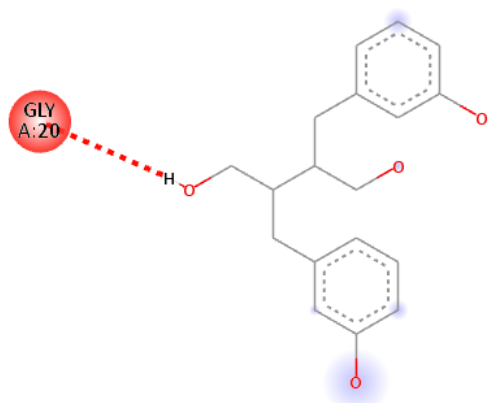
F5. Thellungianin g- EPSP synthase



Interactions

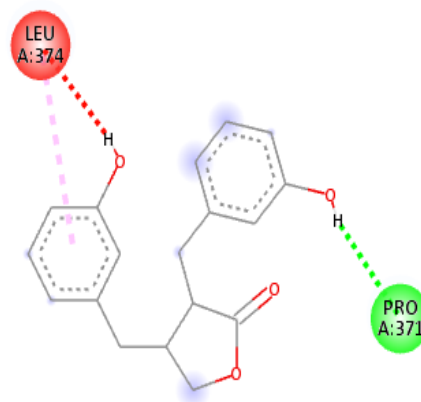
- Carbon Hydrogen Bond
- Pi-Anion

F6. Enterolactone-EPSP synthase



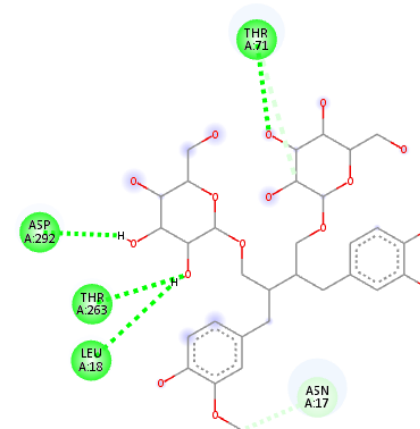
Interactions
■ Unfavorable Donor-Donor

F7. Enterodiol-EPSP synthase



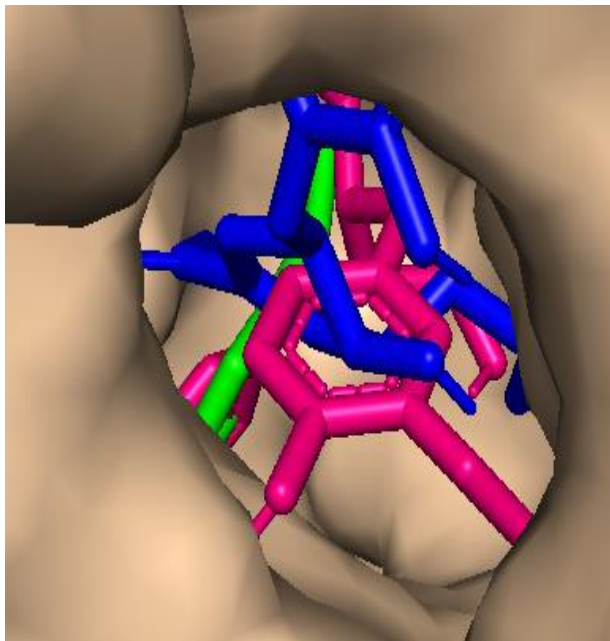
Interactions
■ Conventional Hydrogen Bond
■ Unfavorable Donor-Donor
■ Pi-Alkyl

F8. SDG-EPSP synthase



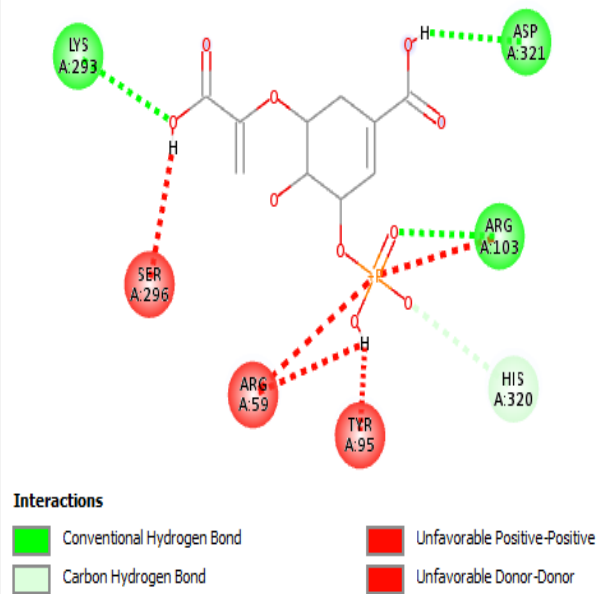
Interactions
■ Conventional Hydrogen Bond
■ Carbon Hydrogen Bond
■ Unfavorable Donor-Donor
■ Unfavorable Acceptor-Acceptor

G. CS

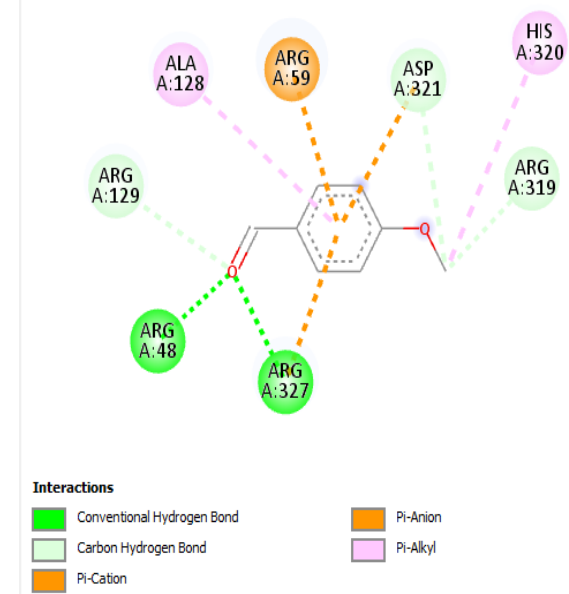


Blue: EPSP, green: p-anisaldehyde, hot pink: SECO

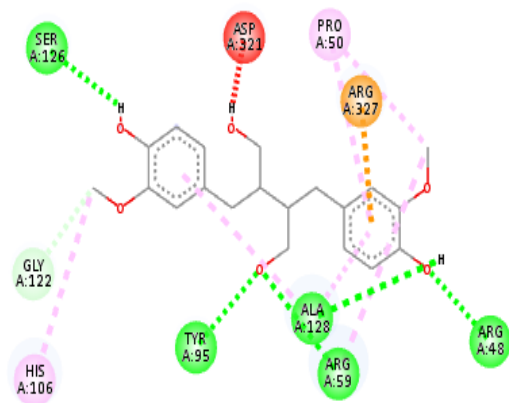
G1. EPSP-CS









G2. P-anisaldehyde-CS



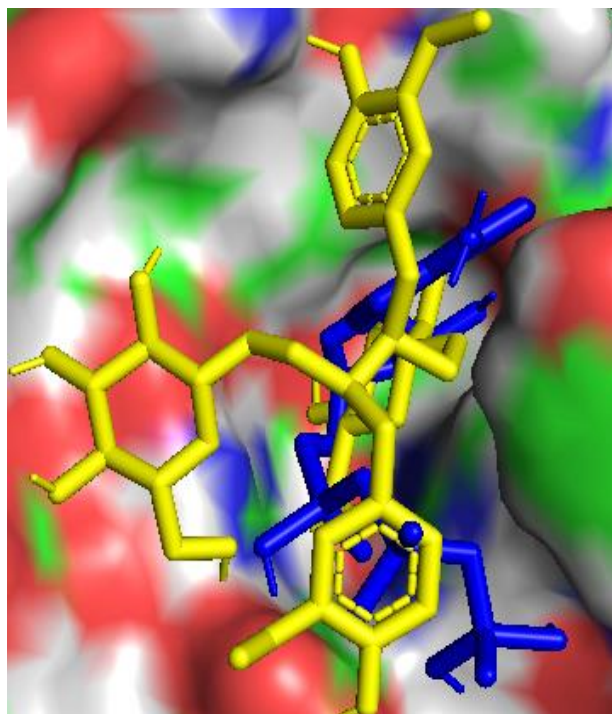
G3. SECO-CS



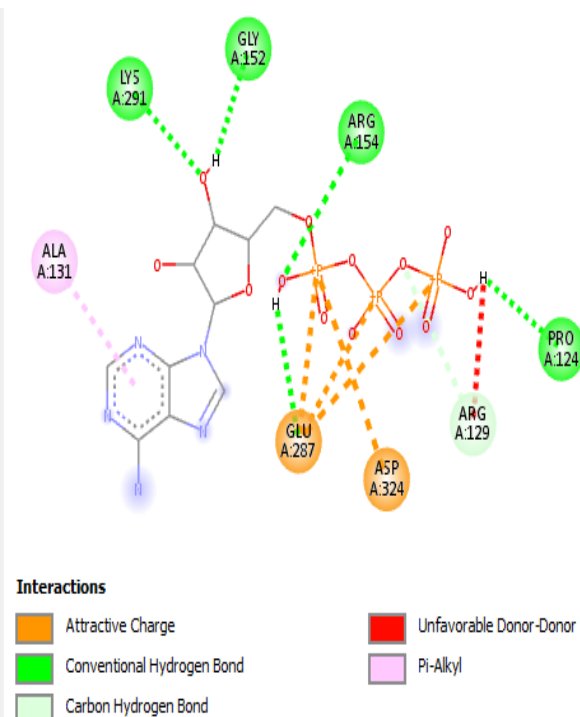
Interactions

 Conventional Hydrogen Bond	 Pi-Cation
 Carbon Hydrogen Bond	 Alkyl
 Unfavorable Donor-Donor	 Pi-Alkyl

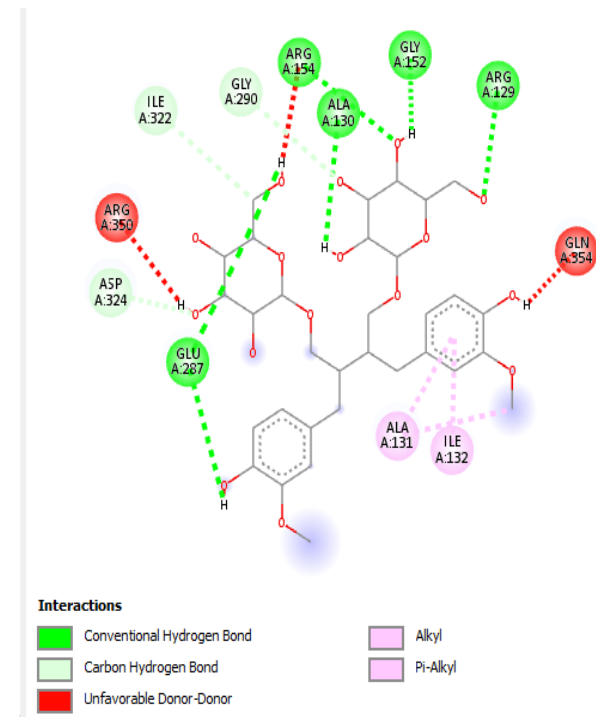
H. T3SS ATPase



H1. ATP-T3SS ATPase



H2. SDG- T3SS ATPase



Blue: ATP, yellow- SDG

Figure 7. 3D and 2D interactions of ligands with their respective controls in the active sites of the proteins. A: DAHP, B: DHQH, C: DHQH, D: SDHase, E: SK, F: EPSP synthase, G: CS, and H: T3SS ATPase using Pymol. The protein targets are represented as surface and the ligands represented as sticks. The 2D interactions of the ligands and their respective controls with the amino acids at the active site of the protein targets of DAHP (A1 and 2), DHQH (B1-5), DHQH (C1 and 2), SDHase (D1 -5), SK (E1-13), EPSP synthase (F1-8), CS (G1- 3) and T3SS ATPase (H1 and 2) obtained using Discovery Studio Visualizer.

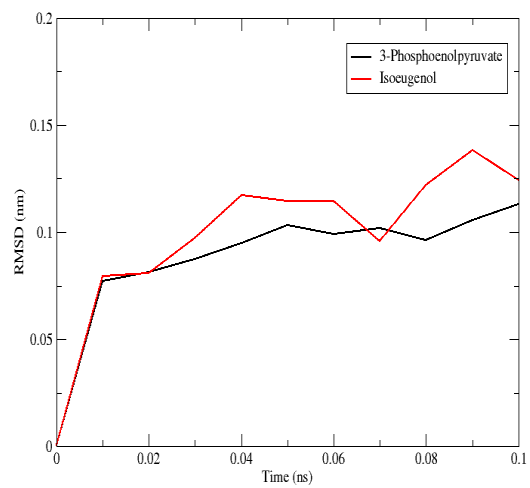
The results of the molecular docking showed that isoeugenol, eugenol, p-anisaldehyde, 4-ethylphenyl 4-methoxybenzoate, 4-hydroxy-3-methoxyphenylacetone, thellungianin g, SECO, SDG, enterodiol, enterolactone, d-carvone, anethole, anisketone and methyl isoeugenol are promising drug candidates as they not only exhibit good binding energies to their protein target(s) but also interacted at the active sites of the protein targets which indicate their potential as competitive inhibitors. Competitive inhibitors compete with the enzyme's substrate for the active site of the enzyme and, therefore, are promising inhibitory compounds. This does not downplay the efficacy of compounds that bind to allosteric site of the enzymes. However, for this study, compounds which interacted with amino acids at the active site of the enzymes were investigated.

3.5. Molecular dynamics (MD) simulation

To authenticate a promising drug candidate, the compound must form a stable complex with the receptor, the protein target. The stabilities of the ligand-receptor complexes were determined by subjecting them to molecular dynamics (MD) simulation. For this, T3SS ATPase and three protein targets from the shikimate pathway: shikimate kinase, 3-dehydroquinate synthase and DAHP synthase were selected. The stability of each ligand-receptor complex during MD simulation (Figure 8A-L) was evaluated using the root mean square deviation (RMSD) of the protein, RMSD of ligands and root mean square fluctuation (RMSF) of the protein. The RMSD value of a protein structure is an indicator of its conformation stability as it measures the average deviation of the protein structure during the MD simulation. The lower the RMSD value of a protein, the more stable the protein. Similarly, the RMSF value of a protein indicates the extent to which the protein's amino acids diverged from their initial states.

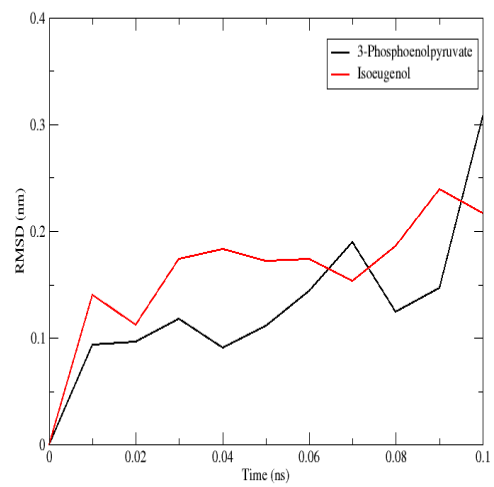
A

RMSD of DAHP



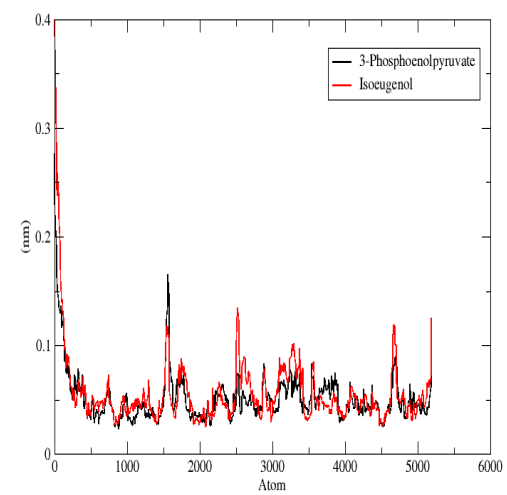
B

RMSD of Ligands with DAHP



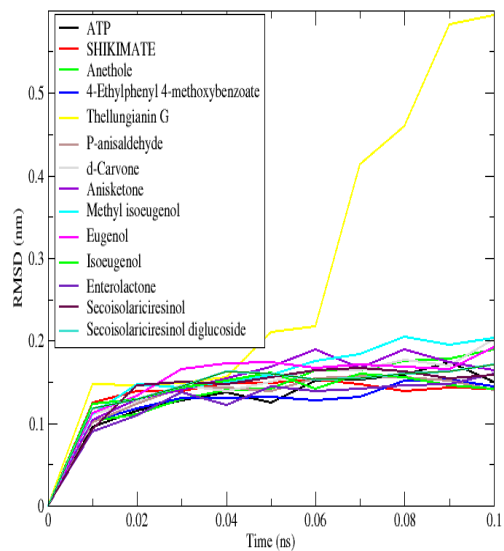
C

RMSF DAHP



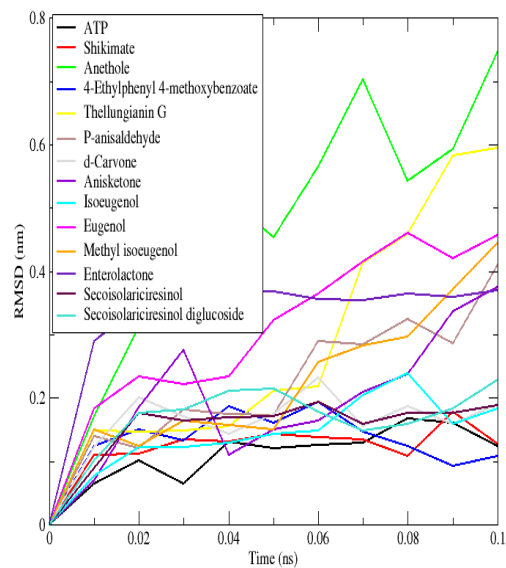
D

RMSD of Shikimate kinase



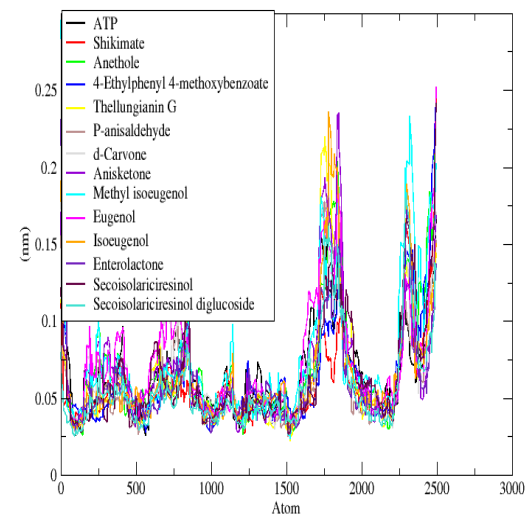
E

RMSD of components of Aniseed oil and Flaxseed oil



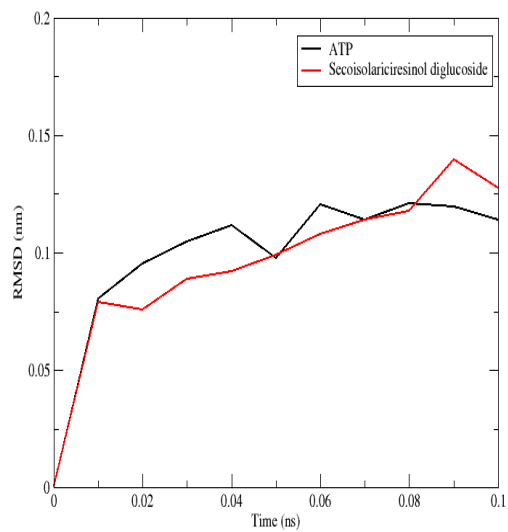
F

RMSF of Shikimate Kinase



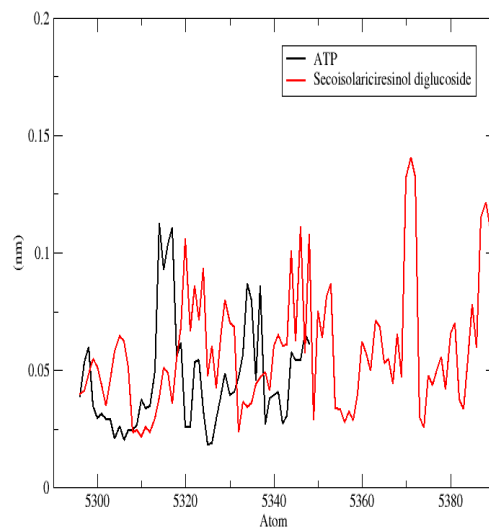
G

RMSD T3SS ATPase



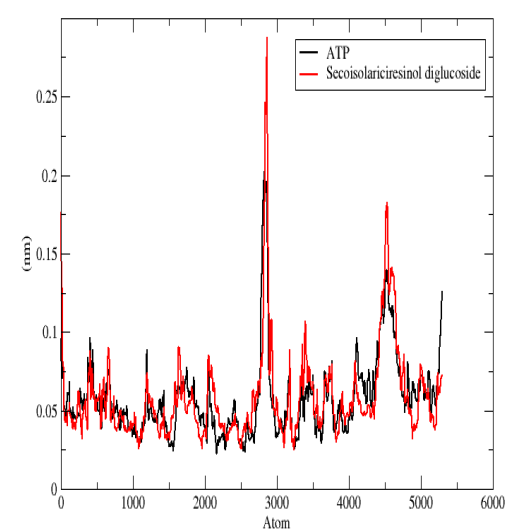
H

RMSF of ATP AND SDG with T3SS ATPase



I

RMSF T3SS ATPase



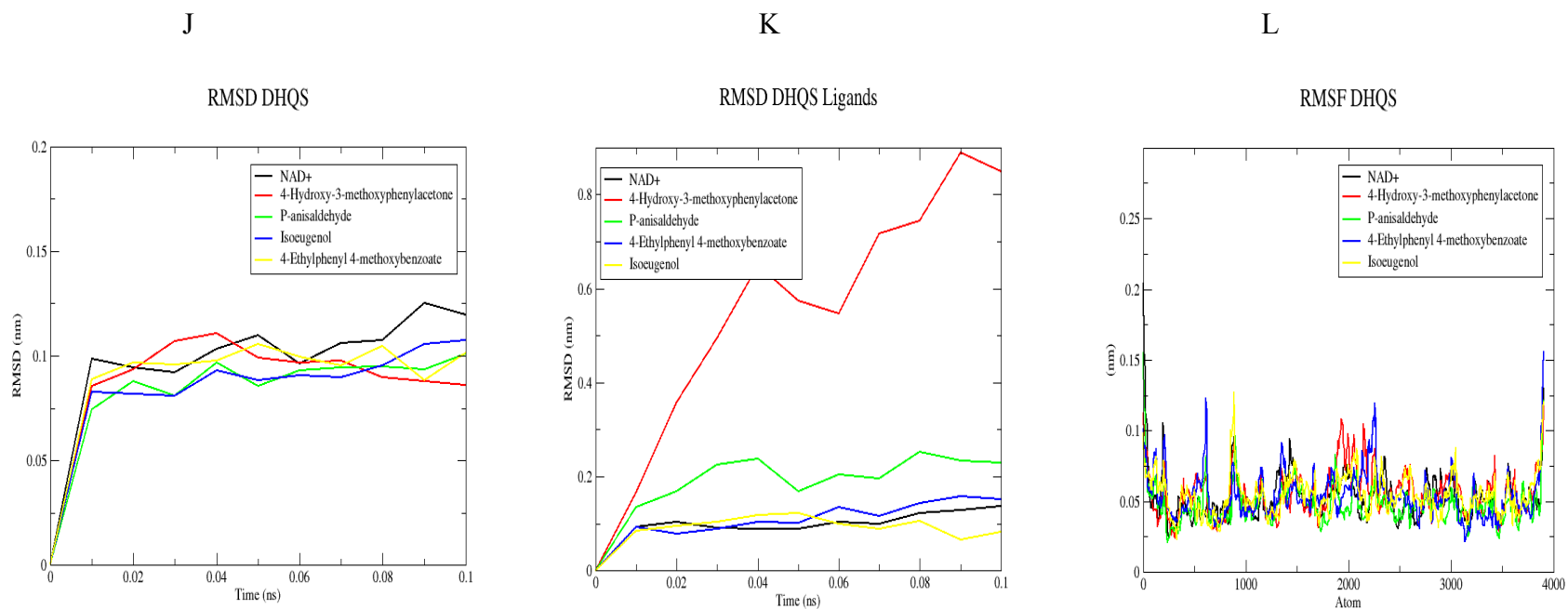


Figure 8A-L. RMSD and RMSF of ligand-protein complex.

A: RMSD of DAHP, B: RMSD of ligands bound to DAHP, C: RMSF of DAHP, D: RMSD of SK, E: RMSD of ligands bound to SK, F: RMSF of SK, G: RMSD of ATPase, H: RMSF of ligand, I: RMSF of ligands bound to ATPase, J: RMSD ligand-DHQS, K: RMSD of ligands bound to DHQS and L: RMSF of ligand-DHQS.

The results revealed that RMSD of all the ligand-protein complex maintained a stable conformation with slight deviation around 2.0 Å except for thellungianin g-SK complex with a RMSD value which increased to over 5.0 Å as shown in Figure 8D. This suggests that SK was largely unstable when bound to thellungianin g which could be because of huge conformational changes in the protein. RMSF of the proteins coupled with the ligands and controls were similar and the observed fluctuations in proteins' atoms could be attributed to the structural changes that the protein undergoes (Figure 8C, F, I and L). This is expected according to Newton's second law of motion which says force is equal to the rate of change of momentum. This implies that fluctuations in the protein atoms were seen because of the force exerted on the protein by the ligands. Conversely, some of the ligands were largely unstable during the MD simulation leading to their high RMSD values. Anethole, anisketone, thellungianin g, eugenol, and methyl isoeugenol when in complex with SK diverged significantly from their initial states and continually diverged with RMSD values between 4.0 Å and 8.0 Å as shown in Figure 8E. Also, 4-hydroxy-3-methoxybenzylacetone in complex with DHQS diverged immensely with RMSD value of over 8.0 Å as shown in Figure 8K. This could be due to weak interactions between the ligands and protein targets. This consequently reduces the potential of these compounds as drug candidates. This is because unstable compounds could be easily displaced from the active site of the enzyme by the enzyme's substrate. In contrast, isoeugenol, p-anisaldehyde, 4-ethylphenyl 4-methoxybenzoate, d-carvone, SDG, SECO and enterolactone did not diverge notably from their initial structure and maintained RMSD around 2Å (Figure 8B, E and K). These results suggest high binding energies and interactions between the ligand and receptor. This indicates that isoeugenol, p-anisaldehyde, 4-ethylphenyl 4-methoxybenzoate and d-carvone from aniseed are promising antimicrobial agents against the shikimate pathway. Also, SDG from flaxseed is a promising antimicrobial agent against the shikimate pathway and T3SS ATPase. SECO and Enterolactone from flaxseed are promising antimicrobial agents against the shikimate pathway.

3.6. Absorption, Distribution, Metabolism, Excretion and Toxicity (ADMET) profiles of the most promising compounds

High attrition rates of drug candidates in the clinical stage are mostly attributed to their poor ADMET profiles. Hence, screening based on these criteria is essential. Ampicillin was studied as control. The drug-likeness of the compounds were screened by the evergreen Lipniski rule of five which states: a molecule should have a molecular mass (MW) less than 500 Da, no more than 5 hydrogen bond donors (HBD), no more than 10 hydrogen bond acceptors (HBA), and an octanol–water partition coefficient log P not greater than 5 (Paramashivam et al. 2015). However, this rule is not to be slavishly followed as it was devised to aid the development of orally bioavailable drugs (Neidle 2012). All the compounds assessed passed this screening except for secoisolariciresinol diglucoside having MW>500, nHBA>10, nHBD>5. Thus, this compound violated three indices and this may reduce its oral absorption. This, however, does not hinder SDG as a drug candidate as it could be administered intravenously. Isoeugenol, p-anisaldehyde, d-carvone and 4-ethylphenyl 4-methoxybenzoate from aniseed fulfilled the drug-likeness requirement. However, only SECO and enterolactone from flaxseed meet the required properties for drug-likeness whereas SDG did not meet the requirements. The gastrointestinal absorption potential of the compounds was screened based on their Madin-Darby canine kidney (MDCK) permeability. This assay measures whether a compound is a permeability-glycoprotein (p-gp) substrate or inhibitor. All the examined compounds were seen to have good MDCK permeability as shown in Table 4. This suggests they have a high chance of being subjected to active efflux. To assess distribution, blood brain barrier (BBB) penetration was investigated. Apart from ampicillin, isoeugenol, 4-ethylphenyl 4-methoxybenzoate and enterolactone that were impermeable to the BBB, p-anisaldehyde, d-carvone, SECO and SDG could penetrate the BBB. For the compounds that did not penetrate the BBB, this feature may be an advantage as there is higher certainty of no effect on the central nervous system (CNS). However, this does not mean that those that penetrate are harmful as they may have no effect on the CNS.

Evaluation of the metabolism of the compounds was performed by investigating their inhibitory effect on cytochrome p450 (CYP450) monooxygenase family isoforms. CYP450 is greatly responsible for the metabolism of substances and inhibition of one or

more of its isoforms may hinder the biotransformation of the compound. This could result in bioaccumulation of the compounds and ultimately could lead to an increase in toxicity profile. D-carvone and secoisolariciresinol diglucoside do not inhibit any of the five isoforms of CYP450 enzyme which indicates a high chance of its metabolism. Isoeugenol and p-anisaldehyde inhibit the CYP 1a2 isoform of CYP 450 and may lead to poor bioavailability except if co-administered with CYP 1a2 inducers. However, 4-ethylphenyl 4-methoxybenzoate and enterolactone inhibit four and five isoforms of CYP 450 respectively, which indicates a high probability of poor metabolism.

Excretion was assayed by clearance of the compound. All but two compounds showed adequate clearance profile and this may be a good indication of low toxicity profiles. The exceptions were secoisolariciresinol diglucoside and ampicillin (the control) whose clearance profiles were low and may result in high toxicity profiles from bioaccumulation. Lastly, the toxicophore of the compounds, toxicity associated with a chemical structure, was evaluated. All compounds except d-carvone had no functional group that could cause acute toxicity and cancers. D-carvone, on the other hand, had a functional group that may be carcinogenic. Modification of the functional group of d-carvone may circumvent this challenge but may also affect its potency. Also, all of the investigated compounds have functional groups to which the skin may be sensitive.

Based on all of the aforementioned screening, isoeugenol and p-anisaldehyde from aniseed and secoisolariciresinol from flaxseed were selected for in vitro analysis. However due to the presence of secoisolariciresinol in diglucoside form in flaxseed, in vitro analysis was conducted with SDG.

Table 4. ADMET profiles of most promising compounds from aniseed and flaxseed.

Compound	Druglikeness	Absorption	Distribution	Metabolism	Excretion	Toxicophore
Ampicillin (control)	Lipinski rule: yes	MDCK permeability: yes	BBB penetration: no	CYP 1a2 inhibitor:no CYP2c19 inhibitor: no CYP2c9 inhibitor: no CYP2d6 inhibitor:no CYP3a4 inhibitor : no	Clearance: low	Acute toxicity: none Genotoxic carcinogenicity:none Nongenotoxic carcinogenicity: none Skin sensitivity: yes
Isoeugenol	Lipinski rule: yes	MDCK permeability: yes	BBB penetration: no	CYP1a2 inhibitor:yes CYP2c19 inhibitor: no CYP2c9 inhibitor: no CYP2d6 inhibitor:no CYP3a4 inhibitor : no	Clearance: moderate	Acute toxicity: none Genotoxic carcinogenicity:none Nongenotoxic carcinogenicity: none Skin sensitivity: yes
P-anisaldehyde	Lipinski rule: yes	MDCK permeability- yes	BBB penetration: yes	CYP1a2 inhibitor: yes CYP2c19 inhibitor: no CYP2c9 inhibitor: no	Clearance: moderate	Acute toxicity: none Genotoxic carcinogenicity: none Nongenotoxic carcinogenicity: none Skin sensitivity: yes

				CYP2d6 inhibitor: no CYP3a4 inhibitor: no		
4-ethylphenyl 4-methoxybenzoate	Lipniski rule: yes	MDCK permeability-yes	BBB penetration: no	CYP1a2 inhibitor: yes CYP2c19 inhibitor: yes CYP2c9 inhibitor: yes CYP2d6 inhibitor: yes CYP3a4 inhibitor: no	Clearance: moderate	Acute toxicity: none Genotoxic carcinogenicity: none Nongenotoxic carcinogenicity: none Skin sensitivity: yes
D-carvone	Lipniski rule: yes	MDCK permeability-yes	BBB penetration: yes	CYP1a2 inhibitor: no CYP2c19 inhibitor: no CYP2c9 inhibitor: no CYP2d6 inhibitor: no CYP3a4 inhibitor: no	Clearance: moderate	Acute toxicity: none Genotoxic carcinogenicity: yes Non-genotoxic carcinogenicity: none Skin sensitivity: yes
Secoisolariciresinol (seco)	Lipniski rule: yes	MDCK permeability-yes	BBB penetration: yes	CYP1a2 inhibitor: yes CYP2c19 inhibitor: no CYP2c9 inhibitor: no	Clearance: moderate	Acute toxicity: none Genotoxic carcinogenicity: none Non genotoxic carcinogenicity: none Skin sensitivity: yes

				CYP2d6 inhibitor: no CYP3a4 inhibitor: no		
Secoisolariciresinol diglucoside	Lipniski rule: no	MDCK permeability-yes	BBB penetration: yes	CYP1a2 inhibitor: no CYP2c19 inhibitor: no CYP2c9 inhibitor: no CYP2d6 inhibitor: no CYP3a4 inhibitor: no	Clearance: low	Acute toxicity: none Genotoxic carcinogenicity: none Non genotoxic carcinogenicity: none Skin sensitivity: yes
Enterolactone	Lipniski rule: yes	MDCK permeability-yes	BBB penetration: no	CYP1a2 inhibitor: yes CYP2c19 inhibitor: yes CYP2c9 inhibitor: yes CYP2d6 inhibitor: yes CYP3a4 inhibitor: no	Clearance: high	Acute toxicity: none Genotoxic carcinogenicity: none Non genotoxic carcinogenicity: none Skin sensitivity: none

3.7. Qualitative and quantitative analysis of the inhibitory ability of the aniseed and flaxseed EO and their bioactive components

To confirm the inhibitory activity of the compounds suggested by molecular docking and molecular dynamic simulation results, antimicrobial analysis of the crude essential oil from aniseed and flaxseed was performed against *S. sonnei*. The bioactive components from aniseed and flaxseed as revealed from the in silico analysis was also investigated for their antimicrobial potencies. Each value reported represents the mean of three different replicates \pm standard deviation (SD).

3.7.1. Qualitative analysis of aniseed and flaxseed EO for inhibition of *S. sonnei* growth

Qualitative analysis was carried out by agar disc diffusion method to determine the inhibitory effect of aniseed and flaxseed oil against *S. sonnei*. The zones of growth inhibition as shown in Table 5 and Figure 9 indicate the zone of growth inhibition exerted by aniseed and flaxseed. The results showed that the zone of bacteria growth inhibition by aniseed and flaxseed were 9 ± 0.02 mm and 8 ± 0.01 mm, respectively.

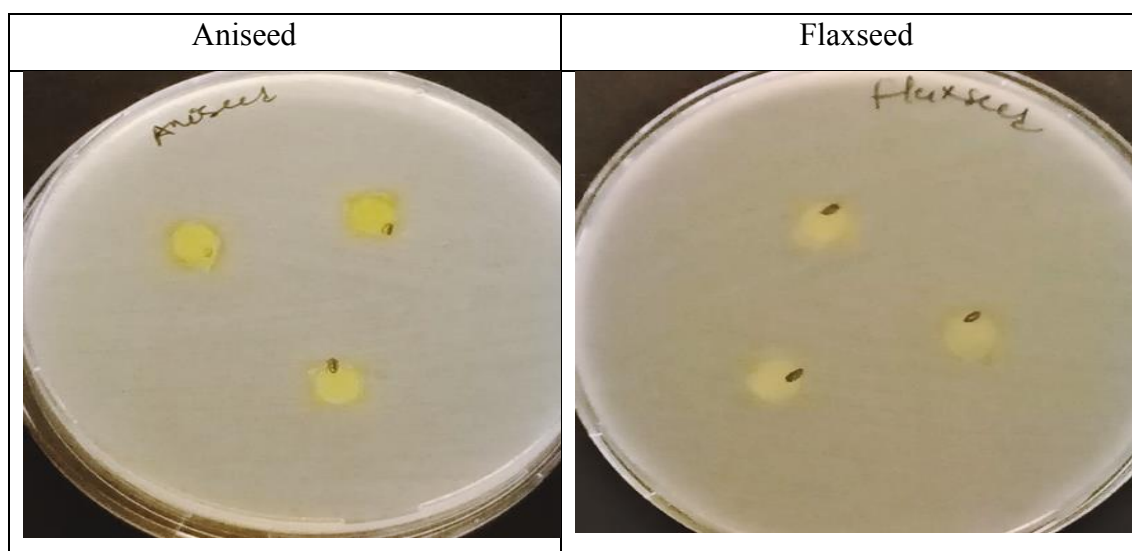


Figure 9. Agar disc diffusion assay of aniseed and flaxseed EO.

Table 5. Qualitative result of EO from aniseed and flaxseed.

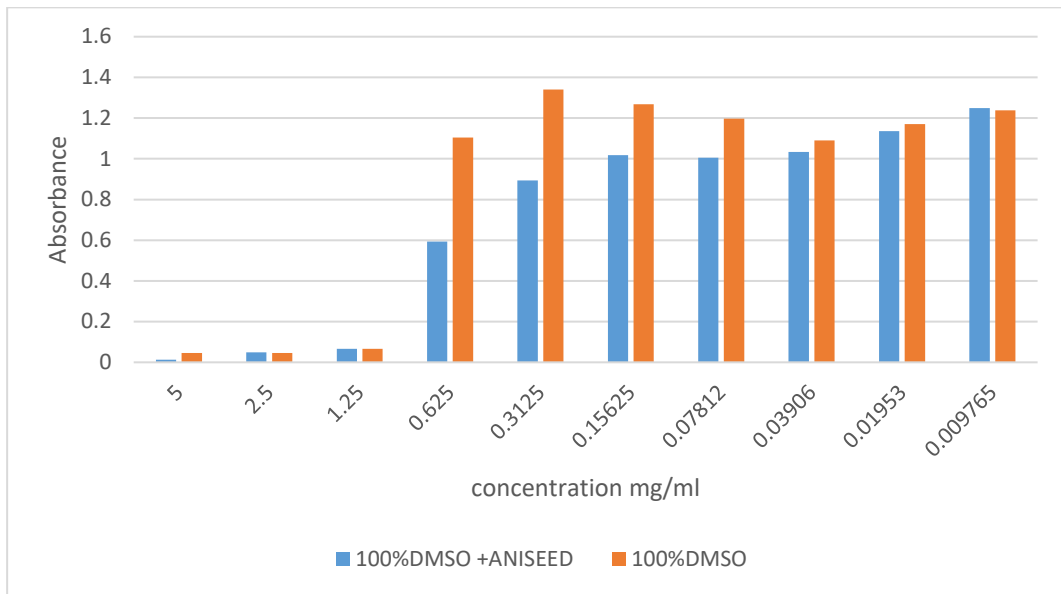
EO	Zone of growth inhibition (mm)
Aniseed	9 ± 0.02
Flaxseed	8 ± 0.01

3.7.2. Quantitative analysis of *S. sonnei* growth inhibition by aniseed and flaxseed EO

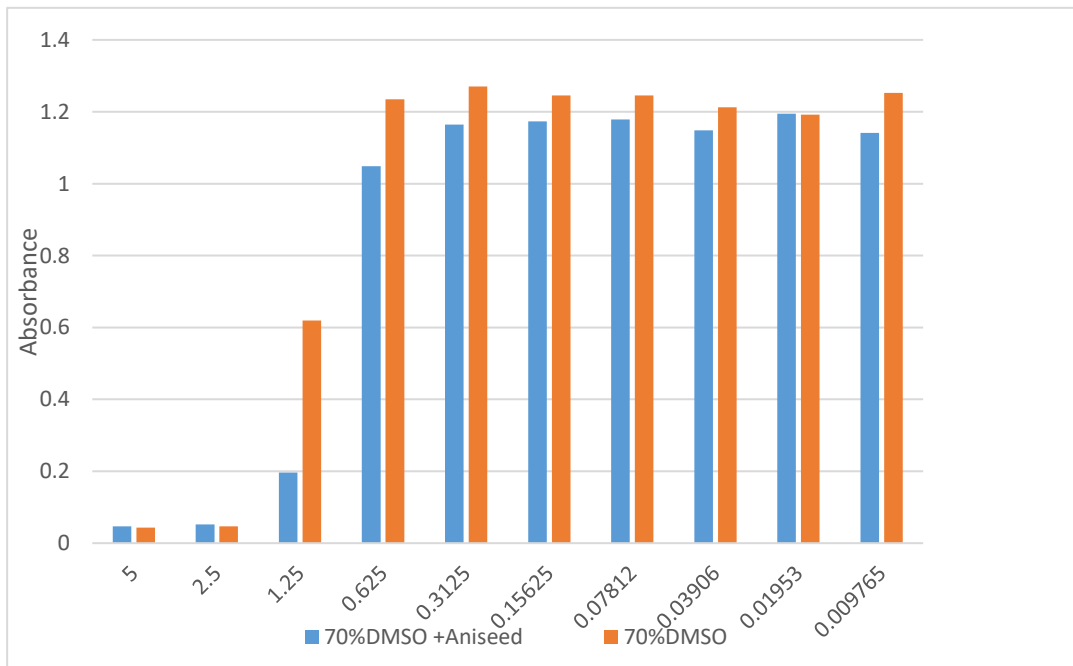
The minimum inhibitory concentration (MIC) assay was used to determine the minimum concentration of aniseed and flaxseed EO required to inhibit bacterial growth using micro-broth dilution method. The oil was dissolved in dimethyl sulfide (DMSO) at different percentages of DMSO (100%, 70%, 50% and 10%) and decreasing concentrations of EO. Histograms of MIC values of the EO from aniseed and flaxseed in DMSO at different concentrations against *S. sonnei* are shown in Figure 10. In each case, the different percentages of DMSO without the EO were also investigated for their antimicrobial activities as controls (orange bars in the graphs).

The result showed that aniseed EO dissolved in 100%DMSO exerted antimicrobial effect on the bacteria. However, 100% DMSO without aniseed showed similar antimicrobial effects (Figure 10A). The concentration of DMSO was reduced to 70% and similar results as those obtained with 100% DMSO were seen (Figure 10B). This led to a reduction in the % DMSO to 50%. Again, similar results as the first two assays were observed with aniseed EO + 50% DMSO and 50% DMSO showing identical antimicrobial effect against *S. sonnei* (Figure 10C). To ascertain the antimicrobial impact of aniseed EO, the starting concentration of aniseed EO was increased from 5 mg/ml to 100 mg/ml and the % DMSO was decreased to 10%. With these changes, the antimicrobial effect of 10% DMSO was very small compared to 100 mg/ml and 50 mg/ml aniseed EO + 10%DMSO (Figure 10D). The technical replicates of these experiments were not conducted due to the observed antimicrobial impact of DMSO.

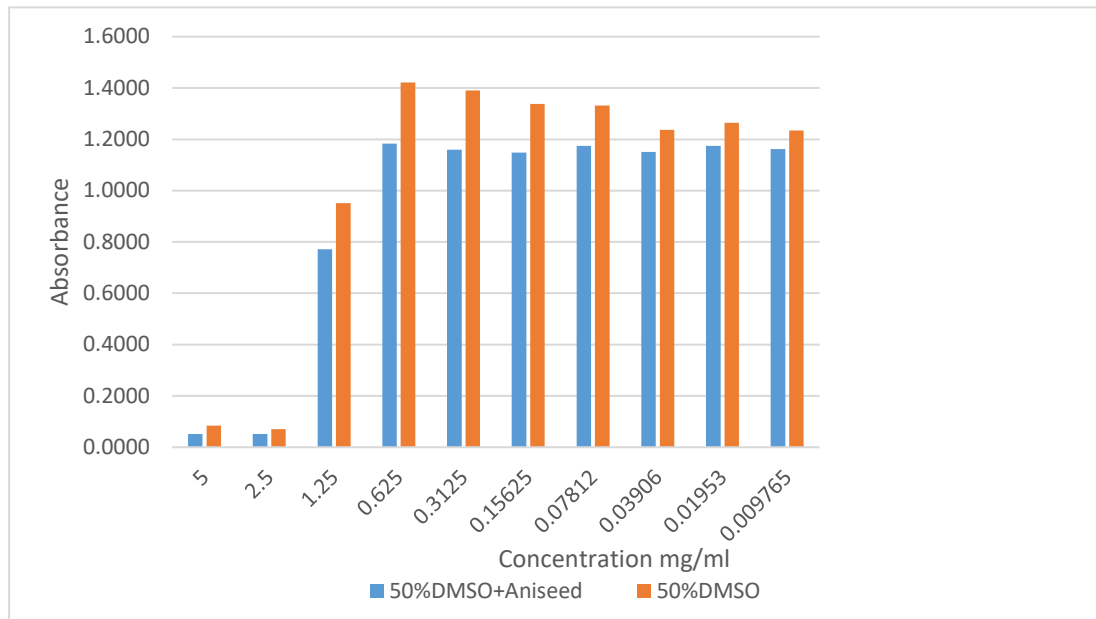
A



B



C



D

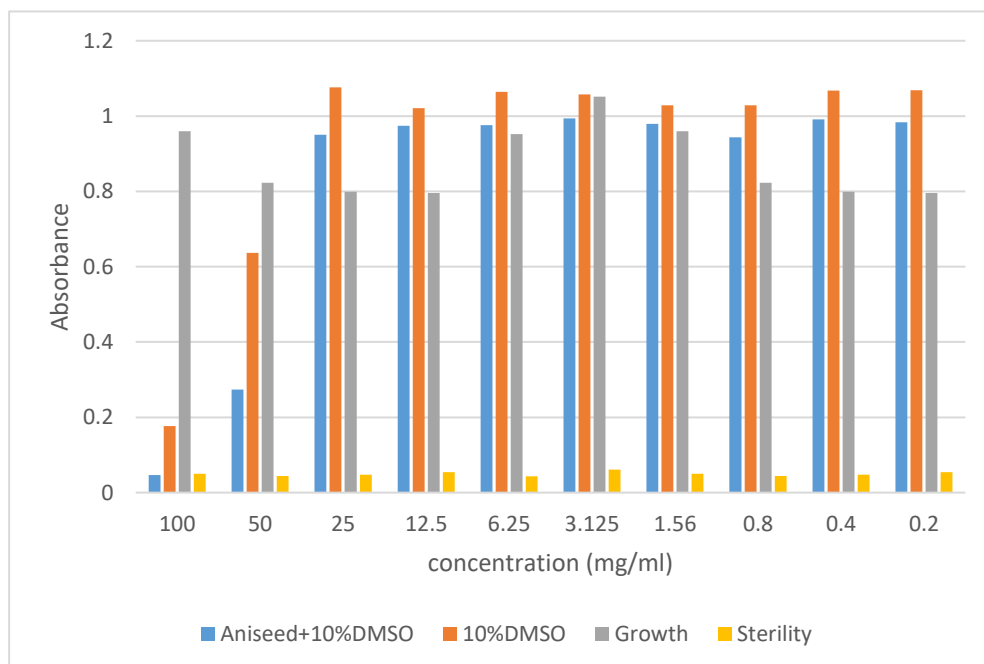
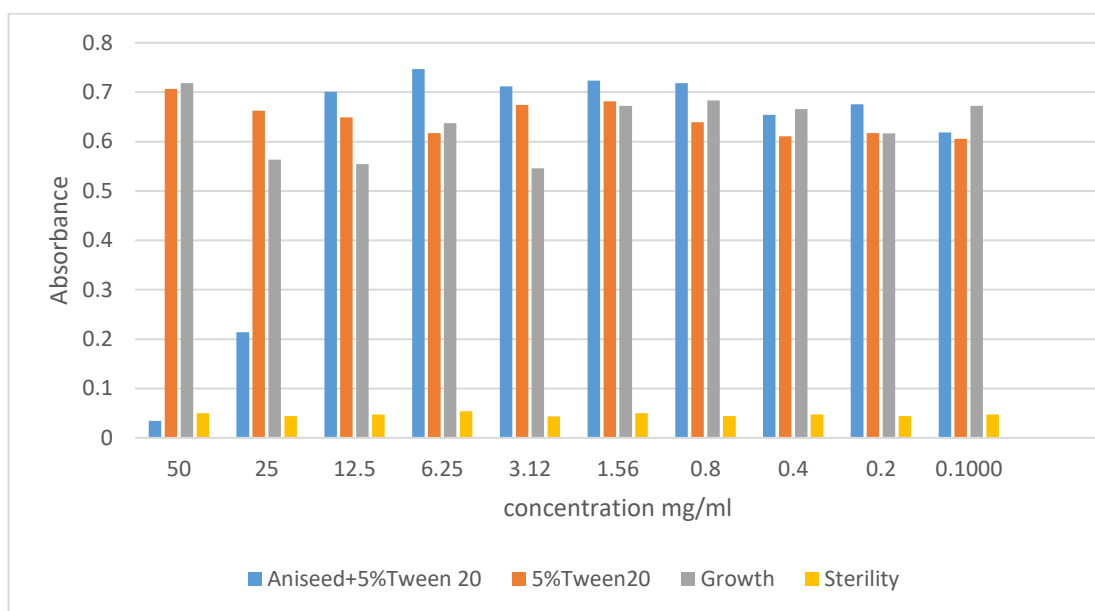


Figure 10. MIC assay of aniseed EO dissolved in DMSO. A: aniseed EO +100% DMSO, B: aniseed EO+70% DMSO, C: aniseed EO + 50% DMSO and D: aniseed EO + 10% DMSO. Colours indicate different conditions tested. Blue: aniseed EO +DMSO, orange: DMSO, gray: growth of bacteria without aniseed EO or DMSO and yellow: sterility control containing Mueller Hinton broth alone.

Although there was significant antimicrobial impact of aniseed EO (100 mg/ml and 50 mg/ml) on the growth *S. sonnei* compared to the impact of 10% DMSO as shown in Figure 10D, 10% DMSO still showed some inhibitory effect on the bacteria. To circumvent this, different concentrations of Tween 20 were used to dissolve the oil. The effect of Tween 20 on the bacteria without the essential oil was also investigated. The results showed that 5% and 2% Tween 20 had no antimicrobial effect on the growth of the bacteria as growth of *S. sonnei* in those levels of Tween 20 without aniseed EO was identical to the growth of the bacteria without aniseed or Tween 20.

A



B

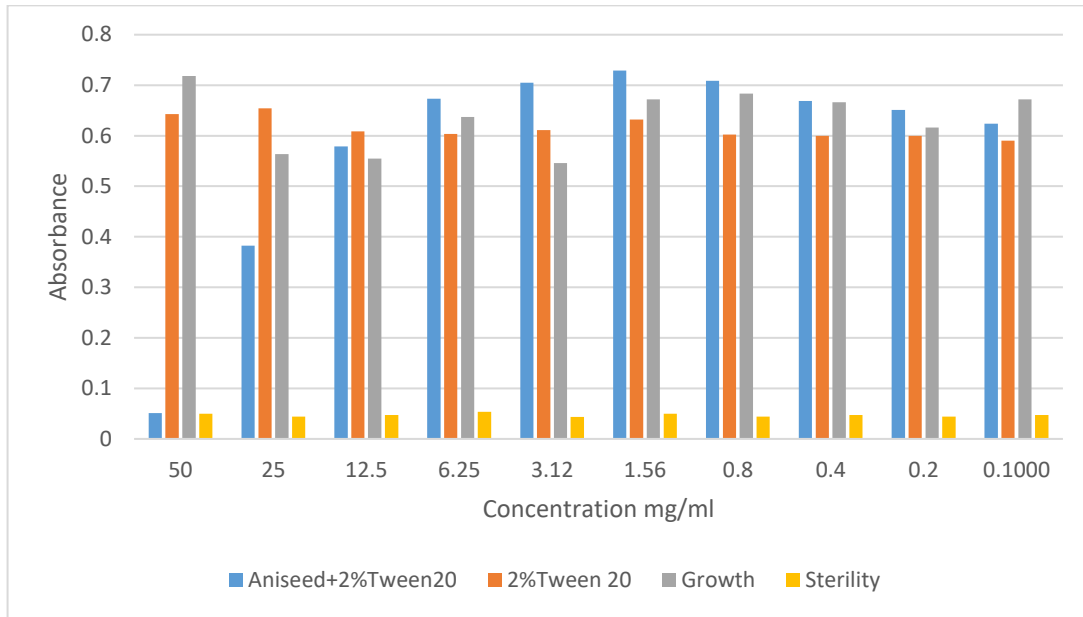


Figure 11. MIC assay of aniseed EO dissolved in Tween 20. A: aniseed EO +5% Tween 20 and B: aniseed EO + 2% Tween 20. Colours indicate different conditions tested. Blue: aniseed EO +Tween 20, orange: Tween 20, gray: growth of bacteria without EO or Tween 20 and yellow: sterility control.

Tween 20 was further reduced to 1%. Due to the solubility of the EO in 1% Tween 20 and the fact that these levels of Tween 20 had no antimicrobial activity (data not shown), the three technical replicates of the MIC assay were conducted with 1% Tween 20 as the solvent as shown in Table 6. The MIC of aniseed EO against *S. sonnei* was determined. The aniseed EO was dissolved in 1% Tween 20. Growth control, sterility control and 1% Tween 20 without aniseed EO were reported. The MIC results as shown in Table 6 and Figure 12 indicated that the MIC of aniseed EO was 50 mg/ml.

Table 6. Minimum inhibitory assay of aniseed EO.
Concentration of EO (mg/ml)

Sample	100	50	25	12.5	6.25	3.125	1.56	0.78	0.39	0.19
Growt h control	0.60 5 ± 0.00 3	0.605 ± 0.003	0.605 ± 0.003	0.605 ± 0.003	0.605 ± 0.003	0.605 ± 0.003	0.605 ± 0.003	0.605 ± 0.003	0.605 ± 0.003	0.605 ± 0.003
Sterilit y control	0.05 6 ± 0.00 2	0.056 ± 0.002	0.056 ± 0.002	0.056 ± 0.002	0.056 ± 0.002	0.056 ± 0.002	0.056 ± 0.002	0.056 ± 0.002	0.056 ± 0.002	0.056 ± 0.002
1% Tween 20	0.66 7 ± 0.02	0.652 ± 0.02	0.605 ± 0.02	0.608 ± 0.02	0.622 ± 0.02	0.633 ± 0.02	0.608 ± 0.02	0.598 ± 0.02	0.592 ± 0.02	0.582 ± 0.02
Anisee d EO +1% Tween 20	0.05 1 ± 0.02	0.051 ± 0.04	0.382 ± 0.04	0.578 ± 0.009	0.673 ± 0.05	0.705 ± 0.02	0.728 ± 0.01	0.668 ± 0.05	0.650 ±0.01	0.524 ± 0.01

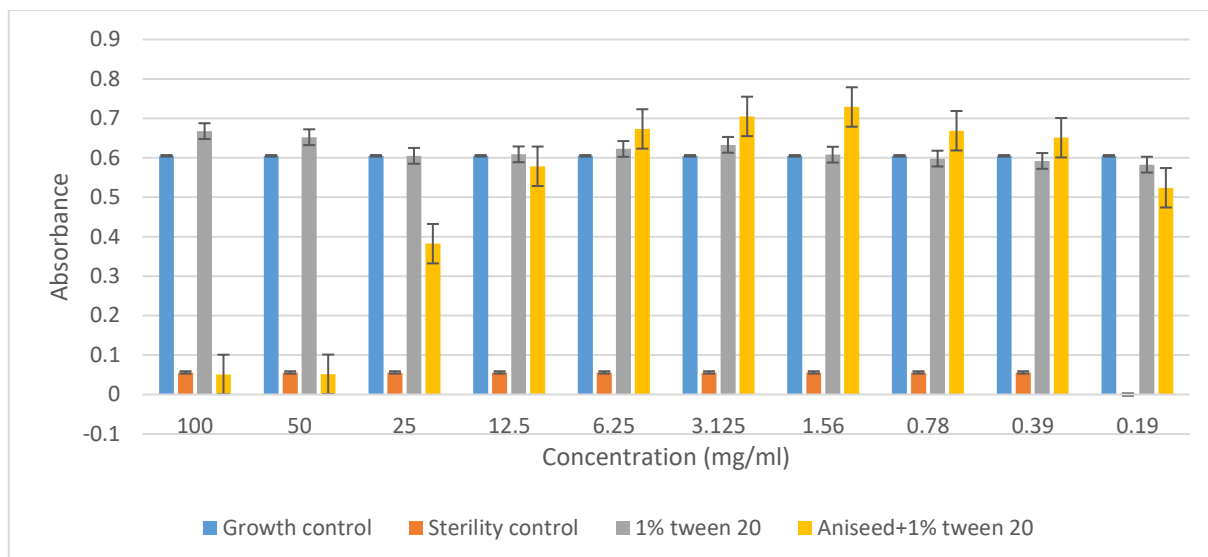


Figure 12. Histogram showing the growth rate of *S. sonnei* at decreasing concentrations of aniseed EO + 1% Tween 20. Colours indicate different conditions tested. Yellow: aniseed+Tween 20, gray: Tween 20, blue: growth of bacteria without aniseed nor Tween 20 and orange: sterility control (no bacteria).

The MIC of flaxseed EO against *S. sonnei* was also determined. The flaxseed EO was dissolved in 1% Tween 20. Growth control, sterility control and 1% Tween 20 without flaxseed EO were also tested. The MIC result as shown in Table 7 and Figure 13 indicated that the MIC of flaxseed EO against *S. sonnei* was 100 mg/ml which was two-fold higher than that of aniseed.

Table 7. Minimum inhibitory assay of flaxseed EO.

Concentration of EO (mg/ml)

Sample	100.00 0	50.000	25.000	12.50 0	6.250	3.125	1.560	0.780	0.390
Growth control	0.605 ± 0.003	0.605 ± 0.003	0.605 ± 0.003	0.605 ± 0.003	0.605 ± 0.003	0.605 ± 0.003	0.605 ± 0.003	0.605 ± 0.003	0.605 ± 0.003
Sterility control	0.056 ± 0.002	0.056 ± 0.002	0.056 ± 0.002	0.056 ± 0.002	0.056 ± 0.002	0.056 ± 0.002	0.056 ± 0.002	0.056 ± 0.002	0.056 ± 0.002
1% Tween 20	0.668 ± 0.020	0.652 ± 0.020	0.605 ± 0.020	0.609 ± 0.020	0.623 ± 0.020	0.633 ± 0.020	0.608 ± 0.020	0.598 ± 0.020	0.592 ± 0.020
Flaxseed EO+ 1% Tween 20	0.076± 0.010	0.347 ± 0.010	0.499 ± 0.020	0.685 ± 0.050	0.627 ± 0.008	0.703 ± 0.030	0.675 ± 0.020	0.622 ± 0.010	0.627 ± 0.008

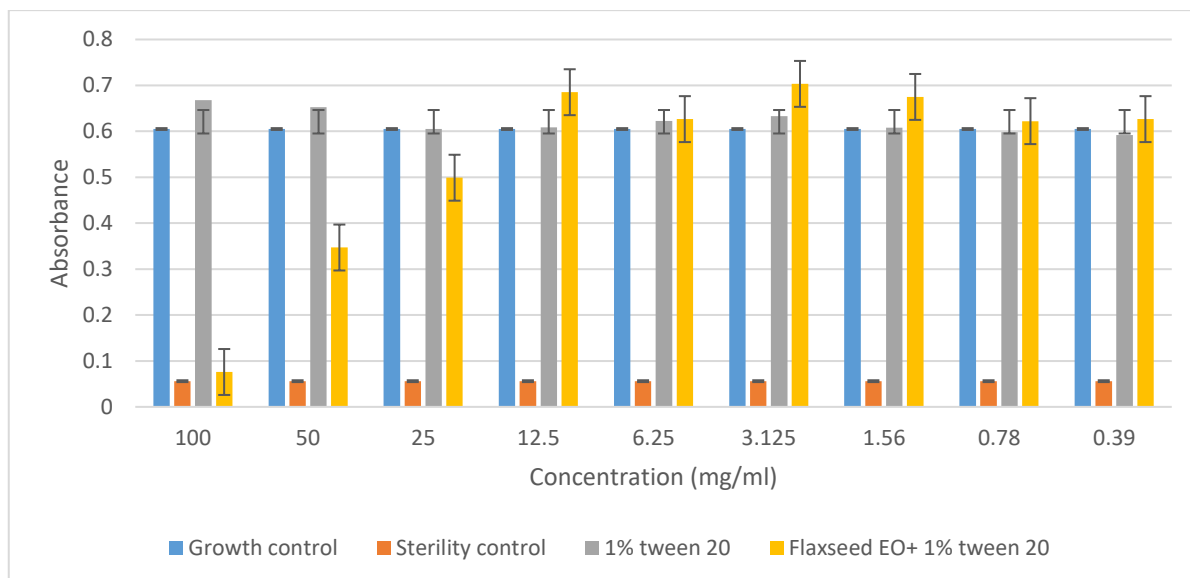
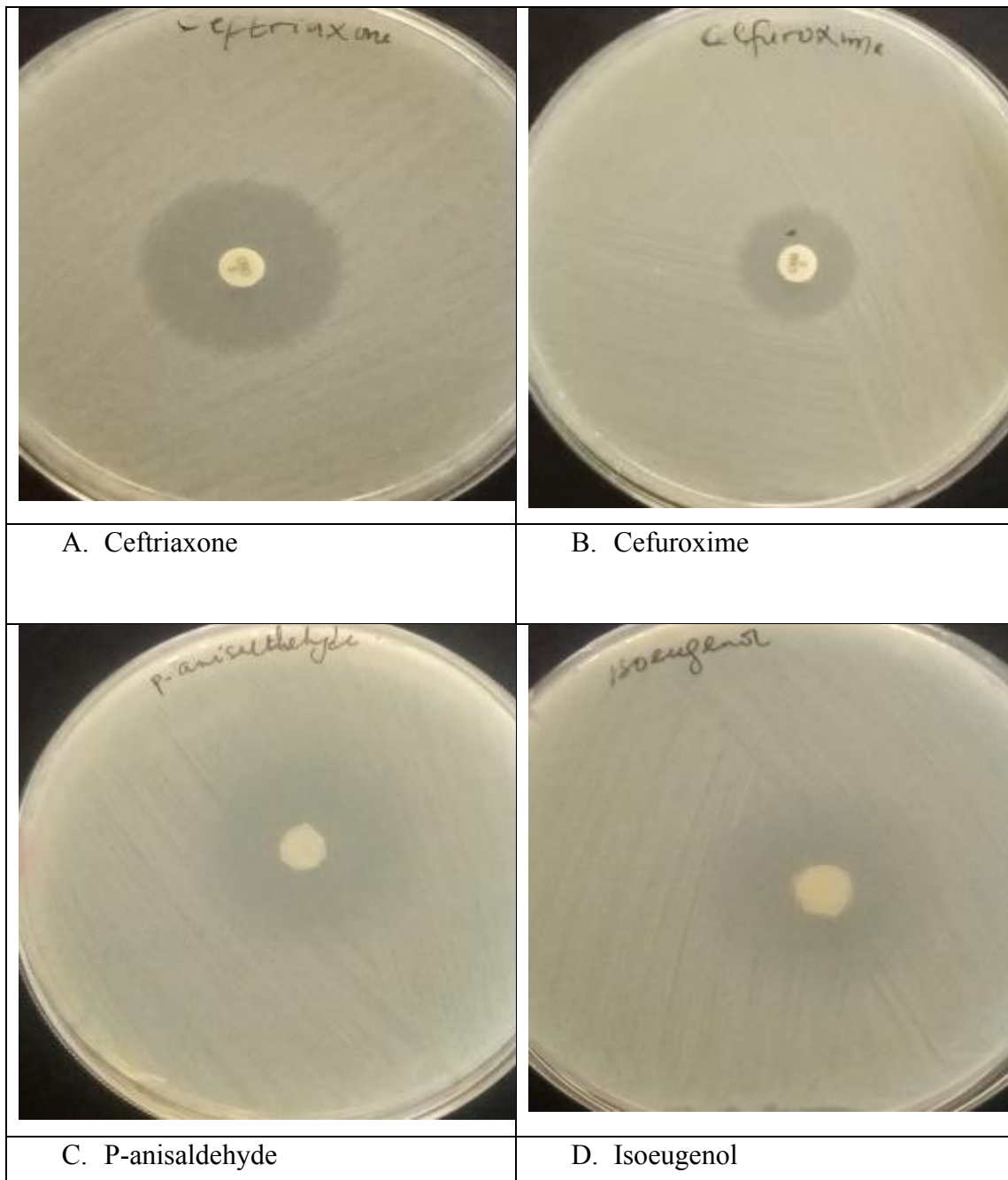


Figure 13. Histogram showing the growth rate of *S. sonnei* at decreasing concentrations of flaxseed EO + 1% Tween 20. Colours indicate different conditions tested. Yellow: aniseed+Tween 20, gray: Tween 20, blue: growth of bacteria without aniseed nor Tween 20 and orange: sterility control.

3.7.3. Qualitative and quantitative analysis of the most promising compounds from aniseed and flaxseed

Agar disc diffusion and MIC assays were carried out to evaluate the antimicrobial activity of the most promising components of aniseed (isoeugenol and p-anisaldehyde) and flaxseed (SDG) on *S. sonnei* in vitro. The effects of anethole, a major component of aniseed oil, were also tested to confirm its low potency as an antimicrobial agent as revealed from the in-silico analysis. The growth inhibitory activity of the most promising compounds was inspected and the zones of growth inhibition for each compound are shown in Figure 14A- F. Ceftriaxone and cefuroxime were used as controls because they are administered as antibiotics against Shigella infection. The histogram representation of the zone of *S. sonnei* growth inhibition is shown in Figure 15. The results showed that *S. sonnei* was highly susceptible to the control antibiotic ceftriaxone, p-anisaldehyde and isoeugenol from aniseed with zones of inhibition of 34 mm, 32 mm and 34 mm, respectively. The bacteria were also sensitive to the antibiotic cefuroxime and SDG from flaxseed with each showing a zone of inhibition of 20 mm. Anethole, however, showed a zone of inhibition of 10 mm. This result suggests that low concentrations of p-

anisaldehyde, isoeugenol and SDG would be required to inhibit the growth of the bacteria. Moreover, these phytochemicals were just as effective as the antibiotics at controlling bacterial growth. For anethole, a higher concentration would be required. These assumptions were confirmed by the quantitative analysis (MIC) where the minimum inhibitory concentration of each compound was determined.



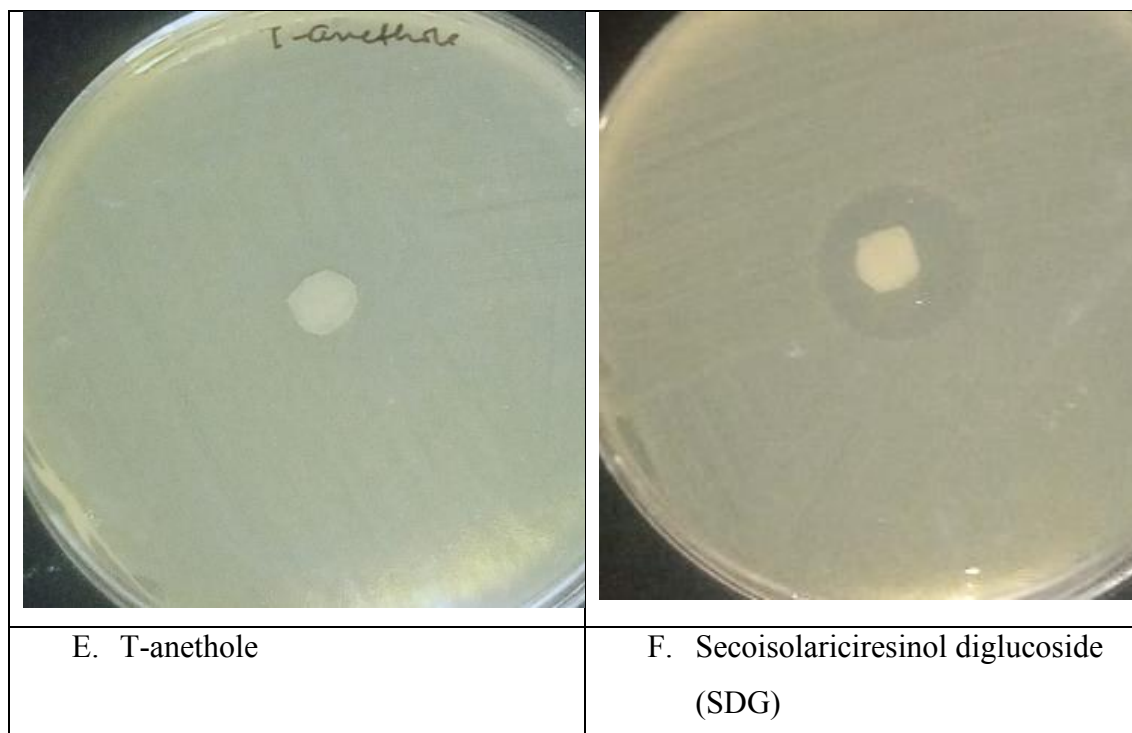


Figure 14. A and B show the zones of growth inhibition by antibiotic control, ceftriaxone, and cefuroxime, respectively. C and D shows zones of growth inhibition by the most promising compounds; isoeugenol and p-anisaldehyde from aniseed. E shows the zone of growth inhibition by anethole, a component of aniseed. Figure F shows the zone of growth inhibition by SDG from flaxseed.

Following the qualitative assay, the MIC of each compound against the bacteria was determined. Table 8, 9,10, 11 and 12 display the MIC assays of ampicillin, p-anisaldehyde, isoeugenol, anethole and SDG against *S. sonnei* respectively. The ΔOD_{600nm} of *S. sonnei* in Mueller-Hinton broth (MHB) without any antimicrobial agent or control and MHB alone were also observed as growth and sterility controls, respectively. Ampicillin was used as control. Table 13 gives a summary the MIC values of the studied phytocompounds, and it shows that isoeugenol from aniseed had the lowest inhibitory concentration of 0.042 mg/ml followed by p-anisaldehyde from aniseed with MIC of 0.17 mg/ml. SDG from flaxseed came third with MIC of 0.25 mg/ml which was like ampicillin with MIC of 0.25 mg/ml. These MIC values were significantly low compared to those of the crude aniseed EO and flaxseed EO. The reason for this could be the low quantity of isoeugenol and p-anisaldehyde (0.13% and 0.25%, respectively) observed in aniseed and 6% w/w SDG recovered from flaxseed which indicates a need to

genetically enhance the synthesis of these phytochemicals in their respective sources and isolating them prior to use as antibiotic. The MIC of anethole, 49.4 mg/ml, was the highest. This was expected as the in silico assay predicted its instability with the protein targets. The chemical structures of the most promising compounds are shown in Figure 15.

Table 8. Minimum inhibitory assay of ampicillin
Concentration of Ampicillin (mg/ml)

Sample	2.000	1.000	0.500	0.250	0.120	0.060	0.030	0.010	0.007	0.003
MHB + bacteria	1.001 ± 0.030	1.001 ± 0.030	1.001 ± 0.030	1.001 ± 0.030	1.001 ± 0.030	1.001 ± 0.030	1.001 ± 0.030	1.001 ± 0.030	1.001 ± 0.030	1.001 ± 0.030
MHB	0.047 ±0.0 02	0.047 ± 0.002	0.047 ± 0.002	0.047 ±0.0 02	0.047 ±0.0 02	0.047 ±0.0 02	0.047 ±0.0 02	0.047 ±0.0 02	0.047 ±0.0 02	0.047 ±0.0 02
MHB + bacteria +Ampicil lin	0.055 ± 0.002	0.049 ±0.0 01	0.047 ±0.0 01	0.053 ±0.0 10	0.945 ± 0.100	1.042 ± 0.060	1.049 ± 0.030	1.035 ± 0.050	1.043 ± 0.008	1.035 ± 0.001

Table 9. Minimum inhibitory assay of p-anisaldehyde

Concentration of p-anisaldehyde (mg/ml)

Sample	11.1	5.59	2.79	1.39	0.67	0.35	0.17	0.09	0.04	0.02
	90	0	0	0	0	0	0	0	0	0
MHB + bacteria	1.00	1.00	1.00	1.00	1.00	1.00	1.00	1.00	1.00	1.00
	1	1	1	1	1	1	1	1	1	1
	±	±	±	±	±	±	±	±	±	±
	0.03	0.03	0.03	0.03	0.03	0.03	0.03	0.03	0.03	0.03
	0	0	0	0	0	0	0	0	0	0
MHB	0.04	0.04	0.04	0.04	0.04	0.04	0.04	0.04	0.04	0.04
	7	7	7	7	7	7	7	7	7	7
	±0.0	±0.0	±0.0	±0.0	±0.0	±0.0	±0.0	±0.0	±0.0	±0.0
	02	02	02	02	02	02	02	02	02	02
MHB + bacteria +p- anisaldeh yde	0.05	0.05	0.05	0.05	0.04	0.04	0.04	1.05	0.98	1.00
	8	4	9	9	9	9	8	1	5	1
	±	±	±	±	±	±	±	±	±	±
	0.02	0.00	0.04	0.00	0.00	0.02	0.00	0.05	0.00	0.01
		4	0	5	1	0	8	0	3	0

Table 10. Minimum inhibitory assay isoeugenol

Concentration of Isoeugenol (mg/ml)

Sample	10.8 00	5.40 0	2.70 0	1.30 0	0.67 0	0.33 0	0.16 0	0.08 0	0.04 2	0.02 0
MHB + bacteria	1.00 1 ± 0.03 0	1.00 1 ± 0.03 0	1.00 1 ± 0.03 0	1.00 1 ± 0.03 0	1.00 1 ± 0.03 0	1.00 1 ± 0.03 0	1.00 1 ± 0.03 0	1.00 1 ± 0.03 0	1.00 1 ± 0.03 0	1.00 1 ± 0.03 0
MHB	0.04 7 ±0.0 02	0.04 7 ±0.0 02	0.04 7 ±0.0 02	0.04 7 ±0.0 02	0.04 7 ±0.0 02	0.04 7 ±0.0 02	0.04 7 ±0.0 02	0.04 7 ±0.0 02	0.04 7 ±0.0 02	0.04 7 ±0.0 02
MHB + bacteria +Isoeuge nol	0.05 5 ± 0.00 3	0.05 4 ±0.0 06	0.05 9 ± 0.00 1	0.04 9 ± 0.02 0	0.04 6 ± 0.01 5	0.04 6 ± 0.00 4	0.04 9 ± 0.03 0	0.05 8 ± 0.03 0	0.05 0 ± 0.00 5	0.82 2 ± 0.01 0

Table 11. Minimum inhibitory assay of anethole

Concentration of anethole (mg/ml)

Sample	98.8	49.4	24.7	12.3	6.17	3.09	1.54	0.77	0.38	0.19
	00	00	00	50	0	0	0	0	0	0
MHB + bacteria	1.00 1 ± 0.03 0	1.00 1 ± 0.03 0	1.00 1 ± 0.03 0	1.00 1 ± 0.03 0	1.00 1 ± 0.03 0	1.00 1 ± 0.03 0	1.00 1 ± 0.03 0	1.00 1 ± 0.03 0	1.00 1 ± 0.03 0	1.00 1 ± 0.03 0
MHB	0.04 7 ±0.0 02	0.04 7 ±0.0 02	0.04 7 ±0.0 02	0.04 7 ±0.0 02	0.04 7 ±0.0 02	0.04 7 ±0.0 02	0.04 7 ±0.0 02	0.04 7 ±0.0 02	0.04 7 ±0.0 02	0.04 7 ±0.0 02
MHB + bacteria +Aneth ole	0.05 0 ± 0.04 0	0.04 7 ± 0.02 0	0.95 3 ± 0.00 1	0.94 8 ± 0.00 6	1.00 3 ±0.0 10	0.97 6 ± 0.00 5	0.96 3 ± 0.05 0	0.96 9 ± 0.04 0	1.07 0 ± 0.00 3	1.00 2 ± 0.00 4

Table 12. Minimum inhibitory assay of SDG

Concentration of SDG (mg/ml)

Samp le	1.000	0.500	0.250	0.120	0.060	0.030	0.015	0.008	0.004	0.002
MHB	1.001	1.001	1.001	1.001	1.001	1.001	1.001	1.001	1.001	1.001
+ bacte ria	± 0.030	± 0.030	± 0.030	± 0.030	± 0.030	± 0.030	± 0.030	± 0.030	± 0.030	± 0.030
MHB	0.047	0.047	0.047	0.047	0.047	0.047	0.047	0.047	0.047	0.047
	±0.00	±0.00	±0.00	±0.00	±0.00	±0.00	±0.00	±0.00	±0.00	±0.002
	2	2	2	2	2	2	2	2	2	
MHB	0.054	0.047	0.058	0.678	0.822	0.986	0.793	0.978	0.822	1.009
+ bacte ria +SD G	± 0.010	± 0.001	± 0.050	± 0.007	± 0.020	± 0.003	± 0.010	± 0.004	± 0.006	± 0.009

Table 13. Minimum inhibitory concentrations of most promising compounds against *S.**sonnei*

Phytocompounds	MIC (mg/ml)
Ampicillin (control)	0.25
P-anisaldehyde	0.17
Isoeugenol	0.04
Secoisolariciresinol diglucoside (SDG)	0.25
Anethole	49.4

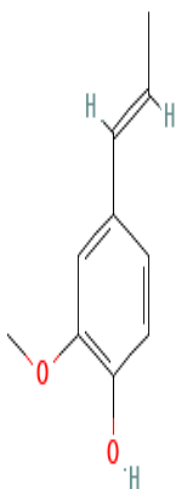
3.7.4 Mode of action

The mode of action of an antimicrobial agent could either be bactericidal or bacteriostatic with the former meaning the antimicrobial agent kills 99.9% of the bacteria. Bacteriostatic means that the antimicrobial agent suppresses the bacteria growth by restraining it at its stationary phase. MBC of crude aniseed EO, flaxseed EO, anethole, isoeugenol, p-anisaldehyde and SDG were investigated as shown in Table 14. MBC is the minimum concentration of an antimicrobial agent required to kill 99.9% of the bacteria. The result shows that the MBCs of p-anisaldehyde, isoeugenol and SDG were twice their MICs while ampicillin has the same MBC value as its MIC. Although the ΔOD_{600nm} of *S. sonnei* treated with anethole, aniseed and flaxseed at concentration 49.4 mg/ml, 50 mg/ml, and 100 mg/ml, respectively, was approximately 0.05 which indicates their MIC, their MBC values were not obtained which suggests they may have a bacteriostatic effect on *S. sonnei*.

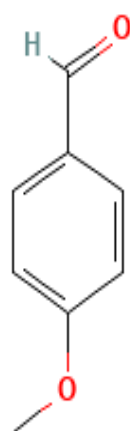
Table 14. Minimum bactericidal concentrations of EO and phytochemicals.

Antimicrobial agents	MBC (mg/ml)
Ampicillin	0.25
P-anisaldehyde	0.34
Isoeugenol	0.084
Secoisolariciresinol diglucoside (SDG)	0.50
Anethole	-
Aniseed EO	-
Flaxseed EO	-

Isoeugenol



P-anisaldehyde



SDG

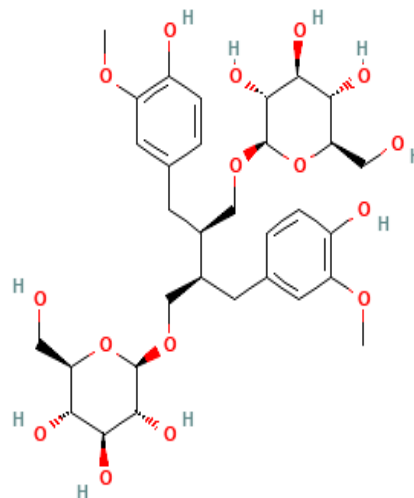


Figure 15. Chemical structures of the most promising antimicrobial agent from aniseed and flaxseed.

3.8. The bioactive compounds

This study indicates that isoeugenol and p-anisaldehyde are the most promising antimicrobial agents from aniseed while SDG is the most promising compound from flaxseed when tested against *S. sonnei*. Similarly, Ehab et al. (2008) and Rosa et al. (2019) reported isoeugenol's efficacy against *Mycobacterium smegmatis* and *Staphylococcus aureus*, respectively. Likewise, Chung et al. (2023) reported the antibacterial impact of p-anisaldehyde when cross-linking with kiwifruit DNA against *Klebsiella pneumoniae*, *Pseudomonas aeruginosa* and *Staphylococcus aureus*. Rajesha et al. (2010) reported the antimicrobial effect of SDG against *Pseudomonas aeruginosa*, *Staphylococcus aureus*, *Bacillus subtilis*, *Agrobacterium tumefaciens*, *Bacillus cereus* and *Escherichia coli*. Bai et al. (2022) reported that eugenol has an antimicrobial effect on *Shigella flexneri* with a MIC of 0.5 mg/ml which was higher compared to the MIC of isoeugenol, p-anisaldehyde and SDG as shown in Table 13. Mathabe et al. (2008) also reported the antimicrobial effect of *Spirostachys africana* stem bark against *S. sonnei*. Although the report showed that the MIC of the plant crude extract was 0.625mg/ml which is lower than the MIC of crude aniseed and flaxseed as shown in Table 6 and 7, the isolated bioactive compounds

of the plant which were acetyl aleuritic acid, lupeol, ent-2,6 α -dihydroxy-norbeyer-1,4,15-trien-3-one (diosphenol 2) and ent-3 β -hydroxy-beyer-15-ene-2-one each had MIC of 0.2 mg/ml which was higher than the MIC obtained from isoeugenol (0.04 mg/ml) and p-anisaldehyde (0.17 mg/ml). On the other hand, 4-methoxysalicylaldehyde from *Periploca sepium* oil showed similar inhibitory activity (MIC: 0.04 mg/ml) as isoeugenol against *S. sonnei* which was also 0.04 mg/ml. These results further emphasize the importance of identifying and isolating bioactive components of a plant in plant-based drug discovery.

CHAPTER 4

CONCLUSION

The aim of this study was to evaluate the pharmaceutical potential of aniseed and flaxseed EO against *S. sonnei* and this was achieved through study of their antimicrobial potential both *in silico* and *in vitro*. Firstly, the major phytoconstituents of both plants were identified and investigated for their antimicrobial effect *in silico* against the enzymes of the shikimate pathway and T3SS ATPase. The promising compounds revealed from the molecular docking and molecular dynamics simulation studies were then assessed for their ADMET properties where the result presented isoeugenol and p-anisaldehyde as most promising compounds from aniseed and SECO from flaxseed. Furthermore, *in vitro* analyses to determine the antimicrobial activity of crude aniseed and flaxseed EOs and their promising phytochemicals against *S. sonnei* were performed which confirmed that isoeugenol, p-anisaldehyde and SDG are promising antimicrobial agents against *S. sonnei*. Conclusions cannot be inferred as regards whether isoeugenol or SDG was the more potent antimicrobial agent as the isoeugenol used was synthesized and chemically standardized contrary to SDG which was isolated in-house. However, the result obtained from the antimicrobial analysis of the crude aniseed and flaxseed EO indicates the importance of isolating the bioactive components of these plants as their respective individual bioactive compounds showed higher potency than the crude oil. To further ascertain the mechanism of action of isoeugenol, p-anisaldehyde and SDG, proteomic assay of the bacterium treated with these phytochemicals should be conducted. This could show whether other metabolic pathway(s) are affected by the phytochemicals.

REFERENCES

- Abraham M.J., Murtola T., Schulz R., Páll S., Smith J.C., Hess B. 2015. “GROMACS: High performance molecular simulations through multi-level parallelism from laptops to supercomputers”. *SoftwareX*, 1-2.
- Afroze F., Ahmed, T., Sarmin M., Shahid A., Shahunja K. M., Shahrin L., Chisti M. J. 2017. “Risk factors and outcome of Shigella encephalopathy in Bangladeshi children”. *PLoS Neglected Trop. Dis.* 11 (4), e0005561 DOI: 10.1371/journal.pntd.0005561.
- Ahmed M. Amer, Usama I. Aly. 2019. “Antioxidant and antibacterial properties of anise (*Pimpinella anisum L.*)”. *Egyptian Pharmaceutical Journal*, 18:68–73.
- Anderson A.C. 2003. “The process of structure-based drug design”. *Chem. Biol.*, 10, pp. 787-97.
- Apoorva B Badiger, Triveni M Gowda, Rajarajeshwari S, Satish Saswat Majhi, Tarun Kumar and DS Mehta. 2019. “Antimicrobial effect of flaxseed (*Linum usitatissimum*) on periodontal pathogens: An in vitro study”. *International Journal of Herbal Medicine*; 7(3): 16-19.
- Arora N., Banerjee A.K. and Murty U.S.N. 2010. “*In silico* characterization of Shikimate Kinase of *Shigella flexneri*: A potential drug target”. *Interdiscip Sci Comput Life Sci* 2, 280–290. <https://doi.org/10.1007/s12539-010-0012-2>.
- Baker S., The H.C. 2018. “Recent insights into Shigella”. *Current Opinion in Infectious Diseases* 31: 449–54.
- Bai X, Li X, Liu X, Xing Z, Su R, Wang Y, Xia X, Shi C. 2022. “Antibacterial Effect of Eugenol on *Shigella flexneri* and Its Mechanism.” *Foods*; 11(17):2565. <https://doi.org/10.3390/foods11172565>.
- Balachandran N., Heimhalt M., Liuni P., To F., Wilson D.J., Junop M.S., Berti P.J. 2016. “Potent Inhibition of 3-Deoxy-d-arabinoheptulosonate-7-phosphate (DAHP) Synthase by DAHP Oxime, a Phosphate Group Mimic”. *Biochemistry* 55: 6617-6629.
- Barbary O.M., El-Sohaimy S.A., El-Saadani M.A., Zeitoun A.M.A. 2010. “Antioxidant, Antimicrobial and Anti-HCV Activities of Lignan Extracted from Flaxseed”. *Research Journal of Agriculture and Biological Sciences*, 6(3): 247-256.
- Basma Ezzat Mustafa, Pram Kumar Subramaniam, Nazih Shaban Mustafa, Muhannad Ali Kashmoola, Khairani Idah Mokhtar, Haitham Qaralleh. 2018. “The anti-fungal effect of flax seed on oral candidiasis: Comparative In-Vitro Study” Clinical article. *J Int Dent Med Res*; 11(2): pp. 580-586.
- Basma Ezzat Mustafa Alahmad, Muhannad Ali Kashmoola, Pram Kumar Subramaniam, Khairani Idah Binti Mokhta, Nazih shaban Mustafa, Omar Abdul

- Jabbar Abdul Qader, Nur Dalila Binti Zolkofli , Wan Nor Syahirah Binti Wan Hassan , Mustafa Nameer Shaban, Nurul Fatimah Mohamed Yusoff. 2018. *Journal of pharmacy and pharmaceutical sciences*; 7 (11), 1-11.
- Berendsen H.J.C., Van der Spoel D., Van Drunen. R. 1995. "GROMACS: A message-passing parallel molecular dynamics implementation". *Computer Physics Communications*, 91 (1), pp. 43-56.
- Berendsen H. J. C., Postma J. P. M., Gunsteren W. F. V, DiNola A., Haak J. R. 1984. "Molecular dynamics with coupling to an external bath". *The Journal of Chemical Physics.*, 81 (8), pp. 3684-3690.
- Bergeron J.R.C., Worrall L.J., Sgourakis N.G., DiMaio F., Pfuetzner R.A., Felise H.B., Vuckovic M., Yu A.C., Miller S.I., Baker D. 2013. "A refined model of the prototypical Salmonella SPI-1 T3SS basal body reveals the molecular basis for its assembly". *PLOS Pathog.*, 9, e1003307.
- Bernal I., Börnicke J., Heidemann J., Svergun D., Horstmann J.A., Erhardt M., Tuukkanen A., Uetrecht, C., Kolbe M. 2019. "Molecular organization of soluble type III secretion system sorting platform complexes". *J. Mol. Biol.*, 431, 3787–3803.
- Berube B.J., Murphy K.R., Torhan M.C., Bowlin N.O., Williams, J.D., Bowlin, T.L., Moir, D.T., Hauser, A.R. 2017. "Impact of type III secretion effectors and of phenoxyacetamide inhibitors of type III secretion on abscess formation in a mouse model of *Pseudomonas aeruginosa* infection". *Antimicrob. Agents Chemother.*, 61, e01202-17.
- Bilal Shaker, Sajjad Ahmad, Jingyu Lee, Chanjin Jung, Dokyun Na. 2021. "In silico methods and tools for drug discovery". *Computers in Biology and Medicine*;137,104851.
- Billones J.B, Carrillo M.C, Organo V.G, Sy J. B, Clavio N. A, Macalino S. J, Emnacen I. A, Lee A. P, Ko P. K, Concepcion G. P. 2017. "In silico discovery and in vitro activity of inhibitors against Mycobacterium tuberculosis 7, 8-diaminopelargonic acid synthase (Mtb Bioa)". *Drug Des Devel Ther.* 11:563.
- BIOVIA D.S. 2015. "Discovery studio modeling environment" San Diego, Dassault Systemes, Release, 4.
- Bjelkmar P., Larsson P., Cuendet M.A., Hess B., Lindahl E. 2010. "Implementation of the CHARMM Force Field in GROMACS: Analysis of Protein Stability Effects from Correction Maps, Virtual Interaction Sites, and Water Models". *Journal of Chemical Theory and Computation*, 6 (2) pp. 459-466.
- Blair J.M.A., Webber M.A., Baylay A.J., Ogbolu D.O., Piddock L.J.V. 2015. "Molecular mechanisms of antibiotic resistance". *Nature Reviews Microbiology*, 13:42–51.

- Bloedon L.T, Balikai S., Chittams J. 2008. “Flaxseed and cardiovascular risk factors: results from a double blind, randomized, controlled clinical trial”. *J Am Coll Nutr*; 27(1):65-74
- Borriello S.P., Setchell K.D.R., Axelson M., Lawson A.M. 1985. “Production and metabolism of lignans by the human faecal flora”. *J. Appl. Bacteriol.*, 58, p. 37.
- Bovee L., Whelan J., Sonder G.J., van Dam A.P., van Den Hoek A. 2012. “Risk factors for secondary transmission of Shigella infection within households: implications for current prevention policy.” *BMC Infectious Diseases*, 12: 347.
- Browne S.H., Hasegawa P. Okamoto S., Fierer J., Guiney D.G. 2008. “Identification of Salmonella SPI-2 secretion system components required for SpvB-mediated cytotoxicity in macrophages and virulence in mice”. *FEMS*, 1, 194–201.
- Buch, T. Giorgino, G. De Fabritiis. 2011. “Complete reconstruction of an enzyme-inhibitor binding process by molecular dynamics simulations”. *Biophysics and computational biology* 108 (25) 10184-10189.
- Carayol N., Nhieu G.T.V. 2013. “The inside story of Shigella invasion of intestinal epithelial cells”. *Csh Perspect Med* 3: 1–13.
- Case H.B., Dickenson N.E. 2018. “Kinetic characterization of the Shigella type three secretion system ATPase Spa47 using α -³²P ATP”. *Bio-Protocol*, 8, e3074.
- Choo E.J., Rhee Y.H., Jeong S.J., Lee H.J., Kim H.S., Ko H.S., Kim J.H., Kwon T.R., Jung J.H., Kim J.H., Lee H.J, Lee H.J., Lee E.O., Kim D.K., Chen C.Y., Kim S.H. 2011. “Anethole Exerts Antimetastatic Activity via Inhibition of Matrix Metalloproteinase 2/9 and AKT/Mitogen-Activated Kinase/Nuclear Factor Kappa B Signaling Pathways”. *Biological and Pharmaceutical Bulletin*, 34: 41-46.
- Chen Z., Li Y., Chen E., Hall D.L., Darke P.L., Culberson C., Shafer J.A., Kuo L.C. 1994. “Crystal structure at 1.9-Å resolution of human immunodeficiency virus (HIV) II protease complexed with L-735,524, an orally bioavailable inhibitor of the HIV proteases”. *J. Biol. Chem.*, 269, pp. 26344-8.
- Christina Krogsgård Nielsen, Jørgen Kjems, Tina Mygind, Torben Snabe, Karin Schwarz, Yvonne Serfert, Rikke Louise Meyer. 2017. “Antimicrobial effect of emulsion-encapsulated isoeugenol against biofilms of food pathogens and spoilage bacteria”. *International Journal of Food Microbiology*; 242, 7-12.
- Chow H.S., Garland L.L., Hsu C.H., Vining D.R., Chew W.M., Miller J.A. 2010. “Resveratrol modulates drug-and carcinogen metabolizing enzymes in a healthy volunteer study”. *Cancer Prev Res.*, 3 pp. 1168-1175.
- Cohen D., Sela T., Slepon R., Yavzori M., Ambar R., Orr N., Robin G., Shpielberg O., Eldad A., Green M. 2011. “Prospective cohort studies of shigellosis during military field training”. *European Journal of Clinical Microbiology & Infectious Diseases*, 20: 123–126.

- Cowan M.M. 1999. "Plant products as antimicrobial agents". *Clinical Microbiology Reviews*, 12: 564–582.
- Daina A., Michielin, O., Zoete, V. 2017. "SwissADME: a free web tool to evaluate pharmacokinetics, drug-likeness and medicinal chemistry friendliness of small molecules". *Sci Rep* 7, 42717. <https://doi.org/10.1038/srep42717>.
- Darden T., York D., Pedersen L. 1993. "Particle mesh Ewald: An N·log(N) method for Ewald sums in large systems". *The Journal of Chemical Physics*, 98 (12), pp. 10089-10092.
- Dobbins, T.A., Wiley, D.B. 2004: US20046806356.
- Duncan M.C., Linington R.G., Auerbuch V. 2012. "Chemical inhibitors of the type three secretion system: Disarming bacterial pathogens". *Antimicrob. Agents Chemother.*, 56, 5433–5441.
- Ehab A. Abourashed, Ahmed M. Galal, Atef M. Shebl, Jaber S. Mossa. 2008. "Enhancing Effect of Isoeugenol on the Antimicrobial Activity of Isoniazid, 6-Paradol and 6-Shogaol". *Journal of Herbs, Spices and Medicinal Plants*, 13:4, 95-103, DOI: [10.1080/10496470801946075](https://doi.org/10.1080/10496470801946075).
- Eric Pettersen F., Thomas Goddard D., Conrad Huang C., Gregory Couch S., Daniel Greenblatt M., Elaine Meng C., Thomas Ferrin E. 2004. "UCSF Chimera—A visualization system for exploratory research and analysis". *Journal of Computational Chemistry*, 25: 1605-1612.
- Erler F., Ulug I., Yalcinkaya B. 2006. "Repellent activity of five essential oils against *Culex pipiens*". *Fitoterapia*, 77: 491–494.
- Fang-Yu Chung, Yi-Zhen Lin, Cheng-Rung Huang, Kuan-Wen Huang, Yu-Fon Chen. 2023. "Crosslinking kiwifruit-derived DNA with natural aromatic aldehydes generates membranolytic antibacterial nanogels". *International Journal of Biological Macromolecules*;255. <https://doi.org/10.1016/j.ijbiomac.2023.127947>.
- Fleming N. 2018. "How artificial intelligence is changing drug discovery". *Nature*. 2018; 557: S55-S57.
- Frank J., Eliasson C., Leroy-Nivard D., Budek A., Lundh T., Vessby B. 2004. "Dietary secoisolariciresinol diglucoside and its oligomers with 3-hydroxy-3-methyl glutaric acid decrease vitamin E levels in rats". *Br. J. Nutr.* 92 169–176. [10.1079/BJN20041154](https://doi.org/10.1079/BJN20041154).
- Franklyn De Silva S. and Jane Alcorn. 2019. "Flaxseed Lignans as Important Dietary Polyphenols for Cancer Prevention and Treatment: Chemistry, Pharmacokinetics, and Molecular Targets". *Pharmaceuticals.*; 12(2): 68.

- Fukumitsu S, Aida K, Shimizu H, Toyoda K. 2010. “Flaxseed lignan lowers blood cholesterol and decreases liver disease risk factors in moderately hypercholesterolemic men”. *Nutr Res.*; 30:441–6.
- Galan, J.E.; Waksman, G. 2018. “Protein-Injection Machines in Bacteria”. *Cell*, 172, 1306–1318.
- Gao, X., Mu, Z., Yu, X., Qin, B., Wojdyla, J., Wang, M., Cui, S. 2018. “Structural Insight into Conformational Changes Induced by ATP Binding in a Type III Secretion-Associated ATPase From *Shigella flexneri*”. *Front Microbiol* 9: 1468-1468.
- Gasteiger J, Marsili M. 1980. “Iterative partial equalization of orbital electronegativity—a rapid access to atomic charges”. *Tetrahedron* 36(22):3219–3228.
- Giri S., Bader A. 2015. “A low-cost, high-quality new drug discovery process using patient-derived induced pluripotent stem cells”. *Drug Discovery Today*, 20, pp. 37-49.
- Gu R., Wang Y., Long B., Kennelly E., Wu S., Liu B., Li P., Long C. 2014. “Prospecting for bioactive constituents from traditional medicinal plants through ethnobotanical approaches”. *Biological and Pharmaceutical Bulletin*, 37: 903–15.
- Gurunathan S., Thangaraj P., Das J., Kim J.H. 2023. Antibacterial and antibiofilm effects of *Pseudomonas aeruginosa* derived outer membrane vesicles against *Streptococcus mutans*. *Heliyon*. Nov 26;9(12)22606.
- Guoli Xiong, Zhenxing Wu , Jiakai Yi , Li Fu, Zhijiang Yang , Changyu Hsieh , Mingzhu Yin , Xiangxiang Zeng , Chengkun Wu , Aiping Lu , Xiang Chen , Tingjun Hou , Dongsheng Cao. 2021. “ADMETlab 2.0: an integrated online platform for accurate and comprehensive predictions of ADMET properties”. *Nucleic Acids Res* 2;49(W1): W5-W14.
- Gyawali R., Ibrahim S.A. 2014. “Natural products as antimicrobial agents”. *Food Control*, 46: 412–429.
- Hajipour M.J., Fromm K.M., Akbar Ashkarran A., Jimenez de Aberasturi D., Larramendi I.Rd., Rojo T., Serpooshan V., Parak W.J., Mahmoudi M. 2012. “Antibacterial properties of nanoparticles”. *Trends in Biotechnology*, 30:499–511.
- Haltalin K. C. and Nelson J. D. 1965. “In Vitro Susceptibility of *Shigella* to Sodium Sulfadiazine and to Eight Antibiotics”. *JAMA* 193, 705– 10
DOI:10.1001/jama.1965.03090090011002.

- Haltalin K. C., Nelson J. D., Ring R., Sladoje M., and Hinton, L. V. 1967. “Double-blind treatment study of shigellosis comparing ampicillin, sulfadiazine, and placebo”. *J. Pediatrics*. 70 (6), 970– 81. DOI: 10.1016/S0022-3476(67)80275-0.
- Haltalin K. C., Nelson J. D., Kusmiesz, H. T. 1973. “Comparative efficacy of nalidixic acid and ampicillin for severe shigellosis”. *Arch. Dis. Child*. 48 (4), 305– 12, DOI:10.1136/adc.48.4.305.
- Hardy, A. V. (1946). “Studies of the acute diarrheal diseases; the sulfonamides in shigellosis”. *Public Health Rep* 61, 857– 66, DOI: 10.2307/4585713.
- Herrmann K. M. 1995. “The shikimate pathway: early steps in the biosynthesis of aromatic compounds”. *Plant Cell* 7:907–919.
- Hess B., Bekker H., Berendsen H.J., Fraaije J.G. 1997. “LINCS: a linear constraint solver for molecular simulations”. *Journal of computational chemistry*, 18 (12), pp. 1463-1472.
- Hosseinian F. S, Muir A. D, Westcott N. D, Krol E. S. 2006. “Antioxidant capacity of flaxseed lignans in two model systems”. *J Am Oil Chem Soc*; 83:835-840.
- Humphrey, W., Dalke, A., Schulten, K. V. M. D. 1996. “Visual molecular dynamics”. *J. Mol. Graph.* 14, 33–38.
- Hyde K.D., Xu J.C., Lumyong S., Rapior S. 2019. “The amazing potential of fungi, 50 ways we can exploit fungi industrially”. *Fungal Diversity*, 97, 1e136.
- İlhami Gülçın, Münir Oktay, Ekrem Kireççi, Ö.İrfan Küfrevioğlu. 2003. “Screening of antioxidant and antimicrobial activities of anise (*Pimpinella anisum L.*) seed extracts”. *Food Chemistry*; 83 (3): 371-382.
- Imran M., Ahmad N., Anjum F.M. 2015. “Potential protective properties of flax lignan secoisolariciresinol diglucoside”. *Nutr J* 14, 71.
- Isidora Samojlik, Vesna Mijatović, Stojan Petković, Biljana Škrbić, Biljana Božin. 2012. “The influence of essential oil of aniseed (*Pimpinella anisum, L.*) on drug effects on the central nervous system”. *Fitoterapia*; 83 (8).
- Jenab M, Thompson L.U. 1996. “The influence of flaxseed and lignans on colon carcinogenesis and beta-glucuronidase activity”. *Carcinogenesis*.;17:1343–8.
- Jeong E.Y., Lee M.J., Kang M.S., Lee, H.S. 2018. “Antimicrobial agents of 4-methoxysalicylaldehyde isolated from *Periploca sepium* oil against foodborne bacteria: structure–activity relationship”. *Applied Biological Chemistry*, 61: 397–402.
- Jhoti H., Leach A.R. 2007. “Structure-based Drug Discovery”. Springer.

- Johnsson P., Kamal-Eldin A., Lundgren L. N. A man P. 2000. "HPLC method for analysis of secoisolariciresinol diglucoside in flaxseeds". *J. Agric. Food Chem*; 46, 5216-5219.
- Jorgensen W.L., Chandrasekhar J., Madura J. D., Impey R.W., Klein M.L. 1983. "Comparison of simple potential functions for simulating liquid water". *The Journal of chemical physics*, 79 (2), pp. 926-935.
- Jumper J., Evans R., Pritzel A. et al. 2021. "Highly accurate protein structure prediction with AlphaFold". *Nature* 596, 583–589. <https://doi.org/10.1038/s41586-021-03819-2>.
- Kahsay A.G., Muthupandian S.A. 2016. "Review on Sero diversity and antimicrobial resistance patterns of Shigella species in Africa, Asia and South America, 2001-2014". *BMC Research Notes*, 2016; 9: 422.
- Kaithwas G., Mukerjee A., Kumar P. et al. 2011. "*Linum usitatissimum* (linseed/flaxseed) fixed oil: antimicrobial activity and efficacy in bovine mastitis". *Inflammopharmacol* 19, 45–52. <https://doi.org/10.1007/s10787-010-0047-3>.
- Kempf D.J., Marsh K.C., Denissen J.F., McDonald E., Vasavanonda S., Flentge C.A., Green B.E., Fino L., Park C.H., Kong X.-P. 1995. "ABT-538 is a potent inhibitor of human immunodeficiency virus protease and has high oral bioavailability in humans". *Proc. Nat. Acad. Sci.*, 92, pp. 2484- 2488.
- Keyser P., Elofsson M., Rosell S., Wolf-Watz H. 2008. "Virulence blockers as alternatives to antibiotics: Type III secretion inhibitors against Gram-negative bacteria". *J. Intern. Med.*, 264, 17–29.
- Khalil I.A., Troeger C., Blacker B.F., Rao P.C., Brown A., Atherly D.E., Brewer T.G., Engmann C.M., Houpt E.R., Kang G., et al. 2018. "Morbidity and mortality due to Shigella and enterotoxigenic *Escherichia coli* diarrhoea: the Global Burden of Disease Study 1990–2016". *The Lancet Infectious Diseases*, 18: 1229-1240.
- Knaggs A.R. 2003. "The biosynthesis of shikimate metabolites". *Nat Prod Rep* 20:119–136.
- Kotloff K.L., Riddle M.S., Platts-Mills J.A. 2018. "Shigellosis". *Lancet*; 391:801–12.
- Kotloff K.L., Riddle M.S., Platts-Mills J.A., Pavlinac P., Zaidi A.K.M. 2018. "Shigellosis". *The Lancet*, 391: 801–12.
- Krohn A., Redshaw S., Ritchie J.C., B.J. Graves, M.H. Hatada. 1991. "Novel binding mode of highly potent HIV-proteinase inhibitors incorporating the (R)-hydroxyethylamine isostere". *J. Med. Chem.*, 34, pp. 3340-3342.

- Lipinski C. A, Lombardo F., Dominy B.W., Feeney P.J. 1997. “Experimental and computational approaches to estimate solubility and permeability in drug discovery and development settings”. *Adv Drug Deliv Rev* 23(1-3):3–25.
- Livivo S., Strockbine N.A., Panchalingam S., Tennant S.M., Barry E.M., Marohn M.E., Antonio M., Hossain A., Mandomando I., Ochieng J.B., et al. 2014. “Shigella isolates from the global enteric multicenter study inform vaccine development”. *Clinical Infectious Diseases*, 59: 933–41.
- Lyvia Layanne Silva Rosa, José Lucas Ferreira Marques Galvão, Hermes Diniz Neto, Jefferson Rodrigues Nóbrega, Daniele de Figuerêdo Silva, Francisco Patricio de Andrade Júnior, Pedro Thiago Ramalho de Figueiredo, Shellygton Lima Silva, Lâisa Vilar Cordeiro, Abrahão Alves de Oliveira Filho and Edeltrudes de Oliveira Lima. 2019. “Isoeugenol efficacy against Staphylococcus aureus”. *International Journal of Development Research*;09 (10):30877-30879.
- Ma X, Wang R, Zhao X, Zhang C, Sun J, Li J, et al. 2013. “Antidepressant-like effect of flaxseed secoisolariciresinol diglycoside in ovariectomized mice subjected to unpredictable chronic stress”. *Metab Brain Dis.*; 28:77–84.
- Majewski D.D., Worrall L.J., Hong C., Atkinson C.E., Vuckovic M., Watanabe N., Yu Z., Strynadka N.C.J. 2019. Cryo-EM structure of the homohexameric T3SS ATPase-central stalk complex reveals rotary ATPase-like asymmetry. *Nat. Commun.*, 10, 626.
- Manoj Kumar, Shikha Verma, Sujata Sharma, Alagiri Srinivasan, Tej P. Singh, Punit Kaur. 2010. “Structure-Based In silico Design of a High-Affinity Dipeptide Inhibitor for Novel Protein Drug Target Shikimate Kinase of Mycobacterium tuberculosis”. *Chemical Biology and Drug Design*; 76(3):277-84.
- Marcus Hanwell D., Donald Curtis E., David Lonie C., Tim Vandermeersch, Eva Zurek and Geoffrey Hutchison R. 2012. “Avogadro: An advanced semantic chemical editor, visualization, and analysis platform”. *Journal of Cheminformatics*, 4:17.
- Martin Y.C., Kofron J.L., Traphagen L.M. 2002. “Do structurally similar molecules have similar biological activity?”. *J. Med. Chem.*, 45, pp. 4350-4358.
- Marteyn B., West N.P., Browning D.F., Cole J.A., Shaw J.G., Palm F., Mounier J. Prévost M.-C., Sansonetti P., Tang C.M. 2010. “Modulation of Shigella virulence in response to available oxygen in vivo”. *Nat. Cell Biol.*, 465, 355S–358.
- Matlakala Christina Mathabe, Ahmed A. Hussein, Roumiana V. Nikolova, Adriaan E. Basson, J.J. Marion Meyer, Namrita Lall. 2008. “Antibacterial activities and cytotoxicity of terpenoids isolated from *Spirostachys Africana*”. *Journal of Ethnopharmacology*.116 (1), 194-197.<https://doi.org/10.1016/j.jep.2007.11.017>.
- Michel G., Roszak A.W., Sauve V., Maclean J., Matte A., Coggins J.R., Cygler M., Laphorn, A.J. 2003. “Structures of shikimate dehydrogenase AroE and its

- Paralog YdiB". A common structural framework for different activities". *J Biol Chem* 278: 19463-19472.
- Minamino T., Kawamoto A., Kinoshita M., Namba K. 2019. "Molecular organization and assembly of the export apparatus off flagellar type III secretion systems". *Curr. Topics Microbiol. Immunol.*, 427, 91–107.
- Newman D.J., Cragg G.M., Snader K.M. 2002. "Natural products as sources of new drugs over the period 1981-2002" *Journal of Natural Products*. 66: 1022–37.
- Nissim-Eliraz E., Nir E., Shoval I., Marsiano N., Nissan I., Shemesh H., Nagy N., Goldstein A.M., Gutnick M. Rosenshine I. 2017. "Microvascular thrombosis and ischemic enteritis in human gut xenografts infected with enteropathogenic *E. Coli*". *Infect. Immun.*, 85, e00558-17.
- Nordmann P., Naas T., Fortineau N., Poirel L. 2007. "Superbugs in the coming new decade; multidrug resistance and prospects for treatment of *Staphylococcus aureus*, *Enterococcus* spp. and *Pseudomonas aeruginosa* in 2010". *Current Opinion in Microbiology*, 10: 436-440.
- Nunes José E. S., Mario A. Duque, Talita F. de Freitas, Luiza Galina, Luis F. S. M. Timmers, Cristiano V. Bizarro, Pablo Machado, Luiz A. Basso, and Rodrigo G. Ducati. 2020. "Mycobacterium tuberculosis Shikimate Pathway Enzymes as Targets for the Rational Design of Anti-Tuberculosis Drugs". *Molecules*;25(6): 1259.
- Odeh A., Allaf A.W. 2017. "Determination of polyphenol component fractions and integral antioxidant capacity of Syrian aniseed and fennel seed extracts using GC–MS, HPLC analysis, and photochemiluminescence assay". *Chemical Papers*, 71: 1731–1737.
- Ogborn M R, Nitschmann E, Bankovic-Calic N, Weiler HA, Aukema HM. 2006. "Effects of flaxseed derivatives in experimental polycystic kidney disease vary with animal gender". *Lipids*; 41:1141–9.
- Paramashivam S.K., Elayaperumal K., Natarajan B., Devi M., Ramamoorthy, S. Balasubramanian, K.N. Dhiraviam. 2015. "In silico pharmacokinetic and molecular docking studies of small molecules derived from *Indigofera aspalathoides* Vahl targeting receptor tyrosine kinases". *Bioinformation*, 11, p. 73.
- Park I.K., Choi K.S., Kim D.H., Choi I.H., Kim L.S., Bak W.C., Choi J.W., Shin S.C. 2006. "Fumigant activity of plant essential oils and components from horseradish (*A Armoracia rusticana*), anise (*Pimpinella anisum*) and garlic (*Allium sativum*) oils against *Lycoriella ingenua* (Diptera: Sciaridae)." *Pest Management Science*, 62: 723– 728.
- Parrinello M., Rahman A. 1980. "Crystal Structure and Pair Potentials: A Molecular-Dynamics Study". *Physical Review Letters*, 45 (14), pp. 1196-1199.

- Paul S.M., Mytelka D.S., Dunwiddie C.T., Persinger C.C., Munos B.H., Lindborg S.R., Schacht A.L. 2010. "How to improve R&D productivity: the pharmaceutical industry's grand challenge." *Nat. Rev. Drug Discov.*, 9, pp. 203-214.
- Penumathsa S. V, Koneru S, Zhan L.2008. "Secoisolariciresinol diglucoside induces neovascularization-mediated cardioprotection against ischemia-reperfusion injury in hypercholesterolemic myocardium". *J Mol Cell Cardiol*; 44 (1):170-179.
- Pettersen, E. F. 2004. "UCSF Chimera—A visualization system for exploratory research and analysis". *Journal of Computational Chemistry* 25, 1605–1612.
- Peterson J, Dwyer J, Adlercreutz H, Scalbert A, Jacques P, McCullough M L. 2010. "Dietary lignans: physiology and potential for cardiovascular disease risk reduction". *Nutr Rev.*; 68:571–603.
- Platts-Mills J.A., Taniuchi M., Uddin M.J., Sobuz S.U., Mahfuz M., Gaffar S.A., Petri W.A. 2017. "Association between enteropathogens and malnutrition in children aged 6-23 mo in Bangladesh: a case-control study". *American Journal of Clinical Nutrition*, 105: 1132–38.
- Prajapati V., Tripathi A.K., Aggarwal K.K., Khanuja S.P.S. 2005. "Insecticidal, repellent and oviposition-deterrent activity of selected essential oils against *Anopheles stephensi*, *Aedes aegypti* and *Culex quinquefasciatus*." *Bioresource Technology*, 96: 1749–1757.
- Prasad K. 2001. "Secoisolariciresinol diglucoside from flaxseed delays the development of type 2 diabetes in Zucker rat". *J Lab Clin Med*; 138:32–9.
- Prasad K. 1997. "Hydroxyl radical-scavenging property of secoisolariciresinol diglucoside (SDG) isolated from flaxseed". *Mol Cell Biochem*; 168:117-123.
- Prasad K.: US20026486126 (2002).
- Prasad K. 2007. "A study on regression of hypercholesterolemic atherosclerosis in rabbits by flax lignan complex". *J Cardiovasc Pharmacol Ther.*;12:304–13.
- Prasad K. 2009. "Flax lignan complex slows down the progression of atherosclerosis in hyperlipidemic rabbits". *J Cardiovasc Pharmacol Ther.*;14:38–48.
- Puzari M., Sharma M., Chetia P. 2018. "Emergence of antibiotic resistant *Shigella* species: A matter of concern". *Journal of Infection and Public Health* 11: 451–454.
- Rajasha J., Ranga A., Madhusudhan Ra. and Karunakumar M. 2010. "Antibacterial Properties of Secoisolariciresinol Diglucoside Isolated from Indian Flaxseed Cultivars". *Current Trends in Biotechnology and Pharmacy* 4 (1): 551-560.

- Ranga Rao A., Harshavardhan Reddy A., Aradhya S. M. 2010. Antibacterial properties of *Spirulina platensis*, *Haematococcus pluvialis*, *Botryococcus braunii* micro algal extracts. *Current Trends in Biotechnology and Pharmacy* Vol. 4 (3) 807-817. ISSN 0973-8916.
- Rebey I.B., Wannan W.A., Kaab S.B., Bourgo S., Tounsi M.S., Ksouri R., Fauconnier M.L. 2019. "Bioactive compounds and antioxidant activity of *Pimpinella anisum* L. accessions at different ripening stages". *Scientia Horticulturae*, 246: 453–461.
- Rhee Y, Brunt A. 2007. "Effects of flaxseed lignan on mitogen stimulated lymphocyte proliferation". *FASEB J.*; 21:702–11.
- Robinson B.S., Riccardi K.A., Gong Y.F., Guo Q., Stock D.A., Blair W.S., Terry B.J., Deminie C.A., Djang F., Colonna R.J. 2000. "A highly potent human immunodeficiency virus protease inhibitor that can be used in combination with other available antiretroviral agents". *Antimicrob. Agents Chemother.*, 44, pp. 2093-2099.
- Rogawski E.T., Liu J., Platts-Mills J.A., Kabir F., Lertsethtakarn P., Sigua M., Khan S.S., Praharaj I., Murei A., Nshama R., et al. 2018. "Use of quantitative molecular diagnostic methods to investigate the effect of enteropathogen infections on linear growth in children in low-resource settings: longitudinal analysis of results from the MAL-ED cohort study" *The Lancet Global Health*.
- Romanowski M.J., Burley S.K. 2002. "Crystal structure of the *Escherichia coli* shikimate kinase I (AroK) that confers sensitivity to mecillinam". *Proteins* 47: 558-562.
- Romilde Iannarelli, Oliviero Marinelli, Maria Beatrice Morelli, Giorgio Santoni, Consuelo Amantini, Massimo Nabissi, Filippo Maggi. 2018. "Aniseed (*Pimpinella anisum* L.) essential oil reduces pro-inflammatory cytokines and stimulates mucus secretion in primary airway bronchial and tracheal epithelial cell lines". *Industrial Crops and Products*; 114, 81-86.
- Rutenber E.E., Stroud R.M. 1996. "Binding of the anticancer drug ZD1694 to *E. coli* thymidylate synthase". *Assessing specificity and affinity structure*, 4, pp. 1317-1324.
- Sağdıç O., Özcan M. 2003. "Antibacterial activity of Turkish spice hydrosols" *Food Control*, 14: 141-143.
- Sajjad Ahmad, Shehneela Baseer, Afifa Navid, Faisal Ahmad, Syed Sikander Azam. 2018. "An integrated computational hierarchy for identification of potent inhibitors against Shikimate Kinase enzyme from *Shigella sonnei*, a major cause of global dysentery". *Gene Reports*; 1, 283-293. <https://doi.org/10.1016/j.genrep.2018.04.010>.
- Satya Tapas, Abhinav Kumar, Sonali Dhindwal, Preeti, Pravindra Kumar. 2011. "Structural analysis of chorismate synthase from *Plasmodium falciparum*: A

novel target for antimalaria drug discovery”. *International Journal of Biological Macromolecules*; 49, (4),767-777.

Seedman.com. flax seed and flax plant.

Schonbrunn E., Eschenburg S., Shuttleworth W.A., Schloss J.V., Amrhein N., Evans, J.N., Kabsch W. 2001. Interaction of the herbicide glyphosate with its target enzyme 5-enolpyruvylshikimate 3-phosphate synthase in atomic detail”. *Proc Natl Acad Sci U S A* 98: 1376-1380.

Schroeder G.N., Hilbi H. 2008. “Molecular pathogenesis of *Shigella* spp.: controlling host cell signaling, invasion, and death by type III secretion”. *Clin. Microbiol. Rev.*, 21, pp. 134-156.

Shahin K., Bouzari M., Wang R., Khorasgani M.R. 2019. “Distribution of antimicrobial resistance genes and integrons among *Shigella* spp. isolated from water sources”. *Journal of Global Antimicrobial Resistance*, 19: 122–128.

Sebastian Reichau, Wanting Jiao, Scott R. Walker, Richard D. Hutton, Edward N. Baker, Emily J. Parker. 2011. “Potent Inhibitors of a Shikimate Pathway Enzyme from *Mycobacterium tuberculosis*”. *Journal of Biological Chemistry*; 286(18): 16197–16207.

Shobha R.I. 2013. “Antioxidant, Anti-Diabetic and Hypolipidemic Effects of Aniseeds (*Pimpinella anisum* L.): In vitro and in vivo Studies”. *Conference Proceedings*.

Spence J. D, Thornton T, Muir A. D, Westcott N. D. 2003. “The effect of flax seed cultivars with differing content of alpha-linolenic acid and lignans on responses to mental stress”. *J Am Coll Nutr.*;22:494–501.

Stevens T.C., Ochoa C.D., Morrow K.A., Robson M.J., Prasain N., Zhou C., Alvarez D.F., Frank D.W., Balczon R., Stevens T. 2014. “The *Pseudomonas aeruginosa* exoenzyme Y impairs endothelial cell proliferation and vascular repair following lung injury”. *Am. J. Physiol. Cell. Mol. Physiol.*, 306, L915–L924.

Sumathi S., Poornima A., Muthukumari D., Padma P.R. 2018. “Cytotoxicity and in-silico studies of anethole in triple negative breast cancer cells”. *International Journal of Pharmaceutical Sciences and Research*, 9: 3414- 3419.

Tai A.Y.C., Easton M., Encena J., Rotty J., Valcanis M., Howden B.P., Slota-Kan S., Gregory J. 2016. “A review of the public health management of shigellosis in Australia in the era of culture independent diagnostic testing”. *Australian and New Zealand Journal of Public Health*, 40: 588–91.

Taneja N., Mewara A. 2016. “Shigellosis epidemiology in India”. *Indian Journal of Medical Research*, 143: 565–576.

- Tepe B., Daferera D., Sokmen A., Sokmen M., Polissiou M. 2005. "Antimicrobial and antioxidant activities of the essential oil and various extracts of *Salvia tomentosa* Miller (Lamiaceae)". *Food Chemistry*, 90: 333–340.
- The encyclopedia britannica, 2023. Anise.
- Trott O, Olson A.J. 2010. "AutoDock Vina: improving the speed and accuracy of docking with a new scoring function, efficient optimization and multithreading". *Journal of Computational Chemistry*, 31: 455-461.
- Ud-Din, A. I., Wahid, S. U., Latif, H. A., Shahnaaj, M., Akter, M., Azmi, I. J., Hasan, T. N., Ahmed, D., Hossain, M. A., Faruque, A. S., Faruque, S. M., and Talukder, K. A. 2013. "Changing trends in the prevalence of *Shigella* species: emergence of multi-drug resistant *Shigella sonnei* biotype g in Bangladesh". *PLoS One* 8 (12), e82601. DOI: 10.1371/journal.pone.0082601.
- Vanommeslaeghe K., Hatcher E., Acharya C., Kundu S., Zhong S., Shim J. 2010. "CHARMM General Force Field (CGenFF): A force field for drug-like molecules compatible with the CHARMM all-atom additive biological force fields". *Journal of computational chemistry*, 31 (4) pp. 671-690.
- Veber D.F, Johnson S.R, Cheng H.Y, Smith B.R, Ward K.W, Kopple K.D. 2002 "Molecular properties that influence the oral bioavailability of drug candidates". *J Med Chem* 45(12):2615–2623.
- Vanommeslaeghe K., Hatcher E., Acharya C., Kundu S., Zhong S., Shim J., Darian E., Guvench O., Lopes P., Vorobyov I. 2010. CHARMM General Force Field (CGenFF): A force field for drug-like molecules compatible with the CHARMM all-atom additive biological force fields". *J Comput Chem*. Mar; 31(4): 671–690.
- Vidal D., Garcia-Serna R., Mestres J. 2011. "Ligand-based Approaches to in Silico pharmacology". *Chemoinformatic and Computational Chemical Biology*, Springer, pp. 489-502.
- Vincent Zoete, Michel Cuendet A., Aurélien Grosdidier, Olivier Michielin. 2011. "SwissParam: A fast force field generation tool for small organic molecules". *Journal of computational chemistry*:32 (11); 2359-2368.
- Yutani M., Hashimoto Y., Ogita A., Kubo I., Tanaka T., Fujita K. 2011. "Morphological Changes of the Filamentous Fungus *Mucor Mucedo* and Inhibition of Chitin Synthase Activity Induced by Anethole". *Phytoteraphy Research*, 25: 1707-1713.
- Wagner S. Diepold A. 2020. "A unified nomenclature for injectisome-type type III secretion systems". *Curr. Topics Microbiol. Immunol.*, 427, 1–10.
- Williams, P. C. M. and Berkley, J. A. 2018. "Guidelines for the treatment of dysentery (shigellosis): a systematic review of the evidence". *Paediatr Int. Child Health* 38 (sup1), S50– S65, DOI: 10.1080/20469047.2017.1409454.

- Williams P., Berkley J. 2016. "Dysentery (shigellosis) current who guidelines and the WHO essential medicine list for children: world Health Organization (WHO)". *Case Rep Pediatr.* (33). doi:10.1155/2016/1691290.
- World Health Organization (WHO). 2022. "Disease outbreak news; Extensively drug resistant *Shigella sonnei* infections". <https://www.who.int/emergencies/disease-outbreak>.
- World Health Organization. 2005. "Guidelines for the Control of Shigellosis, Including Epidemics Due to *Shigella dysenteriae* Type 1".
- World Health Organization (WHO). 2014. "Antimicrobial resistance: global report on surveillance".
- Zainab G. Hussien and Raghad A. Aziz. 2021. "Chemical Composition and Antibacterial Activity of *Linum Usitatissimum* L. (Flaxseed)". *Sys Rev Pharm*;12(2):145-147.
- Zanwar, A. A., et al. 2014. "Antihyperlipidemic activity of concomitant administration of methanolic fraction of flax lignan concentrate and omega-3-fatty acid in poloxamer-407 induced experimental hyperlipidemia". *Industrial Crops and Products*, 52; 656– 663.
- Zhang W, Wang X, Liu Y. 2008. "Dietary flaxseed lignin extract lowers plasma cholesterol and glucose concentrations in hypercholesterolaemic subjects". *Br J Nutr.*; 99:1301–9.
- Zhang L., Mei M., Yu C., Shen W., Ma L., He J., Yi L. 2016. "The functions of effector proteins in *Yersinia virulence*". *Pol. J. Microbiol.*, 65, 5–12.
- Zoete V., Cuendet M.A., Grosdidier A., Michielin O. 2011. "SwissParam: a fast force field generation tool for small organic molecules". *Journal of computational chemistry*, 32 (11), pp. 2359-2368.